Identification and Characterization of Regulators of 2-Cys-Peroxiredoxin A in *Arabidopsis thaliana*

Inaugural-Dissertation
to obtain the academic degree
Doctor rerum naturalium (Dr. rer. nat.)

submitted to the Department of Biology, Chemistry and Pharmacy
of Freie Universität Berlin

by

Wei Guo

from Hohhot (China)

Berlin, 2013

The investigations described in the following thesis were started under supervision of Prof. Dr. Margarete Baier at the Institute of Plant Sciences of the Heirich-Heine University Düsseldorf (09.2008- 11.2010) and continued after moving of the group at the Institute of Biology, department of Plant Physiology of the Freie Universität Berlin (12.2010-08.2013).

1st Reviewer: Prof. Dr. Magarete Baier

2nd Reviewer: Prof. Dr. Wolfgang Schuster

Date of defence: 24.10.2013

Table of contents

Summary

In this project, retrograde redox signaling from chloroplasts to the nucleus was studied by identifying and characterizing regulators of 2-Cys-Peroxiredoxin A transcription in *Arabidopsis thaliana.* The *r*edox *imb*alanced mutants (*rimb*) were used to identify *2CPA* regulators. The mutant loci *rimb3* and *rimb6* were mapped in the Arabidopsis genome by next generation sequencing and characterized. In addition, a 2CPA expression's QTL (eQTL) was identified with SSLP markers based on the genetic variation of Arabidopsis accessions Col-0 and L*er*.

RIMB3 (At4g01290) is a PAT1 domain containing protein which coexpresses with RIMB1 and CDC48. It may function in a pathway upstream of RIMB1. RIMB3 may activate 2CPA expression directly or via Rap2.4a or CDC48 in a development-dependent manner.

RIMB6 is identified as an F-Box containing protein (At4g12560), which negatively regulates the plant defense system by constitutive repression of PR and SCN1 genes. RIMB6 may activate 2CPA expression by repression of an unknown negative regulator of *2CPA*. Furthermore RIMB6 is also involved in regulatory system of metal homeostasis, in which metal channels and/or transporters are regulated.

The eQTL (At3g21660) was determined as an UBX containing protein, which may physically interact with CDC48. The eQTL positively regulates expression of 2CPA and 2CPB. It is proposed that it acts via CDC48 and an unknown positive regulator of *2CPA* downstream of CDC48. The eQTL coexpresses with ASK9 and ASK16, which physically interact with RIMB6.

The three different *2CPA* regulators play important roles in the network of redox retrograde signaling pathway from chloroplast to nucleus. Their regulatory mechanism could further contribute to the understanding of cross-talk between retrograde signaling, ubiquitination, plant defense responses and metal homeostasis in plant cells.

Zusammenfassung

Im Rahmen dieses Projektes wurde die retrograde Signaltranduktion vom Chloroplasten zum Zellkern untersucht, und zwar anhand der Identifizierung und Charakterisierung der Regulatoren von 2-Cys-Peroxiredoxin A (2CPA) in *Arabidopsis thaliana*. Es wurden Mutanten mit gestörten Redoxsystem Kontrollen (*r*edox *imb*alanced, *rimb*) genutzt, um die Regulatoren von 2CPA zu bestimmen. Die mutierten Gen loci *rimb3* und *rimb6* wurden mittels Hochdurchsatzsequenzierung (Next Generation Sequencing) im Genom von Arabidopsis kartiert. Anschließend wurden diese beiden Genloci charakterisiert. Darüber hinaus wurde ein sogenannter expressional quantitative trait locus (eQTL) identifiziert, womit ein Genlocus gemeint ist, welcher Veränderungen der Expression von Genen bedingt, in diesem Fall die Expression von 2CPA. Die Identifizierung dieses eQTLs gelang mit Hilfe von SSLP Markern basierend auf der genetischen Variation der Arabidopsis-Akzessionen Col-0 und Ler.

Bei RIMB3 (At4g01290) handelt es sich um ein Gen, das für ein Protein mit einer PAT1 Domäne kodiert. Es co-expremiert mit RIMB1 und CDC48. RIMB3 aktiviert die Expression von 2CPA, entweder direkt, über Rap2.4a oder über CDC48.

Das Gen RIMB6 (At4g12560) kodiert für ein Protein mit einer F-Box. Es reguliert auf negative Weise das Abwehrsystem der Pflanze durch konstitutive Repression von PR Genen und SCN1. Es wird postuliert, dass RIMB6 die Expression von 2CPA aktiviert indem es einen bisher unbekannten negativen Regulator von 2CPA repremiert. Außerdem ist RIMB6 auch in das Regulationssystem der Metall-homöostase involviert.

Der eQTL At3g21660 kodiert hingegen für ein Protein, das eine UBX Domäne enthält. Es könnte mit CDC48 interagieren. Der eQTL reguliert positiv die Expression von 2CPA und 2CPB, wahrscheinlich über CDC48 und einem bisher unbekanntem positiven Regulator von 2CPA, der unterhalb von CDC48 agiert. Außerdem co-expremiert der eQTL mit ASK9 und ASK16, die wiederum mit RIMB6 interagieren.

Die drei unterschiedlichen 2CPA Regulatoren spielen eine wichtige Rolle im Netzwerk des redoxbedingten retrograden Signalwegs vom Chloroplasten zum Zellkern. Die Untersuchung ihres regulatorischen Mechanismus könnte das Verständnis über das Zusammenspiel von retrograder Signalweiterleitung, Ubiquitinierung, Pflanzen-Abwehr-Antworten und Metall-Homöostase in Pflanzenzellen erweitern.

List of abbreviations

$^1O_2$	singlet oxygen
A.tumefaciens	*Agrobacterium tumefaciens*
aa	amino acids
ABC	ATP-binding cassette
Apx	ascorbate peroxidase
ARE	antioxidant response elements
ASK	binding Arabidopsis-S-phase kinase-associated protein-like proteins
At	*Arabidopsis thaliana*
bp	base pairs
CAB	nuclear genes encoding LHCP
CaLCuV	cabbage leaf curl virus
CBF	C-repeat/DRE binding factor
CDC	cell division control protein
CDD	Conserved Domains Database
cDNA	complementary DNA
CDS	Cu/ZnSODs
CEO1	Clone Eighty One1 (= RCD1)
Chl	chlorophyll
CNG channels	cyclic nucleotide-gated ion channels
Col-0	*Arabidopsis thaliana* ecotype Columbia-0
cpCK2(PTK)	a chloroplast-targeted protein closely related to the α-subunit of nucleocytosolic casein kinase 2
CPR30	constitutive expresser of PR genes 30
cps	counts per second
Csd	copper/zinc superoxide dismutase
Ct	cycle threshold
Cul	cullin
DBMIB	2,5,-dibromo-3-methyl-6-isopropyl-p-benzoquinone
DCMU	3'-4'-dichlorphenyl-1,1-dimethyl urea
DNA	deoxyribonucleic acid
dNTPs	deoxyribonucleotid triphosphates
DREB	dehydration responsive element binding factor
E. coli	*Escherichia coli*
EDS1	Enhanced Disease Susceptibility1
EDTA	ethylene diamine-N tetra acetid acid
ELIP2	early light-induced proteins
EMS	ethyl methanesulfonate
eQTL	expression quantitative locus
EX1	EXECUTER1
eyc	Saccharomyces cerevisiae Shp1, Drosophila melanogaster eyes closed gene
FLN	fructokinase-like proteins
FSD	FeSOD
GDA	geldanamycin
GLK	Golden 2-like1 and 2
GRx	glutaredoxin
gun	genome uncoupled
GUS	β-glucuronidase
H_2O_2	hydrogen peroxide
$HO^{\cdot}$	hydroxyl radicals
HPL	hydroperoxide lyase
HSP	geldanamycin
ICP-MS	inductively coupled plasma mass spectrometry
IRT1	Iron-Regulated Transporter -1
JA	jasmonic acid
kb	kilo base pairs
LB	left borde

LB medium	Lysogeny broth medium
L*er*	*Arabidopsis thaliana* accession Landsberg *erecta*
Luc	luciferase
LHCB	light-harvesting chlorophyll-a/b proteins
m	micro
M	molar
MEcPP	Methylerythritolcyclodiphosphate
MeJA	methyl jasmonate
MEP	methylerythritol phosphate
MES	monohydrate 2-(Nmorpholino) ethanesulfonic acid
Mg-ProtoIX	Mg-protoporphyrin IX
MOS4	MODIFIER OF snc1-4
mRNA	messenger RNA
MS	Murashige & Skoog
MSD	MnSOD
mTERF	mitochondrial transcription termination factor
n	nano
na	ribonucleic acid
NADPH	Nicotinamide Adenine Dinucleotide Phosphate
NDR1	non race-specific disease resistance 1
NLRs	nucleotide-binding domain and leucine-rich repeats containing proteins
NTC/MAS	nineteen Complex
$O_2^{\cdot}$	superoxide anions
OD	optical density
P. Syringae	Pseudomonas syringae
p2CPA	promoter of 2CPA
PAD4	phytoalexin deficient 4
PAP	3'-phosphoadenosine 5'-phosphate
PAT1	topoisomerase II-associated protein
Pchlide	protochlorophyllide
PCR	polymerase chain reaction
PEP	plastid-encoded RNA polymerase
PETC	photosynthetic electron transport chain
PGE	plastid gene expression
PhANGs	photosynthesis-associated nuclear genes
PHD	plant homeodomain
PPR	pentatricopeptide-repeat
PQ	plastoquinone pool
PRIN2	PLASTID REDOX INSENSITIVE 2
PRL1	PLEIOTROPIC RESPONSE LOCUS 1
PS	photosystem
psbA	a gene encoding the D1 protein of PS II
psaAB	a gene encoding reaction centre apoproteins of PS I
PTK/cpCK2	plastid transcription kinase
PUX	plant UBX-domain containing proteins
R	disease resistance
RB	right border
RbohD	respiratory burst oxidase homolog D
Rbx1	RING-box protein 1
RNA	ribonucleic acid
ROS	reactive oxygen species
SA	salicylic acid
SCF	SKP1-CULLIN1-F-box
SDS	sodium dodecyl sulfate
SEM	standard error of mean
SIG	Sigma factor
SKP1	S-phase kinase-associated protein 1
SNP	single nucleotide polymorphism
SOD	superoxide dismutases

soldat	*Singlet oxygen-linked death activators*
SSLP	simple sequence length polymorphism
TA	annealing temperature
TAC	transcriptionally active chromosome
TAE	tris acetic acid EDTA
Taq	*Thermus aquaticus*
TE	tris EDTA
Tm	melting temperature
Tris	tris(hydroxymethyl)-aminomethane
TRx	thioredoxin
TRXz	plastidial thioredoxin z
U	unit
UTR	untranslated region
v/v	volume per volume
w/v	weight per volume
YEB	yeast extract and beef
ZIP	Zrt/Irt-like protein

Amino acids and nucleic acids were abbreviated according to recommendations given by the IUPAC-IUB Joint Commission on Biochemical Nomenclature (JCBN).

1 Introduction

1.1 Communication between nucleus and organelles

Cells are the basic units of life. They are highly organized systems, in which communication and coordination of nucleus and organelles are crucial to maintain all the processes.

1.1.1 From endosymbionts to organelles

Present-day plants have evolved over a billion years ago through endosymbiosis of free-living bacteria (Guttman and Vitetta, 1967). It is believed that, the early mitochondrial and chloroplast ancestor arose from proteobacteria and cyanobacterias, respectively (Dyall et al., 2004). Nowadays organelles contain several thousand proteins. However over 90% of the organelle proteins, which are encoded in the nucleus, are subsequently synthesized in the cytoplasm, and are further translocated into the organelles (Richly and Leister, 2004).

1.1.2 Communication between plastids and nucleus

Due to the difference of encoding location and function locations of most of the organelles proteins and gene expression needs to be synchronized between the nucleus and the organelles by intracellular communication processes (Adams et al., 1990; Abuharbeid et al., 2004). Intracellular signaling can be classified to anterograde signaling and retrograde signaling, which represent signaling from the nucleus to the organelle and the organelle to the nucleus, respectively (Figure 1-1).

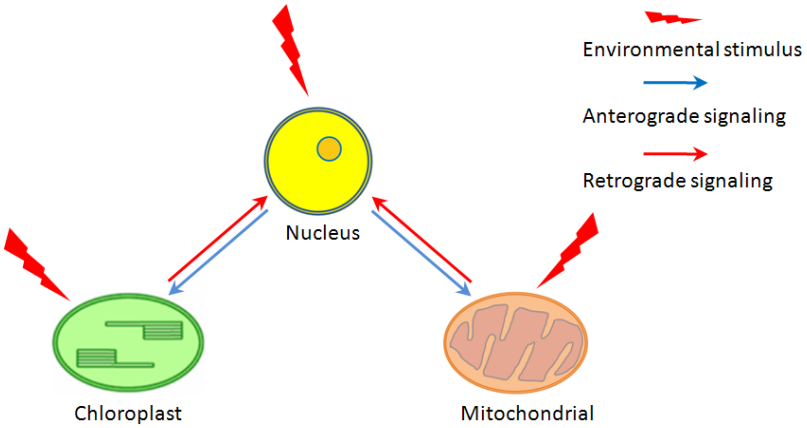

Figure 1-1 Schematics of anterograde and retrograde signaling in plant cells. Signals perceived / generated by the nucleus are communicated to the organelles and lead to changes in the transcription pattern of the organelles in process known as anterograde signaling as indicated by the blue line. Conversely, the signal generated in the organelles is transduced to the nucleus to cause necessary changes in the transcription of nuclear genes in a processed called retrograde signaling as shown by the blue line.

Since nucleus and organelles have their own independent genomes, they have to communicate closely. Signals perceived by the nucleus are communicated to the chloroplasts to adjust gene expression to the stimuli in a process designated anterograde signaling (Pesaresi et al., 2007; Woodson and Chory, 2008). As a result of various biotic and abiotic stresses, cues originated from chloroplast should be transmitted to the nucleus to affect its expression pattern, in a process, which is called retrograde signaling (Rodermel, 2001).

1.2 Retrograde signaling from chloroplast to nucleus

After the early chloroplast ancestors successfully established themselves as a permanent endosymbiont, most of the genetic information was transferred to the nucleus, making it the master regulator. The genome of present-day chloroplasts encode only around hundred proteins (Green, 2011). However, the number of proteins found to be present in the chloroplast by far exceeds the coding capacity of the chloroplast. Therefore, proteins

encoded in the nucleus, have to be processed in the cytosol and subsequently imported into the chloroplast. In this process, the retrograde signaling from chloroplast to nucleus plays a crucial role. Up to now, various signaling pathways have been identified in the chloroplast-to-nucleus retrograde signaling network (Figure 2-2).

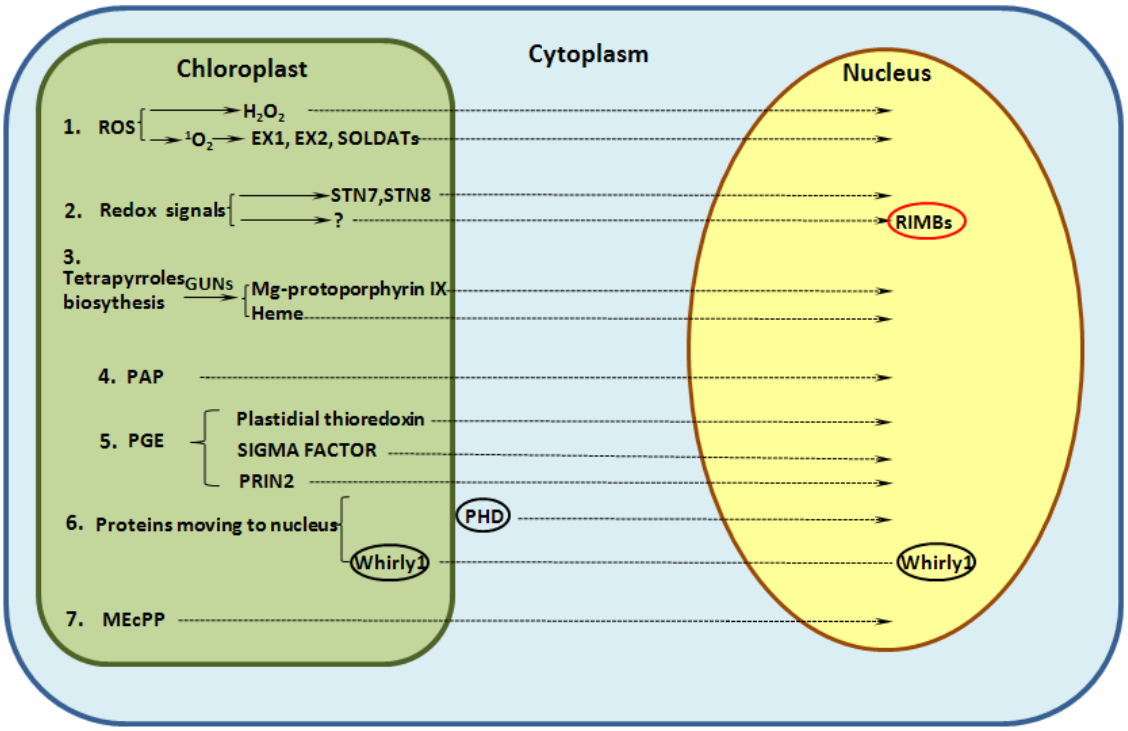

Figure 2-2 Schematic depiction of the various retrograde signaling from chloroplast to nucleus. (1) ROS signals such as hydrogen peroxide and singlet oxygen. Singlet oxygen is communicated to nucleus to effect changes in the expression pattern via EX1, EX2 and SOLDATs as mediators. (2) Redox signals generated in the chloroplast are also communicated to the nucleus through RIMB and STN genes. (3) Tetrapyrrole biosynthesis regulated by GUN genes is indicated to be involved in the chloroplast retrograde signaling. (4) Phosphoadenosine phosphate (PAP) is shown to traverse the membrane to serve as a retrograde signal. (5) Several plastid gene expression (PEG) changes are communicated to the nucleus. (6) Proteins such as Whirly1 and PHD move across the membrane to transduce signals generated in the chloroplast. (7) Methylerythritolcyclodiphosphate (MEcPP) was suggested to be involved in chloroplast retrograde signaling.

1.2.1 Reactive Oxygen Species (ROS)

In plant cells, reactive oxygen species can be accumulated in high amounts, when the plants are exposed to biotic (Doke, 1985) and abiotic stress (Karpinski et al., 1997) and during developmental stages (Pena-Ahumada et al., 2006). If the production of ROS is enhanced, it leads to global changes in gene expression (Vranova et al., 2002), which finally may help cells to avoid irreversible damage to biomolecules (Apel and Hirt, 2004). Although coping with ROS is a priority to avoid its oxidative damage to proteins, DNA, and lipids (Halliwell B, 1989), ROS function as signaling molecules initiating acclimation reactions (Desikan et al., 1998; Mittler et al., 2004)

1.2.1.1 Generation of the ROS

As organelles like chloroplasts, mitochondria and peroxisomes are involved in high energy metabolic flux, various environmental stresses perturb the process which leads to the accumulation of ROS.

In plant cells four main forms of ROS can be found: singlet oxygen ($^1O_2$), superoxide anions ($O_2^{\cdot}$), hydrogen peroxide (H_2O_2), hydroxyl radicals ($HO^{\cdot}$) (Elstner, 1991). In chloroplasts, $^1O_2$ is generated by PSII. It consequently leads to formation of $O_2^{\cdot}$ and $HO^{\cdot}$ in presence of water (Elstner, 1991). Most $O_2^{\cdot}$ is formed at PSI in the Mehler reaction due to excess light energy. It is spontaneously and enzymatically disproportionated into O_2 and H_2O_2 (Mehler, 1951; Asada, 2000).

1.2.1.2 The roles of ROS in plants under biotic and abiotic stresses and plant development

Being recognized initially as toxic products in the plant cells (Halliwell B, 1989), ROS in high concentration are rapidly removed by various cellular enzymatic and nonenzymatic mechanisms (Apel and Hirt, 2004). However, ROS also function as regulators of many biological processes, such as growth, the cell cycle, programmed cell death, hormone

signaling, responses to biotic and abiotic stress, and development (Galvez-Valdivieso and Mullineaux, 2010; Nanda et al., 2010; Swanson and Gilroy, 2010; Suzuki and Mittler, 2012)

ROS generation has been identified in many plant-pathogen interactions involving virulent bacteria, fungi, and viruses (Low and Merida, 1996). ROS have been determined to play a key role in establishing plant defense responses (Levine et al., 1994; Doke et al., 1996; Apel and Hirt, 2004). ROS accumulation precedes the hypersensitive response (HR) cell death, which accompanies pathogen recognition and leads to the incompatible interaction (Levine et al., 1994; Mehdy, 1994).

ROS also play an important role in the different symbiotic interactions: the regulation and the involvement of ROS were reported in Legume – Rhizobia symbiotic relations (Santos et al., 2001; Ramu et al., 2002) and during the establishment of both endo- and ectomycorrhiza (Fester and Hause, 2005; Baptista et al., 2007).

In response to different abiotic stress factors such as high light, low temperature, high temperature, water deficiency, and mechanical stress the ROS production is induced in chloroplast and mitochondria (Apel and Hirt, 2004). The ROS play an important role in to maintaining normal energy and metabolic fluxes and in optimizing different cell functions (Suzuki et al., 2012). Thereby it activates acclimation responses through retrograde signaling, and further controls whole-plant systemic signaling pathways (Suzuki et al., 2012)

In addition, ROS, particularly $O_2^{\bullet}$ and H_2O_2, can act as second messengers in signal transduction cascades during cellular growth and control stomata closing (Pei et al., 2000) as well as programmed cell death (Gechev and Hille, 2005). Furthermore, ROS may play a general role in root developmental regulation (Foreman et al., 2003). Different from Ca^{2+} signaling, ROS signaling is not controlled by messenger storage and release, but by production and scavenging (Mittler et al., 2004).

1.2.1.3 H_2O_2 as chloroplast retrograde signal

H_2O_2 produced in chloroplast plays a role in chloroplast retrograde signaling (Maruta et al., 2012). By moving across biological membranes (Bienert et al., 2006), the low concentrated H_2O_2 still can directly influence the functions of cytosolic signaling components and trigger retrograde signaling from chloroplasts to nucleus, especially in response to stress (Mittler et al., 2011; Maruta et al., 2012). Recently, many studies focused on the mechanism by which the plant cell can recognize the origin of a specific ROS signal and trigger the appropriate responses (Moller and Sweetlove, 2010).

It is reported that the apoplastic ROS-producing enzyme NADPH oxidase RbohD responds to chloroplast redox signals and cell death (Torres et al., 2006). The Arabidopsis Enhanced Disease Susceptibility1 (EDS1) is determined to process H_2O_2 signal to produce counter-balancing activities of salicylic acid (SA) (Wiermer et al., 2005; Straus et al., 2010) .

In the response of plants exposed to excess light, H_2O_2 locally controls of the expression of APX2 and thereby plays a role in intracellular signaling and as an initial signal for the propagation of systemic responses to a wide range of stress conditions (Karpinski et al., 1999; Mullineaux and Karpinski, 2002).

Furthermore, in the response of plants exposed to low temperature, H_2O_2 signaling is identified to control the feedback regulation of cold acclimation by C-repeat/DRE binding factor (CBF1)/DREB1B (Maruta et al., 2012).

1.2.1.4 $^1O_2$ as chloroplast retrograde signal and *flu* mutant

Since $^1O_2$ is has a very short half-life (200 ns) (Gorman and Rodgers, 1992). It is suggested that the singlet oxygen derived plastid signal must exit the chloroplast via second messengers. The conditional fluorescent mutant, *flu*, of Arabidopsis was generated to discover the messengers (Meskauskiene et al., 2001). The *flu* mutant displays an over-

accumulation of protochlorophyllide (Pchlide) in the dark. The mutant produces an oxidative bust of $^1O_2$, if the mutant is transferred into light.

Through a screening for *flu* suppressor mutants, two plastid-localized proteins EXECUTER1 (EX1) and EXECUTER2 (EX2) are identified (Wagner et al., 2004). EX1 and EX2 are suggested to process the $^1O_2$ derived plastid signal to the nucleus (Lee et al., 2007).

Singlet oxygen-linked death activators (*soldat*) were also identified by screening for *flu* suppressor mutants, where $^1O_2$-dependent cell death was abolished without affecting protochlorophyllide accumulation (Baruah et al., 2009; Coll et al., 2009; Meskauskiene et al., 2009). The SOLDAT8 was identified as the sigma factor 6 (SIG6) subunit of the plastid-encoded RNA polymerase (PEP) (Coll et al., 2009) while SOLDAT10 was determined as a plastid-localized protein related to the human mitochondrial transcription termination factor mTERF (Pei et al., 2000). However, the two SOLDAs look like general components essential for chloroplast function but not signaling components specifically involved in the $^1O_2$-triggered signaling (Pei et al., 2000).

In addition, the PLEIOTROPIC RESPONSE LOCUS 1 (PRL1) was identified by screening for novel regulatory components of the $^1O_2$-responsive AAA-ATPase promoter in the *flu* background (Baruah et al., 2009). PRL1 plays a role in plant innate immunity response against pathogens and was identified as a component of the conserved proteolytic NTC/MAS complex together with CDC5 and MOS4 (Palma et al., 2007; Monaghan et al., 2009).

1.2.2 Redox state of the components in the photosynthetic electron transport chain

The redox state of the photosynthetic electron transport chain (PETC) is the link between photosynthetic light reactions and metabolism. It fluctuates under varying light

intensity and quality and triggers signals to nucleus (Woodson and Chory, 2008). Two sources of retrograde redox signals from chloroplast to nucleus have been proposed in the past 20 years: the redox state of the plastoquinone pool (PQ) (Escoubas et al., 1995) and the photosystem I (PSI) acceptor site (Baier et al., 2004). The redox state of the PQ pool correlates with the expression of the plastid encoded genes *psaAB* and *psbA*, which functions in anterograde signaling (Pfannschmidt et al., 2001; Pfannschmidt, 2003). Several studies demonstrated that the redox retrograde signal is complex signaling network, which is more than the simple switch between oxidized and reduced PQ pool (Brautigam et al., 2009).

1.2.2.1 STN7

STN7, a thylakoid protein kinase, has been identified to be involved the redox signaling network and regulation of photosynthetic acclimation (Bellafiore et al., 2005). STN7 is an important element in the regulation of state transition in PSII and PSI, in which STN7 phosphorylates the major photosynthetic light harvesting proteins. In the mutant *stn7*, acclimation to changes in light quality is defective, suggesting that STN7 involves in mediating redox signal from chloroplast to nucleus (Bonardi et al., 2005). However, as demonstrated by the expressional analysis, *stn7* and wild type plant did not have any significant disparity in the transcript abundance of photosynthetic genes. STN7 is therefore determined not to affect the transcripts of Arabidopsis photosynthesis-associated nuclear genes (PhANGs) (Pesaresi et al., 2011). Recently, it was reported that the STN7 functions in chloroplast-to-nucleus retrograde signaling by regulating thylakoid membrane redox balance, which mediates signals reprogramming the hormonal network that operates at all levels of cellular metabolism in the plant cell, via jasmonic acid (JA) and through direct interaction (Tikkanen et al., 2012) .

1.2.2.2 Regulators of 2CPA

In term of the redox state of the PSI acceptor site, the antioxidant enzyme 2-Cys-peroxiredoxin A (2CPA) has been studied widely to understand chloroplast redox signaling (Baier et al., 2004). The transcription of the 2CPA is proven to be under control of the PETC and it is also independent from the PQ state signals (Baier et al., 2004). A correlation was confirmed between activity of 2CPA promoter and the electron pressure on the acceptor site of photosystem I (Baier et al., 2004). Thus, the regulators of the 2CPA could function as the redox signals from chloroplast to nucleus.

1.2.3 Tetrapyrrole biosythesis

Tetrapyrroles have been studied widely in the past 20 years and hypothesized as retrograde signals from chloroplast to nucleus (Susek et al., 1993; Woodson et al., 2011; Kindgren et al., 2012a). In *Arabidopsis thaliana* chlorophyll, heme, siroheme and phytochromobilin are the four tetrapyrrole molecule forms, which are synthesized via a common branched pathway in plastids. Their synthesis in the plant cell is tightly regulated. It was shown that expression of photosynthesis-associated nuclear genes was affected by perturbations in the tetrapyrrole pathway (Susek et al., 1993).

To study the communication between chloroplasts and the nucleus, the mutants *g*enome *un*coupled (*gun*) were isolated by their elevated expression of CAB-GUS in the presence of norflurazon, and they were widely applied to study chloroplast retrograde signaling in background of the tetrapyrrole biosynthesis (Susek et al., 1993). Under photooxidation caused by norflurazon treatment, the mutants express photosynthesis-associated nuclear genes (PhANGs) while wild type plants showed strong suppression of photosynthetic gene expression (Susek et al., 1993). GUN1 was identified as a chloroplast localized pentatricopeptide-repeat (PPR) containing unknown function protein, which mediates the impaired plastid gene expression (PGE) to the nucleus (Susek et al., 1993) and GUN2-GUN6 encode components of tetrapyrrole biosynthesis (Vinti et al., 2000). The *gun* mu-

tants provided strong evidence that the tetrapyrroles are involved in retrograde signaling from the chloroplast to the nucleus in plants.

1.2.3.1 Mg-protoporphyrin IX

GUN4, a Mg-ProtoIX-binding protein (Larkin et al., 2003) and GUN5, H-subunit of Mg-chelatase (Mochizuki et al., 2001) are involved in chlorophyll B synthesis.

Accumulations of Mg-ProtoIX and Mg-ProtoIX-ME have been reported under oxidative stress induced by exposure the plants to low temperatures and inhibitors of photosynthetic electron transport (Wilson et al., 2003; Strand, 2004). Impaired flux through the accumulation of Mg-ProtoIX/Mg-ProtoIX-ME and biosynthesis of chlorophyll is determined as an indicator of changes in the environment and consequently causes changes in PhANG expression (Kindgren et al., 2011; Kindgren et al., 2012a). A disturbed chlorophyll biosynthesis as a result of Mg-ProtoIX/Mg-ProtoIX-ME accumulation due to oxidative stress causes altered PhANG expression. Whether accumulation of Mg-ProtoIX is itself an important part of the tetrapyrrole-mediated signal is still unclear.

The transcription factors Golden 2-like1 and 2 (GLK1/2) were indentified to regulate the genes involved in chlorophyll biosynthesis including the subunits of the Mg-chelatase, and to be responsive to plastid retrograde signals (Waters et al., 2009). It is assumed that GLK1/2 operate downstream of plastid retrograde signaling in more long-term acclimatory responses (Waters et al., 2009).

In addition, Kindgren (2012) suggested a regulatory system, including the HSP90 proteins that respond to the GUN5 signal and the transcription factor HY5, which is modified by tetrapyrroles in response to oxidative stress (Kindgren et al., 2012a). The study on the *hy*5 mutant further suggested that HY5 acts downstream of the GUN5 signal. Moreover the insensitivity of *hy*5 mutant to the treatment with the inhibitor of HSP90, geldanamycin (GDA) also supporting the link between HY5 and HSP90. It is concluded that

HSP90 and HY5 could be two additional components in the GUN5 pathway (Kindgren et al., 2012a).

1.2.3.2 Heme

In animal and yeast cells, accumulation of the heme has been reported to regulate gene expression (Forsburg and Guarente, 1989; Qi et al., 1999; Zhang and Hach, 1999; Ogawa et al., 2001). In *Chlamydomonas reinhardtii* feeding with heme demonstrated global changes in the gene expression and *ca.* 1000 genes significantly changed their expression level. Heme is therefore suggested to act as retrograde signal from chloroplast to nucleus (Voss et al., 2011).

Recently, a new *gun* mutant, gun6-1D, has been identified. It displays a similar phenotype to the gun2–gun5 mutants with high PhANG expression compared to wild type when grown on MS with norflurazon. The GUN6-1D encodes plastid ferrochelatase 1 (FC1, heme synthase). The analysis suggested that the protein contributes to a specific pool of heme which may act as a retrograde signal and that is responsible for the regulation of PhANG expression (Woodson et al., 2011).

In addition, Mg-ProtoIX and heme are cytotoxic. To play a role in signaling from chloroplast to nucleus, they must be emitted from chloroplast to the cytosol. An Arabidopsis tryptophan-rich sensory protein (At-TSPO) was recently identified to bind and scavenge porphyrin during plants stress. It is suggested that the membrane associated protein may play a role in heme trafficking and signaling during plastid development (Vanhee et al., 2011).

1.2.4 Phosphoadenosine phosphate (PAP)

Recently, a phosphonucleotide (3'-phosphoadenosine 5'-phosphate, PAP) was proposed to be a novel chloroplast retrograde signal (Estavillo et al., 2011). Under drought or ex-

posure to excess light PAP accumulates in chloroplasts and acts as a mobile signal altering RNA metabolism by inhibiting a 5' to 3' exoribonucleases. PAP was shown to induce stress-induced genes such as APX2 and ELIP2 (Estavillo et al., 2011). The level of PAP is regulated by a phosphatase SAL1 dephosphorylating PAP to AMP (Quintero et al., 1996). In a response to oxidative stress caused by high light and drought, PAP transmits the signal from chloroplast to nucleus. It was proven that PAP is able to move between cellular compartments as substrate of SAL1. A SAL1-PAP retrograde pathway is conclusively proposed to alter nuclear gene expression during HL and drought stress (Estavillo et al*.,* 2011).

1.2.5 Plastid gene expression

Plastid gene expression (PGE) is essential for the initiation of PhANG expression (Koussevitzky, 2007). Regulation of PGE could be involved in chloroplast retrograde signaling. GUN1, for instance, can mediate the impaired plastid gene expression to the nucleus (Susek et al., 1993). PEP-dependent plastid gene expression is strong effected by photosynthetic activity. Redox signals from the thylakoid membrane are suggested to link to plastid gene expression via complex networks of phosphorylation events (Steiner et al., 2009).

1.2.5.1 SIGMA FACTOR (SIG)

Reversible phosphorylation of sigma factors is proven to influence PGE activity *in vivo*. The activity of SIG1 is modulated by the redox signature of the chloroplast, which in turn affects the expression of psaA gene (Shimizu et al., 2010). It is suggested that the sensor kinase CSK links photosynthetic activity to SIG1 phosphorylation and expression of photosynthesis genes in the chloroplasts. Furthermore, SIG6 was identified as a substrate of the plastid transcription kinase cpCK2 (PTK/cpCK2) through a mutant screening in background of *flu* mutant SIG5 was recently determined to controls circadian rhythms of transcription of several chloroplast genes (Noordally et al., 2013). By SIG5 pathway,

the nuclear-encoded circadian oscillator controls rhythms of chloroplast gene expression. It has been shown that SIG5 transduces light signals to the circadian regulation of plastid genes (Shimizu et al., 2010).

1.2.5.2 Plastidial thioredoxin z and fructokinase-like proteins

A plastidial thioredoxin z (TRXz) was recently determined as one of the components of the transcriptionally active chromosome (TAC) from chloroplasts (Arsova et al., 2010). The TRXz was suggested to be involved in the redox regulation of PEP activity during dark-to-light transition (Arsova et al., 2010; Schroter et al., 2010). Moreover, 2 fructokinase-like proteins (FLN1 and FLN2) were identified as potential TRX z target proteins. It is shown that the FLN2 redox state changes in *vivo* during light/dark transitions mediated by TRXz. Kindgren (2012) reported that the activity of PEP is correlated with the redox regulation of nuclear encoded photosynthesis genes (Kindgren et al., 2012b). Due to the important role of TRXz in the regulation of PEP-dependent transcription in chloroplasts (Arsova *et al.,* 2010), the TRXz was suggested to be responsive to photosynthetic electron transport and further trigger a retrograde signaling, which regulates expression of nuclear encoded photosynthesis genes (Arsova et al., 2010),.

1.2.5.3 PRIN2

The PLASTID REDOX INSENSITIVE 2 (PRIN2) was also identified as a chloroplast component involved in redox-mediated retrograde signaling. In mutants *prin2-1* and *prin2-2*, regulation of PhANGs was disturbed in response to excess light, and photosynthetic electron transport was inhibited. The *prin2* mutant is characterized by having a radiation sensitive phenotype. *LHCB1.1* and *LHCB2.4* are misregulated in the mutant, indicating that fully functional PEP complex is required in the correct expression of LHCB, in response to redox fluctuation in photosynthetic electron transportation (Kindgren et al., 2012b). The high irradiance-sensitive phenotype with significant photoinactivation of PSII in *prin2* suggested that PRIN2 is a part of the PEP machinery. The

PEP complex is assumed to respond to photosynthetic electron transport and generate a retrograde signal from chloroplast to nucleus (Kindgren et al., 2012b).

1.2.6 Proteins moving between plastids and nucleus

Recently, a chloroplast outer membrane-bound plant homeodomain (PHD) transcription factor named PTM was identified to mediate chloroplast signals, which regulates PhANGs (Sun et al., 2011). The PTM contains transmembrane domains a DNA-binding homeobox domain, a different transcription factors (DDT) domain (reviewed in Doerks et al., 2001) and a plant homeodomain (PHD) in its N-terminal and four transmembrane domains in the C-terminal (Sun et al., 2011). It is suggested that PTM functions as a stress sensor in the chloroplast outer envelope membrane. After a proteolytic mechanism is activated by a GUN1-mediated response, the N-terminal part of the protein N-PTM is released and travels to nucleus as a retrograde signal, which induces ABI4 transcription factor (Strand et al., 2012).

Furthermore, Whirly1, which is dually located in nucleus and chloroplast, was determined to be able to move from chloroplast to nucleus, proven by a HA-Whirly1 fusion protein (Isemer et al., 2012). The Whirly1 was identified to modulate the expression of PR1 gene. In chloroplast Whirly1 plays a role in RNA metabolism (Melonek et al., 2010), while it regulates transcription of stress responsive genes the nucleus. It is assumed that Whirly1 acts as a plastid retrograde signal. However, the factor, which triggers the retrograde movement, is up to now still unclear (Isemer et al., 2012).

1.2.7 Methylerythritolcyclodiphosphate (MEcPP)

Methylerythritolcyclodiphosphate (MEcPP) was suggested to be able to elicit the expression of selected genes which mediate stress response, and are encoded in nucleus but targeted to chloroplast, for instance hydroperoxide lyase (HPL) (Xiao et al., 2012). MEcPP is a precursor of isoprenoids produced by the plastidial methylerythritol phos-

phate (MEP) pathway. Abiotic stresses elevate MEcPP levels, inducing the expression of the stress responsive genes. It was suggested that MEP perceives stress cues and orchestrate the expression of stress responsive genes by regulating the levels of MEcPP (Xiao et al., 2012).

1.3 Antioxidant system in chloroplast

1.3.1 Non-enzymatic antioxidants

1.3.1.1 Ascorbate

In plant cells, the most abundant water soluble antioxidant is ascorbate, which is synthesized in mitochondria and exists mostly in the reduced form under physiological conditions in the leaves (Smirnoff and Wheeler, 2000). Ascorbate can scavenge superoxide, hydroxyl, radicals and singlet oxygen due to its ability to donate electrons in many enzymatic and non-enzymatic reactions as co-factor. In the ascorbate-dependent water–water cycle, ascorbate peroxidase (APx) uses two molecules of ascorbate to reduce H_2O_2 to water (Noctor and Foyer, 1998). Additionally ascorbate also has functions to regenerate oxidized α-tocopherols (Niki, 1987) and to donate electron to violaxanthin de-epoxidase (Smirnoff and Wheeler 2000).

1.3.1.2 Glutathione

Glutathione (GSH) is the most important non-enzyme thiol in plant cells. It functions as a key redox buffer in metabolically active tissue (Foyer et al., 1997). The GSH pool is widely reduced and maintained by glutathione reductase (GR) (Foyer et al., 1997). In seeds it is an exception that GSSG (form of oxidized GSH) is accumulated (Foyer and Noctor, 2005). The GSH is regenerated mediated by GR by oxidation of NADPH in chloroplast (Foyer et al., 1997).

1.3.1.3 Carotenoids

Carotenoids are another type of low molecular weight antioxidants. They function as a light harvesting pigment in photoautotrophic organisms (Bouvier et al., 2005). In chloroplasts most carotenoids are located in thylakoid membranes, together with chlorophylls in functional pigment-binding proteins (Demmig-Adams et al., 1996). Carotenoid can scavenge free radicals, for instance $^1O_2$ and therefore plays important roles in photoprotection (Mittler et al., 2004, Bouvier et al., 2005).

1.3.1.4 α-Tocopherol

The antioxidant α-tocopherol is located in the chloroplast envelope, thylakoid membranes and in plastoglobuli (Munne-Bosch, 2005). α-tocopherol scavenges ROS, especially $^1O_2$ and $OH^{\bullet}$ and thereby plays an important role to protect the membranes. α-tocopherol is synthesized in higher plants, algae and some cyanobacterias (Munne-Bosch et al., 2003; Kruk et al., 2005; Munne-Bosch, 2005). To detoxify ROS, α-tocopherol is oxidized by reversible one-electron oxidation to an α-tocopheryl radical anion (Foyer and Noctor, 2000, 2003) or by $^1O_2$ (Stratton and Liebler, 1997). α-tocopherol is subsequently regenerated via α-tocopheryl-hydroquinone by ascorbate oxidation (Munne-Bosch, 2005).

1.3.2 Enzymatic antioxidants in chloroplasts

Apart from low molecular weight antioxidants, in plant cells the enzymatic antioxidants also play an important role in detoxification of the ROS. The $O_2^{\bullet -}$ generated at photosystem I is rapidly dismutated to H_2O_2 and O_2 by superoxide dismutase (SOD) (Asada, 1999). The H_2O_2 is subsequently detoxified and reduced to water by ascorbate peroxidase (APx), peroxiredoxins (Prx), or glutathione peroxidase (GPx). Detoxifying H_2O_2 to water in plants can be achieved in the ascorbate-dependent (Halliwell-Foyer- Asada cy-

cle) (Asada, 1999) or ascorbate-independent water–water cycles (Figure 1-2) (Mccord and Fridovic.I, 1969).

1.3.2.1 Superoxide dismutases (SOD)

In the chloroplast antioxidant system, SOD is an important antioxidant enzyme to detoxify $O_2^{\bullet-}$ generated in the Mehler reaction at PSI. In *Arabidopsis thaliana* SOD can be classified in to 3 isoenzymes, which contain different metal cofactors and are located in different cell compartments (Bowler et al., 1992). The Cu/ZnSOD1 (CSD1) is located in the cytosol, while the CSD2 can be found in the chloroplast, and (CSD3) in the peroxisome. MnSOD (MSD1) is located in the mitochondria and three FeSODs (FSD1, FSD2 and FSD3) are located in the chloroplast (Kliebenstein et al., 1998).

1.3.2.2 Ascorbate Peroxidases and enzymes of the Halliwell-Asada-Cycle

In *Arabidopsis thaliana* ascorbate peroxidases (APxs) are located in various cell compartments. While thylakoid-bound APx (tAPx) is located at thylakoid membrane in chloroplasts (Shigeoka et al., 2002), stromal APx (sAPx) can be found both in mitochondria and plastids (Chew et al., 2003).

In the ascorbate-dependent water-water cycle, also known as Halliwell-Asada-Cycle, APx reduces H_2O_2 to H_2O through an ascorbate regeneration system (Asada, 1999) (Figure 1-3). Scavenging H_2O_2 to H_2O by APx is achieved by oxidation of ascorbate to monodehydroascorbate (MDHA), which can be regenerated by monodehydroascorbate reductase (MDHAR) using NAD(P)H as a reducing agent. MDHA can also spontaneously disproportionate to ascorbate and dehydroascorbate (DHA), which is reduced again to ascorbate mediated by dehydroascorbate reducatase (DHAR).

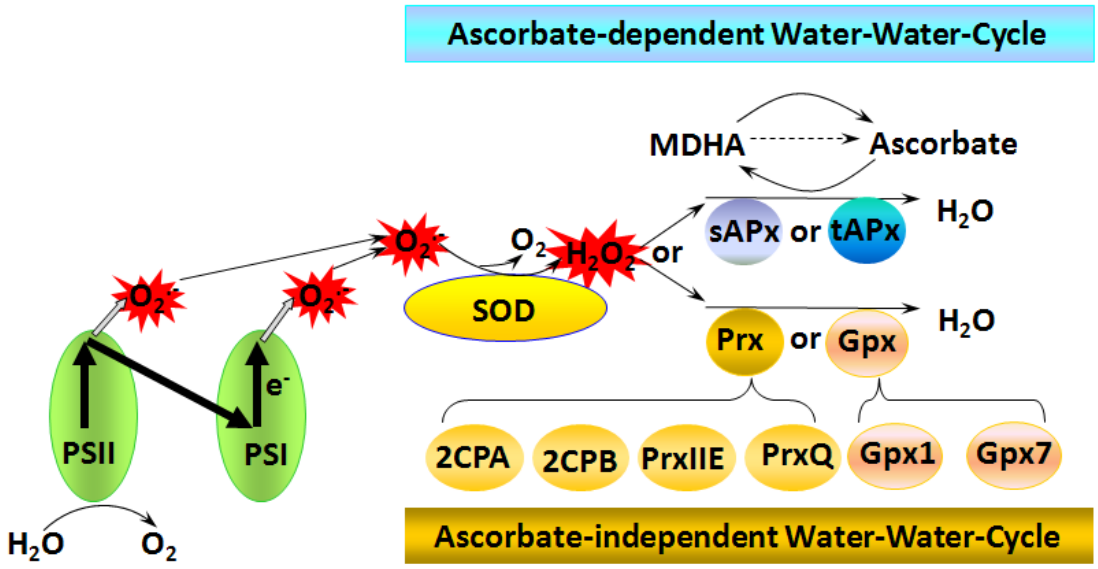

Figure 1-3: A schematics of ascorbate-dependent water–water cycle and ascorbate-independent water–water cycle in chloroplasts of *Arabidopsis thaliana* chloroplasts. $O_2^{\bullet-}$ generated by excess excitation of electrons or various stress condition is dismutated to H_2O_2 by SOD, and H_2O_2 is subsequently reduced to H_2O by ascorbate-dependent (sAPx and tAPx) and ascorbate-independent (via Prx and Gpx) water–water cycle.

1.3.2.3 Peroxiredoxins, glutathione peroxidases and ascorbate-independent water–water cycles

In plant cells, peroxiredoxins (Prxs) belongs to the superfamily of peroxidases. Different from APx, but similar to GPx, the H_2O_2 reducing catalytic activity of Prx is due to their conserved cysteine residues (Chae et al., 1994). The first Prx in plant, 2-Cys Prxs (thio-specific antioxidant), was firstly identified from *Hordeum vulgare* as a homologue of animal and fungal thioredoxin-dependent peroxide reductases and bacterial alkyl hydroperoxide reductases (Baier and Dietz, 1996). In *Arabidopsis thaliana* and most other organisms, Prx can be found in four forms: 1-Cys-Prx (Stacy et al., 1999), 2-Cys-Prx (2-Cys-PrxA, 2-Cys-PrxB) (Baier and Dietz, 1997; Horling et al., 2001), type II Prx (Hofmann et al., 2002) and PrxQ (Jeong et al., 2000; Rouhier et al., 2004; Lamkemeyer et al., 2006). 1-Cys-Prx is located in the cytosol or the nucleus (Stacy et al., 1999), whereas 2-Cys-Prx and PrxQ are chloroplastic and five different PrxIIs are located in cytosol, chloroplast

and mitochondria (Horling et al., 2001). By forming an intra- or inter-molecular dithiol, Prx detoxify H_2O_2 to water. By thiol-disulfide-reactions Prx is subsequently regenerated using small thiols, such as thioredoxins (TRx), glutaredoxins, and glutathione as electron donors (Baier and Dietz, 1997). In the APx knockdown Arabidopsis lines the expression of Prx is induced, indicating a complementary mechanism of APx and Prx in the plant cells, if the plant cell faces insufficient antioxidant protection in chloroplast (Kangasjarvi et al., 2008).

Glutathione peroxidases (GPxs) are localized in the cytosol, chloroplasts, mitochondria and the endoplasmatic reticulum (Mullineaux et al., 1998; Rodriguez Milla et al., 2003; Yang et al., 2006). The GPx reduces H_2O_2 to water via thiols, which act as reducing equivalents. In *Arabidopsis thaliana* chloroplast, GPx has two isoforms: GPx1 and GPx7, while GPx2 and GPx4 are located in cytocol, GPx3 in mitochondria, GPx6 in both cytosol and mitochondria and GPx5 can be found in the endoplasmic reticulum (Rodriguez Milla et al., 2003).

In the ascorbate-independent water-water-cycle (Figure 1-3), the detoxification of H_2O_2 to water is catalyzed by GPx or Prx. In this reaction cycle, small thiols are subsequently used as electron donors to regenerate the GPx or Prx (Baier and Dietz, 1999).

1.4 Transcriptional regulation of the chloroplast antioxidant enzymes

The transcriptional regulation of the chloroplast antioxidant system is a complex network, in which tight coordination of different signaling and metabolic pathways is required between nucleus and chloroplast. In general, the genes encoding chloroplast antioxidant enzymes are less sensitive and they respond slower than cytosolic antioxidant enzymes in response to most stress treatments (Baier et al., 2010).

1.4.1 Different responses of different chloroplast antioxidant enzymes to abiotic stresses

The transcript levels of the chloroplast antioxidant enzymes are differently responsive to most environmental stimuli, according to array experiments (Kilian et al., 2007; Baier et al., 2010). Csd2, for example, was only induced by UV-B light, and DHAR2 expression was up-regulated in response to oxidative stress, UV-B light and osmotic stress as well. Transcript level of GPx7 was exceptionally responsive to cold treatment and UV-B stress after 24 h. It increased transiently 6.22-fold and 10.59-fold, respectively after the treatments. Furthermore, under 24 h treatments of osmotic and salt stresses, transcripts of almost all genes encoding chloroplast antioxidant enzymes were decreased, indicating continuous suppression of signaling under osmotic and salt stress during the long term treatments. However, the transcript levels were kept balanced under treatments with cold, heat, methyl viologen (oxidative stress) and wounding during the first 6h, but increased afterwards up to 12 h of treatment and then decreased (Baier et al., 2010). In addition, under cold stress GPx1 and GPx7 expression levels were strongly increased, while expression of Fsd1 and sAPx were slightly induced. Fsd1 and sAPx showed a slow response to stress, in which their expressions were induced after 12 h under all four stresses (Baier et al., 2010).

Strong increase of the transcript levels of the chloroplast antioxidant enzymes is difficult to induce (Baier et al., 2010). One example is 2CPA, whose expression was slightly induced in response to oxidative stress (Baier and Dietz, 1997; Baier et al., 2004), whereas it strongly decreased under antioxidants treatment (Horling et al., 2003; Nanda et al., 2010).

1.4.2 Transcription factor of sAPx in Arabidopsis

Recently, a transcription factor of sAPx, designated ANAC089, was identified by yeast-one-hybrid screening on the upstream sequence of sAPx start codon (Klein et al., 2012).

The ANAC089 binds to the region of -1262 to -1646 bp upstream of the start codon of sAPx, and suppresses expression of sAPx under a highly reducing condition. The transcription factor, which is located to the *trans*-Golgi network and the ER, is released under reducing treatment and targeted to the nucleus and further regulate the chloroplast antioxidant system (Klein et al., 2012).

1.4.3 Regulation of GPx1 and GPx7 expression in Arabidopsis

The expression of GPx1 is enhanced specifically in response to the combined treatment of cold and light, though the GPx1 transcript level is not significantly changed under cold treatment in the dark (Soitamo et al., 2008). The Arabidopsis GPx1 is homologous to Lotus GPx6 (Ramos et al., 2009), in which the promoter contains motifs similar to the redox regulated antioxidant response elements (ARE) of maize catalase2 (Guan et al., 1996; Scandalios, 2005; Ramos et al., 2009), potentially indicating similar regulatory elements in *Arabidopsis thaliana*.

The GPx7 is the most responsive antioxidant enzyme to stresses in chloroplast according to the array data published by Kilian et al., (2007). In the past 20 years, several light regulated I- and T-boxes (Donald and Cashmore, 1990; Chan et al., 2001) and an ABA-sensitive Myc-ATRD22 motif (Abe et al., 1997) were identified in the GPx7 promoter, however the regulation mechanism of GPx7 is not yet clear.

1.4.4 Regulation of 2-Cys-PrxA (*2CPA*)

1.4.4.1 Transcriptional regulation of *2CPA*

The first peroxiredoxins were cloned the from bacteria such as *E. coli* and *Salmonella typhimurium* over 20 years ago (Storz et al., 1989). Since then the peroxiredoxin genes have been widely studied and the first 2CPA was identified in plant 17 years ago (Baier and Dietz, 1996). The *2CPA* serves now as a model locus to study the mechanism of

regulation of the chloroplast antioxidant system (Baier et al., 2004; Heiber et al., 2007; Shaikhali et al., 2008).

2CPA promoter responds to the oxidative stresses mediated by H_2O_2, ethylene and wounding (Baier et al., 2004), however the 2CPA expression is not induced by methyl viologen and ozone (Baier and Dietz, 1997). In the tAPx and sAPx knock-out line, the antioxidant protection is insufficient and the 2CPA expression is induced, indicating that the APxs and Prxs in chloroplast act complementarily (Kangasjarvi et al., 2008).

Baier et al., (2004) identified a 314 bp core-promoter of *2CPA*, which controls the 2CPA expression according to the stages of leaf development (Baier et al., 2004). Furthermore, a 216 bp *cis*-regulatory domain on upstream of the 2CPA core-promoter was identified and designated ‘‘redox-box’’. Based on this redox-box, a yeast-one-hybrid screen was performed on the *Arabidopsis thaliana* cDNA library. Consequently, a redox-sensitive transcription factor Rap2.4a was identified, which binds to a CE3-like element of the redox-box sequence (Shaikhali et al., 2008). Rap2.4a regulates 2CPA in a redox state dependent manner. In the reduced state the Rap2.4a is in its monomer form. In moderate redox state, it binds on *2CPA* promoter in the dimer form and activates 2CPA expression, and in the oxidized state the Rap2.4a is released from the *2CPA* binding domain through oligomerization (Shaikhali et al., 2008).

By modulating NO_3^- reduction rates and blocking photosynthetic electron transport in the upstream and downstream of the PQ pool, it was concluded that, the *2CPA* activity is dependent on the electron acceptor availability at photosystem I (Baier et al., 2004). A further study of the ABA responsive test revealed that ABA suppresses 2CPA promoter activity. Furthermore, the application of MAPKK-inhibitor PD98059 on the *2CPA* reporter gene line revealed cross-talk of redox signaling and ABA signaling mediated by different MAPKKs (Baier et al., 2004).

1.4.4.2 *Rimb* mutants

To discover the regulators of *2CPA* promoter under redox stresses, a reporter line expressing luciferase under control of *2CPA* promoter was created with Arabidopsis wild type Col-0 (Baier et al., 2004). By application of ethyl methanesulfonate (EMS) to the plants of the reporter gene line, six *r*edox *imb*alanced mutant lines (*rimb*) were generated, which demonstrated impaired regulation of *2CPA* promoter in response to oxidative stress (Heiber et al., 2007). Moreover, the expression of other chloroplast antioxidant enzymes, for instance 2CPB and CDS2, were reduced under photooxidative stresses. It was suggested that independent points of the redox signaling pathway are affected in each *rimb* mutant (Heiber et al., 2007), whose independence from ROS signaling was proven by using marker genes of ROS signaling, like *Fer*, *Cat2*, *Lox2* and *BAP1* (Kiddle et al., 2003; op den Camp et al., 2003).

According the pre-characterization of the six *rimb* mutants, a regulatory network was proposed, in which RIMB3 and RIMB6 play important roles in the central chloroplast-to-nucleus signaling pathway, while RIMB1 and RIMB2 function as general modulators, additionally RIMB5 and RIMB7 are gene-specifically regulators (Heiber et al., 2007). However, the loci of all the RIMBs still needed to be identified in the Arabidopsis genome.

Recently, RIMB1 has been identified as CEO1 (Clone Eighty One; At1g32230) (Hiltscher, 2011), also known as RADICAL-INDUCED CELL DEATH1 (RCD1), which belongs to the (ADP-ribosyl) transferase domain-containing subfamily, that is classified in the WWE protein-protein interaction domain protein family (Aravind, 2001; Ahlfors et al., 2004). CEO1 is localized in the nucleus without stress treatment. However under high salt or oxidative stress CEO1 is also found in the cytoplasm. CEO1 responses to abotic stresses. Experiments of yeast-two-hybrid revealed that CEO1 interacts with Rap2.4a (Sheikhali et al., 2006). It was proposed that CEO1 is induced by H_2O_2, and interacts with Rap2.4a, and that this interaction subsequently increases the DNA-binding activity of Rap2.4a to its binding motif on the target gene (Sheikhali et al., 2006).

1.5 Aim of this study

The present work aims to identify regulators of the chloroplast antioxidant enzyme 2-Cys-Peroxiredoxin A (2CPA), which serves as a model locus to study chloroplast-to-nucleus redox signaling (Baier et al., 2004), and to further elucidate mechanisms of retrograde redox signaling from chloroplast to nucleus, with a particular focus on transcriptional regulation. In this study the *r*edox *imb*alanced (*rimb*) mutants *rimb3* and *rimb6*, which were generated on a reporter gene controlled by the 2CPA promoter (Heiber et al., 2007), were used to investigate the regulation of 2CPA. Identification via genetic mapping and characterization of the loci of RIMBs may lead to a new insight on regulation of chloroplast antioxidant system and the retrograde signal transduction from chloroplast to nucleus.

2 Material and Methods

2.1 Plant materials

The seeds of *Arabidopsis thaliana* natural accessions Columbia-0 (Col-0) and Landsberg *erecta* (L*er*) were obtained from Nottingham Arabidopsis Stock Centre (NASC, Loughborough, UK). The reporter gene line T19-2 expressing luciferase under control of the 2CPA promoter was generated by Agrobacteria transformation of Arabidopsis accession Col-0 (Baier et al., 2004). *Rimb* mutants were generated by EMS mutagenesis of T19-2 (Heiber et al., 2007).

The information of all the T-DNA insertion lines was selected on T-DNA Express Arabidopsis Gene Mapping Tool (http://signal.salk.edu/cgi-bin/tdnaexpress). The seeds were obtained from either the Nottingham Arabidopsis Stock Centre (http://arabidopsis.info) or the Institute National de la Recherche Agronomique (INRA, Paris, France).

2.2 Growth conditions

2.2.1 Sterilization and vernalization of *Arabidopsis thaliana* seeds

The seeds of *Arabidopsis thaliana* were sterilized in 70% ethanol (v/v) for 1 minute, and in 30% household bleach (Glorix, Lever Farbergé, Netherlands) for 8 min, then washed 5 times in sterile water. Afterwards the seeds were stratified under 4°C in the dark for two days.

2.2.2 Growth of *Arabidopsis thaliana* seedlings on sterile MS medium

The *Arabidopsis thaliana* young seedlings were grown under short-day condition on MS medium (Murashige and Skoog, Duchefa, Haarlem, Netherlands) containing 0.5% (w/v) sucrose and 0.4% (v/v) phytagel.

MS medium	
MES - buffer	5 mM
Phytagel	0.4% (w/v)
MS without Vitamin [1 x]	0.43% (w/v)
Sucrose	0.5% (w/v)
Sterile water	ad. 1000 ml

2.2.3 Growth of *Arabidopsis thaliana* plants on soil

2.2.3.1 Nutrient-rich substrate

The Arabidopsis nutrient-rich substrate is a mixture of 42.4% (v/v) P type-soil (Knauf Perlite GmbH, Dortmund, Germany), 42.4% (v/v) T type-soil (Both types of soil were produced by Knauf Perlite GmbH, Dortmund, Germany) and 15.2% (v/v) perlite (Knauf Perlite GmbH, Dortmund, Germany).

2.2.3.2 Nutrient-poor substrate

The Arabidopsis nutrient-poor substrate is a mixture of 33.3% (v/v) P type-soil, 33.3% (v/v) perlite and 33.3% (v/v) vermiculite (Deutsche Vermiculite Dämmstoff GmbH, Sprockhövel, Germany).

2.2.4 Short-day and Long-day growing condition

The plants were cultivated either in a growth chamber or in a controlled environment chamber (Percival Scientific, Inc, Perry, USA) under short day conditions (10 h light, 22°C at 120 µmol photons m^{-2} s^{-1} with white light (OSRAM LUNILUX Cool White 36W) / 14 h dark, 18°C, 50% humidity). Under long-day conditions the plants were grown on soil in the green house (16 h at 120 µmol photons m^{-2} s^{-1} light, 22°C/ 8 h dark, 18°C).

2.3 Crossing of *Arabidopsis thaliana* plants

All the open flowers, buds and mature siliques were removed from the inflorescences of mother plants by a pair of fine forceps. One flower from the father plant was taken and opened. The mature anthers on this flower were rubbed onto the stigma of the emasculated inflorescence. This procedure was repeated on the next day on the same stigma which was closed in a small paper bag to prevent from fertilization by other flowers. After ripening, the siliques were harvested, and the seeds were kept at room temperature for drying. Genotyping was performed from the F1 generation to confirm the crossing. The F2 generation was used for genetic mapping.

2.4 Co-segregation analysis

To confirm the co-segregation of the low luciferase phenotype and the chlorosis phenotype, plants with chlorosis were selected from the F2 generation of the chlorotic mutant with the parental line T19-2. The seeds of chlorotic and wild type like plants were harvested. In these two groups, LUC-screen was performed on the 10 days-old seedling to calculate the ratio of the plants with low luciferase activities within the seedlings with chlorotic and non-chlorotic parents.

2.5 Phenotype analysis of the plants

The wild type plants Col-0, reporter gene line T19-2 and *rimb* mutants were grown in growth chamber and greenhouse under short- and long-day conditions respectively. The plants were photographed once a week. To quantify the rosette diameter of each line, Java-based image processing program ImageJ (http://rsb.info.nih.gov/ij/) was applied. The phenotype analysis was performed for 6 weeks.

2.6 Determination of luciferase activity *in vivo*

2.6.1 Measurement with Fluoskan Ascent FL luminometer

Luciferase reporter gene activities were determined in 10 days old seedlings separately grown on 100 µl MS medium in each well of 96-well microtiter plates. Col-0 and T19-2 were commonly included as negative and positive control lines, respectively. The seedlings were incubated in 3 mM luciferin solution (3 mM Luciferin; 0.01% (v/v) Triton X - 100) in the dark for 5 min by spraying luciferin solution onto the surface of the leaves. The luciferase activities were measured for 20 mS integration time in the Fluoroscan Ascent FL luminometer (Thermo Fisher Scientific, Dreieich, Germany). The photomultiplier tube was kept at the default setting of 828 V. The bioluminescence intensities with emission wavelength 482 nm were measured on 5 points in each well. The luciferase activity of each seedling was represented by the mean value of the luminescence-intensities of the 5 points in each well.

2.6.2 Measurement with NightSHADE LB 985 *in vivo* plant imaging system

The luciferase activities of the plants were imaged using a NightSHADE LB 985 (BERTHOLD TECHNOLOGIES GmbH & Co. KG, Bad Wildbad, Germany). The plants were incubated in luciferin for 10 min in the dark and exposed for 1 minute for imaging. Colors from blue to red on the images indicate the levels of luminescence intensities

from low to high. The activities of the reporter gene of each individual were quantified by software IndiGO.

2.7 Agarose gel electrophoresis

2.7.1 DNA Gelelectrophoresis

DNA samples were analyzed by electrophoretically on 1.2 or 4% (W/V) agarose gels depending on the fragment sizes. The agarose powder was melted in 1 x TAE buffer and supplemented with 0.5 µg m/l ethidiumbromide. The DNA samples were loaded on the gel after mixing them with 25% (v/v) DNA-loading-buffer. The electrophoresis was run at 120 V in 1 x TAE buffer for around 15 min. The DNA fragments were afterwards visualized in a UV-light box with a CCD-camera at 312 nm (INTAS, Göttingen, Germany).

TAE buffer	
Tris-acetate pH 7.5	0.8 mM
EDTA	0.02 mM

Loading buffer	
Bromophenol blue	0.05% (w/v)
Xylenecyanol	0.05% (w/v)
Glycerol	6% (v/v)

2.7.2 RNA Gelelectrophoresis

For RNA MOPS-formaldehyde agarose gels, 1.2% agarose was melted in 3-(N-morpholino) propanesulfonic acid (MOPS) buffer after cooling down to 60°C and adding 0.9% (v/v) formaldehyde. 3µl isolated RNA samples were mixed with 3 µl loading dye and 4.8 µl loading buffer. The mixture was denatured for 15 min at 65°C, then trans-

ferred on ice for *ca.* 2 min and finally loaded on the MOPS agarose gel. The RNA fragments were separated for approximately 20 min at 90 V in 1x MOPS buffer.

1x MOPS buffer	
MOPS pH 7.0	20 mM
Sodium acetate	5 mM
EDTA	1 mM

Loading buffer	
MOPS pH 7.0	3 mM
Sodium acetate	0.75 mM
EDTA	0.15 mM
Formaldehyde	6.5% (v/v)
Formamide	57.5% (v/v)
Ethidium bromide	0.12 mg/ml

Loading dye	
Bromophenolblue	0.03% (w/v)
Tris-HCl pH 7.6	10 mM
Glycerol	60% (v/v)
EDTA	60 mM

2.8 DNA isolation

2.8.1 Isolation of genomic DNA

Genomic DNA was isolated from single leaves (*ca.* 0.25 cm² leaf area), by homogenisation 200 µl REB buffer. The genomic DNA was extracted by mixing the homogenate with 200 µl phenol-chloroform-isoamyl alcohol (25:24:1). After centrifugation the upper water

phase was transferred to 200 µl isopropanol to precipitate DNA at -20°C for 30 min. The precipitate was collected by centrifuging at 20.000 x *g* for 15 min followed by washing the DNA pellet in 70% (v/v) ethanol. Finally the DNA was re-suspended in 100 µl of nuclease-free water and stored at -20°C.

REB buffer	
Tris/HCl pH 8.0	50 mM
EDTA	25 mM
Sodium chloride	250 mM
SDS	0.5% (v/v)

2.8.2 Isolation of nuclei DNA for Illumina sequencing

0.5 – 1 g of the plant tissue was ground to fine powder in liquid nitrogen and mixed with 10 ml of ice-cold Nuclei extraction buffer. The mixture was filtered through two layers of Miracloth (CalBiochem) and mixed with 2 ml Lysis buffer (10% Triton X-100 in Nuclei extraction buffer) for 2 min on ice. The nuclei DNA was pelleted by centrifugation at 4°C and at 2000 x *g*, then re-suspended in 500 µl CTAB extraction buffer followed by incubation at 60°C for 30 min. The mixture was cooled down at room temperature for 5 min. The nuclei DNA was separated from protein solution by mixing 350 µl chloroform/ isoamyl alcohol (24:1). After centrifugation at 4629 x *g* for 10 min the upper phase was collected and mixed with 400 µl isopropanol to precipitate the DNA. By centrifugation at 13000 rpm for 3 min the DNA was pelleted and then washed with 75% (v/v) ethanol. The nuclei DNA was dissolved in 50 µl of nuclease-free water and incubated at 65°C for 30 min to deactivate any DNases, and stored at -20°C.

CTAB extraction buffer	
1M Tris-Cl pH 7.5	100 mM
5M Sodium cholride	0.7 M
0.5 M EDTA	10 mM
BME (2-Mercaptoethanol)	1% (v/v)
CTAB	1% (v/v)
d. Water	

Nuclei extraction buffer	
TRIS-HCl pH 9.5	10 mM
EDTA pH8.0	10 mM
Potasium chloride	100 mM
Sucrose	500 mM
Spermidine	4 mM
Spermine	1 mM
Beta-mercaptoethanol	0.1% (v/v)

2.8.3 Testing the quality of isolated DNA

The concentrations and qualities of DNA were spectrophotometrically evaluated by using NanoPhotometer (Implen, Munich, Germany) in which the absorbances at 260, 280 and 230 nm were measured, indicating the contents of nucleic acids, proteins and other contaminations respectively. The ratios of A260/A280 and A260/A230 were calculated to evaluate the purity of the isolated DNA. The ratios should be over 1.8 and in the range of 2.0 to 2.2, respectively. Furthermore DNA samples were also run in 1.2% agarose gel to test the quality the DNA.

2.9 RNA isolation

2.9.1 Isolation of RNA from the plant material

Around 10 10-day old seedlings of *Arabidopsis thaliana*, which were grown on MS plates, were harvested and frozen immediately in liquid nitrogen. All the plant material was pulverized by using a Retsch Ball Mill (Retsch GmbH, Haan, Germany) at a frequency of 30/s for 60 seconds. The total RNA was isolated by using the GeneMATRIX Universal RNA Purification KIT (EURx, Gdansk, Poland) according to the manufacturer's instructions. The principle of this total RNA isolation kit is based on specific binding of RNA to a silica-gel-membrane under high salt conditions. The cell debris, proteins and most of the DNA were removed by subsequent washing steps. The rest of DNA on the membrane was digested by DNAse. The total RNA was finally eluted in the provided elution buffer and stored at -20°C.

2.9.2 Testing the quality of isolated RNA

The concentration and quality of the isolated RNA were spectrophotometrically analyzed using the NanoPhotometer (Implen, Munich, Germany). For RNA, the ratios of A260/A280 and A260/A230 should be over 2.0 and in the range of 2.0 to 2.2, respectively. To finally confirm the RNA quality, the samples were separated in 1.2% MOPS-formaldehyde agarose gel and analyzed by INTAS gel documentation system. Only samples, which showed sharp RNA bands, were used for further analysis.

2.10 Polymerase chain reaction (PCR)

The primers were designed with online primer designer Primer3 (http://frodo.wi.mit.edu) and synthesized by Sigma-Aldrich Chemie GmbH (Munich, Germany). The primers were dissolved at final concentration of 100 mM and stored at -20°C

2.10.1 Standard PCR

Polymerase chain reaction (PCR) was performed on a Flexibler PCR Thermocycler (Analytika Jena, Germany) with standard protocol-0 of PCR reaction for 20 µl shown in Table 2-1. The heat-stable *Taq* polymerase, which was hetrologously expressed in *E.coli* and isolated, was applied to catalyze the reaction, and the annealing temperatures were according to the melting temperature (T_m) of the gene specific primers.

10x PCR buffer	
Tris/HCl pH 8.4	200 mM
KCl	500 mM
$MgSO_4$	15 mM
$MgCl_2$	1.5 mM

Table 2-1: general PCR reaction system and conditions

PCR reaction system		PCR conditions			
10x PCR buffer	2µl	Pre-denaturartion		95°C	3 min
Primer Forward	0.2 mM		Denaturation	95°C	1 min
Primer Reward	0.2 mM	35 cycles	Annealing	54°C to 60°C	1 min
dNTPs	2 mM		Extension	72°C	1 min
DNA template	5 mM	Extension		72°C	15 min
Taq polymerase	1U	Incubation		4°C	

2.10.2 PCR with Opti*Taq*

To amplify the PCR products over 2 kb the Opti*Taq* polymerase (EURx, Gdansk, Poland) was used. The protocol-0 of the PCR reaction with Opti*Taq* for 50µl is shown in Table 2-2, in which annealing temperature was according to the T_m of primers and extension time is adjusted to the size of the products (one minute per kb length).

Table 2-2: PCR reaction system and conditions of Opti*Taq*

PCR reaction system		PCR conditions			
10x Pol Buffer C	5µl	Pre-denaturartion		95°C	2 min
$MgCl_2$	3.5 mM		Denaturation	95°C	30 sec
Primer Forward	0.2 mM	35 cycles	Annealing	54°C	30 min
Primer Reward	0.2 mM		Extension	72°C	1 min/1kb
dNTPs	0.2 mM	Extension		72°C	7 min
DNA template	5 mM	Incubation		4°C	
Opti*Taq* polymerase	1.25 U				

2.11 Sequencing of PCR fragments and plasmids

The PCR fragments and plasmids were sequenced by GATC Biotech AG (Konstanz, Germany) and Eurofins WMG Operon (Ebersberg, Germany) using ABI 3730xl system.

2.11.1 Sequencing of PCR fragments

After an electrophoresis on a 1.2% agarose gel for quality check the PCR fragments were purified by using Invisorb® Spin DNA Extraction Kit (STRATEC Molecular, Berlin, Germany) according to the manufacturer's instructions. The PCR products binding on the silica membrane were eluted in 30 µl provided elution buffer, while all the other compounds in the PCR reaction were washed out. Together with the specific primers the purified fragments were sent the company for sequencing.

2.11.2 Sequencing of Plasmids

PCR fragments were cloned into pCR2.1 – TOPO vector (Figure 2-1, Invitrogen, Carlsbad, USA). The plasmids were transformed into chemically competent cells DH5α *E. coli* (prepared in our lab) and isolated with GeneMATRIX Plasmid Miniprep DNA Purification Kit (Roboklon GMBH, Berlin, Germany) and sequenced. Primers M13 forward and reward were applied for sequencing the insertion.

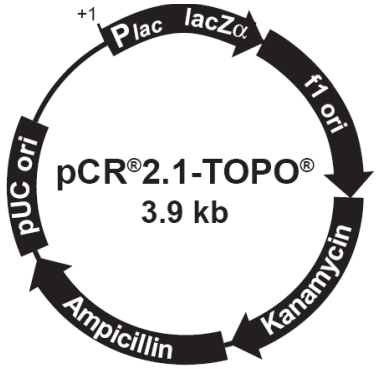

Figure 2-1: Map of pCR2,1-TOPO vector (Invitrogen, Carlsbad, USA). pUC ori: pUC origin of replication; P*lac*: lac promoter; *Lac*Zα: *Lac*Zα fragment; f1 origin: F1 *phage* origin of replication; Kanamycin: Kanamycin resistance gene; Ampicilin: Apmpicilin resistance gene (Invitrogen, Carlsbad, USA).

2.11.3 Sequence analysis

The sequencing results were obtained as regular text and AB1 files, which could be operated by using GATCviewer[tm] (GATC Biotech AG, Konstanz, Germany). The sequences were aligned using two online BLAST tools: Multiple sequence alignment of INRA (http://multalin.toulouse.inra.fr/multalin) (Corpet, 1988) and Clustal Omega - Multiple Sequence Alignment of EMBL-EBI (http://www.ebi.ac.uk/Tools/msa/clustalo).

2.12 Sequencing with Illumina system

Sequencing of *Arabidopsis* genomic DNA with Illumina G2 Analyzer and HiSeq2000 system was performed by Dr. Rowan Beth in collaboration with the group of Prof. Dr. Detlef Weigel (Max Planck Institute for Developmental Biology, Tübingen, Germany).

Before sequencing, the quality of the DNA solution was checked by Qubit® Fluorometer (Life Technologies GmbH, Darmstadt, Germany) and by electrophoresis in a 1.2% (w/v) agarose gel. From the equally pooled DNA samples 1.6 µg of DNA were used for sequencing. The DNA was divided into 4 samples of 400 ng for indexing. Paired-end libraries were prepared with an insert size between 200 – 500 bp. The samples were se-

quenced with 2 x 100 bp reads in the lane of illumina Analyzer. The sequencing processes were culminated in one lane of an Illumina G2 Analyzer with over 30 million raw reads, which covered the *Arabidopsis thaliana* genome 19 times. By using 1/4 of a lane of Hi-Seq 2000 Analyzer the sequencing was ended up with 80 million raw reads covering the *Arabidopsis thaliana* genome 57 times

2.13 Gene expression analysis

2.14 First strand cDNA synthesis

The first strand cDNA was synthesized from total RNA by using High-Capacity cDNA Reverse Transcription Kits (Applied Biosystems, Carlsbad, USA). The reaction was set up with 2 µl 10x RT Buffer, 2 µl 10x random primers, 0.8 µl dNTP mix(100mM), 1 µl MultiScribe^{tm} Reverse Transcriptase and 4.2 µl nuclease-free water in 10 µl reaction system without RNase according to the suppliers recommendations. The synthesized cDNA was stored at -20°C. The reaction conditions are listed in Table 2-3.

Table 2-3: Thermal cycling conditions for reverse transcription

Reaction step	Temperature [°C]	Time [m]
Step 1	25	10
Step 2	37	120
Step 3	85	5
Step 4	4	

2.14.1 Expression Analysis

Reverse transcription quantitative PCR (qRT PCR) was performed to analyze the transcript level of genes of interest.

2.14.1.1 Primer design

The primer pairs for quantitative real-time PCR were designed with desired Amplicon size (60 to 80 bp) on the ‘‘primer design tool for high-throughput qPCR’’ QuantPrime (http://www.quantprime.de). The optimal annealing temperature for each primer pair was determined to ensure the primers binding to their targets efficiently and to prevent both non-specific annealing and primer-dimer formation. Furthermore the primers were designed to span exon–intron borders, to amplify only cDNA from mRNA gene transcripts, but not genomic copies.

The specificities of the primers pairs were verified by analyzing the melting curve of the reaction products and additionally by running PCR products on an agarose gel. Only the primer pairs which had a single peak in the melting curve, corresponding to the single band on the agarose gel, were selected in qPCR reaction. (See primers in Appendix)

2.14.1.2 Reverse transcription quantitative PCR (qRT-PCR)

Analysis of qRT-PCR was performed on a CFX96 thermocycler (BioRad, Hercules, USA) using SYBR Green QPCR Master Mix (Agilent Technology, Santa Clara, USA). The optimal annealing temperature was determined to 60°C, while the efficiency of amplification was verified for each primer pair in a qRT-PCR reaction, which was performed for 10-fold dilution series of respective cDNA sample. The reaction system and the condition are shown in Table 2-4.

Table 2-4: qRT-PCR reaction system and conditions:

qRT-PCR reaction system (10µl)		qRT PCR conditions			
2X SYBR® Green PCR		Pre-denaturartion		95°C	10 min
Master Mix	5µl		Denaturation	95°C	30 sec
Primer Forward	0.2 mM	40 cycles	Annealing	60°C	30 sec
Primer Reward	0.2 mM		Extension	72°C	30 sec
DNA template	5 mM	Post-denaturartion		95°C	10 sec
		Melting Curve test 65°C to 95°C		Increment 0.5°C 5 Sec	

The fluorescent dye SYBR Green preferentially binds to double-stranded DNA and emits a characteristic fluorescence at 585 nm after excitation with 470 nm. The fluorescence signals were read and collected at end of each annealing and extension steps to monitor the melting kinetics of the PCR product. Melting curve tests were performed at the end of the program with gradient temperature from 65°C to 95°C to test the purity of the used buffers and solutions to assess for primer dimer formation with non-template control. Afterwards the cDNA amounts were calculated by the software Bio-Rad CXF manager 2.1 with the equation $\mathrm{R} = 2^{-[\Delta\mathrm{Ct\ sample} - \Delta\mathrm{Ct\ reference}]}$. The expression ratio $\mathrm{R} = 2^{-\Delta\Delta\mathrm{Ct}}$ is based on a statistical real-time PCR efficiency of 2 and with the differences (Δ) of threshold value (Ct) of samples and reference gene.

The cDNA of wild type plants was included as positive control. All reactions were performed for three technical replicates and three biological replicates representing an independent RNA isolation. Transcript levels of the target genes were normalized to the respective transcript level of *Act7* gene (At5g09810) as reference gene.

2.15 Genetic mapping of mutant loci with Single Sequence Length Polymorphisms (SSLP)

The mutant lines, which were generated by EMS mutagenesis on *Arabidopsis thaliana* accession Col-0, were crossing to another accession L*er* (Heiber and Baier 2007). The plants of the segregating F2 population were screened for low luciferase activity and the SSLP genetic mapping was performed on the selected individuals with mutant alleles.

2.15.1 Determination of individuals with mutant alleles from the segregating F2 population

Seedlings growing on MS medium with 0.5% (w/v) sucrose on 96-well microtiter plates were screened for luciferase activity (See chapter 2.6.1). T19-2 was included as positive control line and the luciferase activities of each seedling relative to T19-2 were calculated. About 25% of the individuals were considered as individuals with mutant alleles, which cause the luciferase activities of the plants between positive control (T19-2) and negative control (Col-0), and they were selected for further mapping. All that individuals for mapping were transferred onto soil and grown further in green house.

2.15.2 SSLPs markers design using Cereon database

SSLPs markers were applied in genetic mapping, with which the genetic backgrounds were distinguished between *Arabidopsis thaliana* accession Col-0 and L*er* based on the In/Del polymorphisms (Jander et al., 2002). All the SSLPs markers were designed based on the database of the Cereon/Monsanto Arabidopsis Polymorphism Collections (http://www.arabidopsis.org/browse/Cereon/). The primers were designed to target both sides of the flanking sequence of the SSLPs, which represent Indel polymorphisms between Col-0 and L*er* around 20 bp. The desired PCR product lengths were about 200 bp.

2.15.3 Mapping analysis of the mutant loci with SSLPs markers

To cover the *Arabidopsis thaliana* genome 25 SSLPs markers were applied, 30 F2 plants with low luciferase activity were selected for the first round of genetic mapping. For each marker PCR was performed with the genomic DNA of the 30 plants as templates, and genetic DNA of Col-0*,* L*er* and 1:1 mixture of Col-0 and L*er* DNA were also included as references templates. PCR products were electrophoretically separated on 4% (w/v) agarose gels to determine size differences between Col-0 and L*er* DNA templates.

The linkage of each marker was calculated with the equation for the recombination frequency shown below:

$$recombination\ frequency\ in\ centiMorgen = \frac{number\ of\ recombination\ events}{total\ number\ of\ offsprings} * 100$$

According to the linkage values across the genome, the region of interest with highest allele frequency of Col-0 alleles was determined. More SSLPs markers on this region were applied to search the marker with highest Col-0 allele frequency that represents the position of mutant locus. To confirm the functions the final loci, the transcript analysis was performed then with T-DNA insertion knock-out lines.

2.16 Genetic mapping of mutant loci with next generation sequencing

The segregating F2 population were imaged by NightSHADE LB 985 and screened for low luciferase activity followed by screening for mutant phenotype. Individuals with mutant alleles were selected and pooled to isolate nuclei DNA for Illumina sequencing. The nuclei DNA was sequenced on either Illumina GII analyzer or Hi-Seq 200 Analyzer.

2.16.1 Analyses of the Illumina sequencing results with ShoreMap

Software package ‘‘SHOREmap’’ (Schneeberger et al., 2009) was applied to analyze the deep sequencing data. The reads for the mapping population were separated by using ‘‘SHORE import’’ with the demultiplexing option and aligned to the sequence of accession Col-0 by using ‘‘SHORE mapflowcell’’. The paired-end information was corrected by ‘‘SHORE correct4pe’’ and the files from the first and second read were merged by using ‘‘SHORE merge’’. After consensus lists of polymorphisms (SNPs and small Indels) were obtained with ‘‘SHORE consensus’’ option, consensus subsets of marker positions between the mapping population and L*er* marker list of Weigel’s lab were finished. The ‘‘SHOREmap_interval.pl’’ was applied to plot the allele frequency of Col-0 alleles across the *Arabidopsis thaliana* genome with different windows sizes. All known L*er* markers were excluded from the SNP list for the mapping population. The remaining SNPs should represent EMS-induced mutations in the Col-0 background. The new SNPs were annotated to identify the candidate mutations.

2.16.2 Confirmation of the final candidate locus

After identification of the final candidates, the new SNPs of the mutant lines and the sequence of the same locus in T19-2 were re-sequenced with Sanger sequencing method to confirm the results of Illumina sequencing. To confirm the functions of the final loci, the transcript analysis was performed with T-DNA insertion knock-out lines.

2.17 Genotyping and isolation of homozygous T-DNA insertion lines by PCR

Primers for genotyping of the T-DNA insertion lines were designed by the ‘‘iSect Toolbox’’ (http://signal.salk.edu/tdnaprimers.2.html) in the way to span insertion border. Information about the common border-primers of insertion sequence was obtained from

the providers of the T-DNA lines providers.

For genotyping of the T-DNA insertion lines, two PCR reactions were performed: the primers of flanking sequence were applied for the first PCR, while a primer targeted to the insertion and one of the primers of flanking sequence were used in the second PCR. Only products of insertion sequence could be amplified from the homozygous T-DNA insertion lines, while from wild type and heterozygous lines products of genomic DNA were amplified. In this way the homozygous T-DNA insertion lines were selected, and their progeny were used in further analysis as knock-out/down lines.

2.18 *Escherichia coli* manipulations

2.18.1 Generation of chemically competent *E. coli*

Escherichia coli strain DH5α was grown in 5 ml LB medium overnight at 37°C with agitation at 200 rpm. Afterwards the culture was enlarged to 100 ml LB with the 5 ml prepared pre-culture till OD600 had reached 0.4 to 0.6. After the culture was chilled on ice for 10 min, the cells were harvested by centrifugation at 1600 x *g* for 7 min at room temperature. The pellet was resuspended in 5 ml ice-cold $CaCl_2$ medium, composed of 60 mM $CaCl_2$, 10 mM Pipes, 15% (v/v) glycerol and adjusted with KOH to pH 7.0. The cells were harvested then by centrifugation at 1600 x *g* for 7 min at room temperature. The pellet was again resuspended in 2 ml ice-cold $CaCl_2$ medium and distributed into 1.5 ml tubes with 100 µl in each. The competent *E. coli* cells were immediately frozen in liquid nitrogen and stored at -80°C.

Lysogeny Broth (LB) medium	
Tryptone	1% (w/v)
Yeast extract	0.5% (w/v)
NaCl	1% (w/v)

2.18.2 Plasmid transformation into *E.coli*

The plasmids were transformed into chemically competent DH5α *E. coli* strain by heat shock. The plasmid was mixed with the DH5α cells that were thawed on ice. After incubation on ice for 30 min, the cells were heated to 42°C for 40 seconds and immediately transferred onto the ice and cooled down for 2 min. Afterwards the cells were recovered in 200 µl LB liquid medium at 37°C for 1 h. Positive transformants harboring recombinant plasmids were selected on LB medium plate containing the appropriate antibiotics overnight at 37°C and grown in liquid LB medium for further analyses.

2.19 Plasmid manipulation

2.19.1 Purification of PCR products from agarose gel

Gel slices containing the PCR fragments of interest were cut out of the agarose gel under UV light. Afterwards the DNA fragments were extracted from the gel using the Invisorb® Spin DNA Extraction Kit (STRATEC Molecular, Berlin, Germany) according to the manufacturer's instructions. The DNA was harvested by melting the agarose gel slices in salt buffer and bound to a silica membrane. After wash steps the DNA was eluted in the provided elution buffer.

2.19.2 Cloning into entry vector (PCR8/GW/TOPO)

The purified PCR products were cloned into vector pCR®8/GW/TOPO® (Figure 2-2, Invitrogen, Carlsbad, USA) according to the manufacturer's instructions. The orientation of the inserted sequences in pCR®8/GW/TOPO® was determined by restriction digestion, in which one of the enzymes was cutting the insert and another was cutting the pCR®8/GW/TOPO® backbone. Fast-digestion enzymes were applied to digest 1 µg plasmid DNA in 20 µl reaction system at 37°C for 30 min. The digested fragments were

run on agarose gel electrophoresis and visualized under UV light. The insertion sequence and its orientation were additionally verified by single read sequencing.

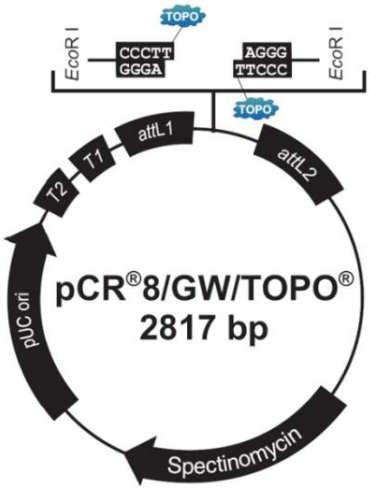

Figure 2-2 Map of pCR8/GW/TOPO vector (Invitrogen, Carlsbad, USA). Spectinomycin: Spectinomycin resistance gene (SpnR); pUC ori: pUC origin of replication; T2/T1: *rrnB* T2 and T1 transcription termination sequences to prevent basal transcription of the PCR product of interest in *E. coli*; *attL1* / *attL2*: sites for recombination-based transfer of the gene of interest into a Gateway® destination vector (Invitrogen, Carlsbad, USA).

2.19.3 Confirmation of the insertion with colony PCR

At least 10 colonies were selected for colony PCR with a pair of insertion specific primers. The PCR conditions for 20 µL reaction system are listed below (Table 2-5). After an electrophoresis in agarose gel, only the reactions with the colonies containing the right insert could show a product with appropriate size.

Table 2-5: Colony PCR

PCR reaction system		PCR conditions			
10x *PCR* buffer	2µl	Pre-denaturartion		95°C	10 min
Primer Forward	0.2 mM		Denaturation	95°C	1 min
Primer Reward	0.2 mM	35 cycles	Annealing	54°C	1 min
dNTPs	2 mM		Extension	72°C	1 min
DNA template	colonies	Extension		72°C	15 min
Taq polymerase	1U	Incubation		4°C	

2.19.4 Isolation of plasmids using miniprep kits

The colonies containing the recombinant vectors were grown in 5 ml Lysogeny Broth (LB) medium containing the appropriate antibiotics and incubated at 37°C overnight by shaking. The plasmids were isolated with GeneMATRIX Plasmid Miniprep DNA Purification Kit (Roboklon GMBH, Berlin, Germany). The plasmid DNA was bound to silica membrane, while the RNA, proteins and other substrate of the cells were washed out by set of washing buffers. The plasmid DNA was eluted in provided elution buffer and stored at -20°C. Finally the insertion of the isolated plasmids was verified by sequencing with primer M13 forward (see Appendix).

2.19.5 LR reaction

The binary vector pHGWL7.0 was used for Gateway® recombination cloning reaction (Karimi et al., 2002). The insertion, flanked by two attL sites in the entry clone pCR®8/GW/TOPO®, was transferred by LR clonase mix into a destination vector pHGWL7.0 carrying two attR sites (Karimi et al., 2002). As a result, luciferase is under the control of the inserted promoter sequence. The sequence containing a *ccd* B lethal gene was exchanged into entry vector and as consequence the growth of clones bearing entry vector was hindered. Moreover, since entry vector pCR®8/GW/TOPO® and destina-

tion vectors pHGWL7.0 (Figure 2-3) have resistance to the same antibiotic, the pCR8®/GW/TOPO® vector was double digested with Psp1406I and EcoRV leading to a fragment containing the inserted promoter sequence flanked by the attL1 and attL2 recombination sites. This approach was to prevent survival of the colonies containing the entry vector pCR8®/GW/TOPO® after the LR recombination reaction.

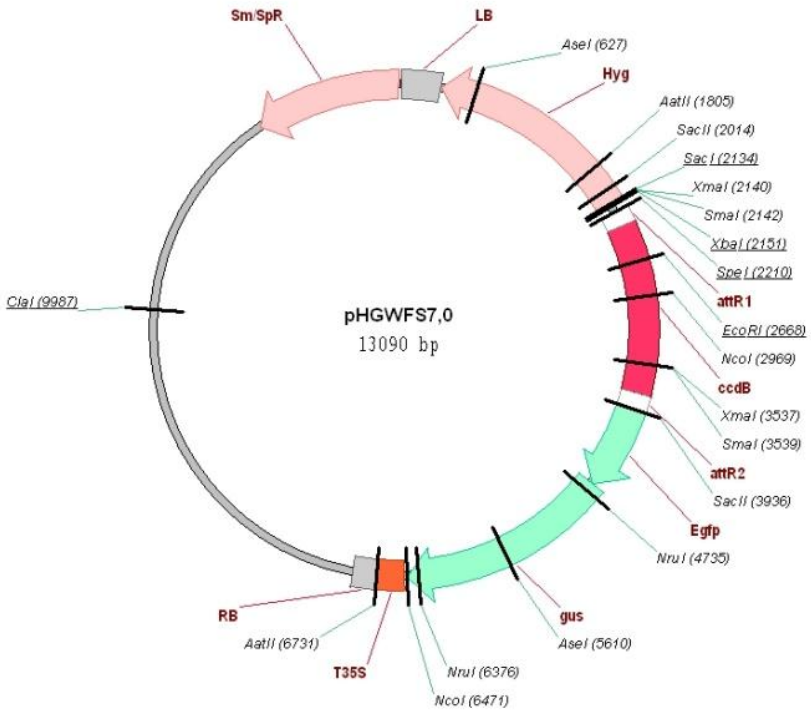

Figure 2-3: map of pHGWFS vector. Sm/SpR: gene which mediates streptomycin-spectinomycin resistance to *E. coli* and *Agrobacteria*; LB: left border of T-DNA; Hyg: plant selectable marker gene which mediates hygromycin B resistance under transcriptional regulation of the nopaline synthase (*nos*) promoter and *nos* terminator; *attR1*/ *attR2*: sites for recombination-based transfer of the gene of interest from any Gateway® entry vector containing *attL1*/*attL2* sites generating *attB1*/*attB2* sites; *ccd*B: F plasmid-encoded gene that inhibits growth of *E. coli* without insert; *Egfp*: enhancer green fluorescent protein reporter gene; *gus*: β-glucuronidase reporter gene, frame fusion with *Egfp* coding region; T35S: 35S terminator; RB: T-DNA right border (Karimi et al., 2002).

The LR reaction was performed using LR Clonase II enzyme mix kit (Invitrogen, Carlsbad, USA) in a 5 µl reaction system with 75 ng linearized entry vector, 75 ng pHGWL7.0 plasmid and 0.5 µl LR Clonase II enzyme mix filled up with TE buffer (pH 8.0). The mix-

ture was incubated at 25°C overnight, followed by termination step with 1 µl proteinase K solution at 37°C for 10 min.

After the LR reaction, the plasmids were transformed into DH5α *E. coli* strain. Positive transformants were selected on LB plates containing 100 µg/ml spectinomycin. The cloning success was verified by testing isolated freshly grown colonies by colony PCR and restriction digestions. The positive ones were grown overnight in 5 ml LB medium at 37°C with agitation at 200 rpm overnight. Afterwards the plasmids were sequenced with a border primer binding at the flanking sequence of the insertion for final confirmation (GATC Biotech, Konstanz, Germany).

2.20 *Agrobacterium tumefaciens* manipulations

2.20.1 Production of competent *A. tumefaciens* cells

Agrobacterium tumefaciens strain GV3101(pMP90) was cultivated in 10 ml YEB medium containing rifampicin (100 µg/ml) and gentamycin (25 µg/ml) and incubated overnight at 28°C and with agitation 180 rpm. From this culture 2 ml were transferred into 50 ml YEB medium containing the appropriate antibiotics and incubated with agitation at 28°C and 180 rpm until OD600 reached at least 0.5.

YEB medium	
Bacto Peptone	5 g /l
Yeast extract	1 g/l
Beef extract	5 g/l
Sucrose	5 g/l
$MgSO_4$ x 7 H_2O	0.5 g/l

After the culture was cooled down to 4°C, the cells were harvested by centrifugation at 5.000 x *g* and 4°C for 5 min. The pellet was resuspended in 1 ml 20 mM $CaCl_2$ and divided into 0.2 ml Eppi tubes and stored at -20°C.

2.20.2 Transformation of *A. tumefaciens*

The freeze-thaw method (Weigel D, 2002) was applied to transform *Agrobacterium tumefaciens* strain GV3101(pMP90). 0.2 ml competent cells and 1 µg plasmid DNA were mixed and incubated for 15 min on ice. Afterwards the cells were frozen in liquid nitrogen for 5 min followed by incubation at 37°C for 5 min. After adding 1 ml YEB medium the cells were incubated for 2 to 4 hours at 28°C. The cells were plated on YEB plates containing 1.5% (w/v) agar, rifampicin (150 µg/ml), gentamycin (25 µg/ml) and spectinomycin (50 µg m/l), and incubated at 28°C for 2 days. Colonies were plated on a fresh YEB plate and incubated at 28°C for 24 hours before transformed Agrobacteria were used for plant transformation.

2.21 Comparison and analysis of promoters in plants

Promoter analysis was performed to check the effects of the natural variation in promoters of different accessions on expression of gene of interest.

2.21.1 Analysis of the promoter sequences in Col-0 and L*er*

Sequences of 2 kb upstream start codon were analyzed to study the promoters. The promoter sequence of gene of interest was obtained with sequence viewer in TAIR (http://www.arabidopsis.org/servlets/sv?action=closeup) (Swarbreck et al., 2008). The polymorphism between Col-0 and L*er* was thoroughly checked by using Cereon database (http://www.arabidopsis.org/browse/Cereon/), and the polymorphism was confirmed again by checking Arabidopsis SNP viewer (http://signal.salk.edu/perlegen.html).

2.21.2 Transient gene expression

The promoter sequences of gene of interest were cloned into vector pHGWL7.0 for transient gene expression.

2.21.2.1 Preparing Agrobacterium suspension for infiltration

In this study the p19 coexpression system (Voinnet et al., 2003) was applied to prevent subsequent gene silencing in plant cell. *Agrobacterium tumefaciens* strain GV3101(pMP90) carrying the constructs p2CPACol-0:LUC, p2CPAL*er*:LUC and strain GV3101(pMP90) carrying the 35S CaMV driven p19 protein of tomato bushy stunt virus were inoculated in 10 ml YEB medium containing the appropriate antibiotics (GV3101(pMP90):rifampicin 100 µg m/l, gentamycin 25 µg m/l; p19 protein: kanamycin 100 µg m/l; pHGWFL7.0: spectinomycin 100 µg m/l) and incubated with agitation at 28°C until OD600 reached at least 0.5. For co-infiltrations, both Agrobacteria cultures were mixed with each other according to the ratios shown below:

$$V_{construct}=V_{final}*0.5/OD_{600} \quad \text{and} \quad V_{P19}=V_{final}*0.3/OD_{600}$$

(V_{final} was 30ml per petri dish)

Cells were harvested by centrifugation at 3000 x *g* at room temperature for 8 min and resuspended in activation buffer (100 mM MES pH 5.6, 10 mM $CaCl_2$ and 150µM acetongsyringon). The agrobacterial suspension was incubated in the activation medium for at least 2 hours at room temperature and then infiltrated into the leaves of 10 days seedling of *Arabidopsis thaliana*.

2.21.2.2 Infiltration of *Arabidopsis* leaves and LUC screening

10 days-old seedlings of *Arabidopsis thaliana* grown on 96 well microtiter plates were used for infiltration. 150 µl of the agrobacterial suspension were added to each well. A desiccator was applied to infiltrate the agrobacterial suspension into the plant leaves for 90 seconds and it was repeated 6 times. The infiltrated plants were transferred onto the MS medium containing 500 mg/l cefotaxim and incubated for 2 days followed by LUC screen with NightSHADE LB 985. T19-2 was used as positive control, while the plants infiltrated with only activation buffer were used as negative control in this experiment.

2.22 Metal content analysis

Plants were grown on nutrient-rich and nutrient-poor soil in growth chamber under short-day condition for 5 weeks. The rosettes were harvested and frozen in liquid nitrogen after determination of the fresh biomass. All plant materials were thoroughly ground to fine powder. Contents of metal elements in the plant materials were measured with inductively coupled plasma mass spectrometry (ICP-MS) in collaboration with the group of Prof. Ute Krämer (Ruhr University Bochum).

2.23 Coexpression analysis and function prediction

In this study, Arabidopsis eFP Browser (http://bar.utoronto.ca/efp/cgi-bin/efpWeb.cgi) (Winter et al., 2007; Patel et al., 2012) was applied to check the specific gene expression pattern in different parts of *Arabidopsis thaliana* at different developmental stages, accessions, and under different treatments and stresses. Based on results of microarray as well as experiments under wide range of conditions, the database gives an graphical expression map with different colors indicating different levels of expression of a specific gene.

In terms of coexpression's data, the relationships of expression of all the genes of interest were studied by using database Genevestigator for plant biology (https://www.genevestigator.com/gv/plant.jsp), which is a database and web-browser data mining interface for Affymetrix Gene Chip data that was generated based on transcripts studies of plant science (Zimmermann et al., 2004; Zimmermann et al., 2005; Laule et al., 2006).

Predictions of protein–protein interactions and functions of genes of interest were performed with database Genemania (http://www.genemania.org), which provides possible information of coexpression, predicted functions, physical interactions shared protein

domains, co-localization and genetic interaction of the investigated genes based on the published literature (Mostafavi et al., 2008; Warde-Farley et al., 2010).

2.24 Analysis of amino acid sequences and protein structures

The DNA sequences were translated into amino acid sequences by using EMBOSS Transeq (http://www.ebi.ac.uk/Tools/st/EMBOss_transeq/), an online nucleic acid sequences translating tool of EMBL-EBI (Rice et al., 2000; Goujon et al., 2010). Amino acid sequences were submitted to the online alignment-based modeling tool SWISS-MODEL (http://swissmodel.expasy.org) (Guex and Peitsch, 1997; Arnold et al., 2006; Kiefer et al., 2009) to predict the 3 D structures that were displayed by using the Swiss-pdbViewer DeepView 4.1 (http://swissmodel.expasy.org/spdbv). The alignments of the sequences for conserved domains were performed by using Conserved Domain Database (CDD) on NCBI (http://www.ncbi.nlm.nih.gov/cdd) (Marchler-Bauer et al., 2011; Marchler-Bauer et al., 2013).

3 Results

To study the regulation of 2CPA expression in *Arabidopsis thaliana*, a homozygous p2CPA:Luc reporter gene line (T19-2) was generated in the background of Arabidopsis accession Col-0 (Baier et al., 2004). By screening the EMS mutagenized reporter gene line for low luciferase activity, seven mutant lines (*r*edox *im*balanced-*rimb*) were isolated, of which five lines showed limitations in redox-box regulation of the 2CPA promoter (Heiber et al., 2007). In the present project *rimb3* and *rimb6* were chosen to investigate the gene regulation in the central chloroplast-to-nucleus signaling pathway (Heiber et al., 2007).

3.1 Phenotypic characterization of *rimb3* and *rimb6* mutants

In order to study the function of the loci RIMB3 and RIMB6, the loss-of-function mutant *rimb3* and *rimb6* were first phenotypically characterized. The plants of *rimb3* and *rimb6* were smaller in rosette diameter, leaves shape, e*t cetera*. Phenotype of *rimb6* was dependent on supplemented mineral nutrients availability (Hiltscher, 2011). Here, the mutant lines *rimb3* and *rimb6* were re-characterized to check low induction of 2CPA expression and secondary phenotypes under the growth condition at Freie Universität Berlin.

3.1.1 Growth habits of the mutants

Under both short-day (10h at 120 µmol photons m^{-2} s^{-1} light/14h dark) and long-day (14h light/8h dark) conditions the *rimb3* and *rimb6* mutants were severely impaired in growth

(Figure 3-1). They exhibited smaller rosettes in comparison to the parental line T19-2 under short- and long-day conditions.

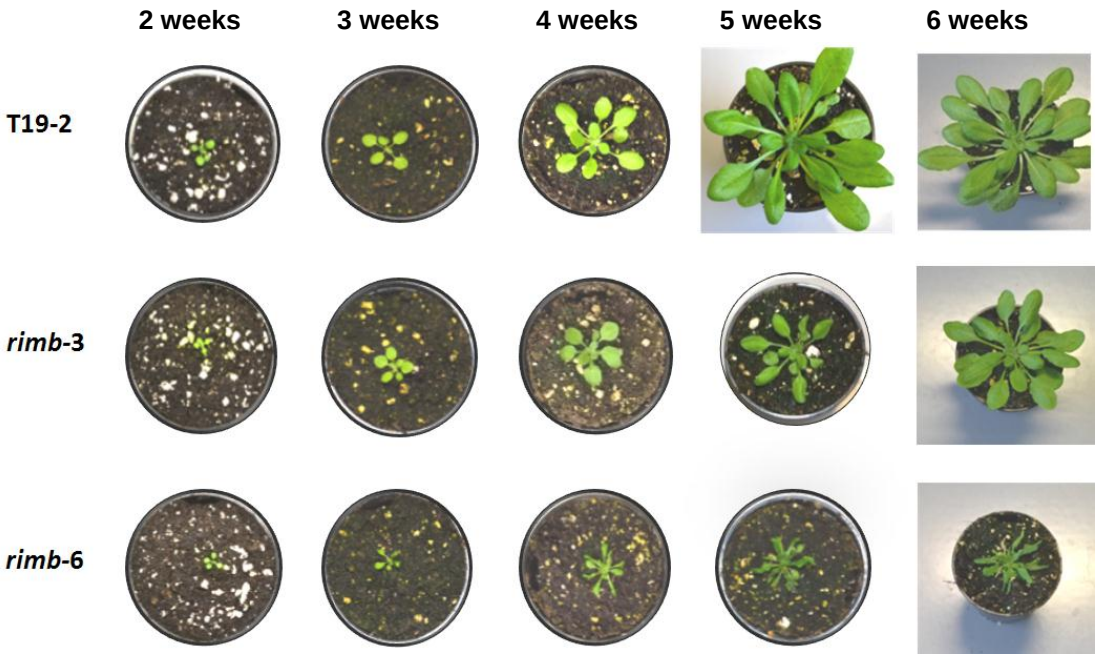

Figure 3-1: The phenotype of T19-2, *rimb3* and *rimb6* under short-day condition. The disturbed growths of *rimb3* and *rimb6* were disturbed likely due photooxidative damage to the chloroplasts.

From two weeks onwards the two mutants grew slower than the parental line T19-2 (Figure 3-1). Moreover the mutant plants displayed smaller rosette diameters than of T19-2 plants. Under short-day condition the rosette diameters of the plants of *rimb3* reached only approximately 60% of the rosette diameters of T19-2 at all the developmental stages (Figure 3-2). The plants of *rimb6* grew in a similar way to *rimb3* in the first four weeks, but afterwards the growth of *rimb6* was slowed down: the rosette diameters of five weeks-old plants of *rimb6* were only 33% relative to the rosette diameters of T19-2 and the rosettes of *rimb6* at the sixth week were 27% of rosettes of T19-2.

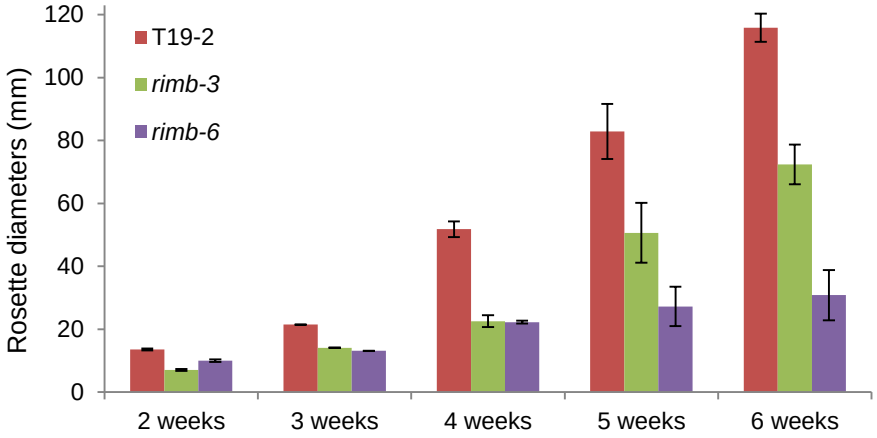

Figure 3-2: Rosette diameters of *rimb3* and *rimb6* of five weeks: rosette diameters of *rimb3* and *rimb6* were clear smaller than the control line T19-2. The data are means of 8-10 parallels.

In *rimb3* plants older than four weeks, chlorosis developed frequently on old leaves under long-day condition (Figure 3-3), potentially indicating that the disturbed growth of *rimb3* plants correlates with photooxidative damage to the chloroplasts (Heiber et al., 2007).

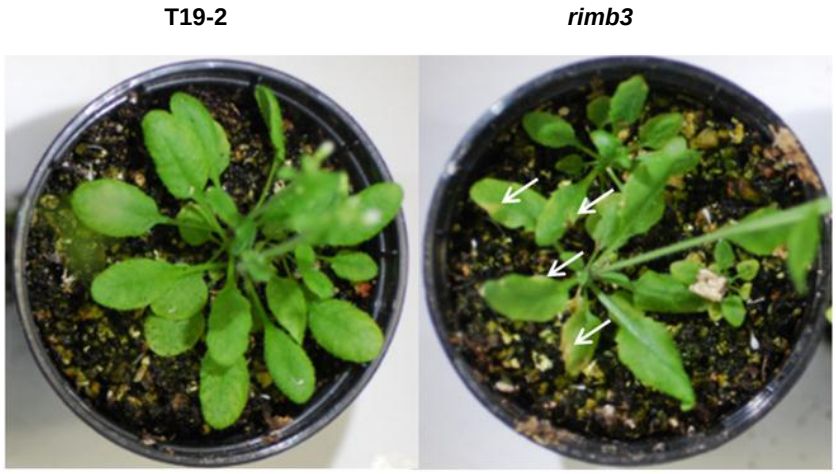

Figure 3-3: Phenotype of *rimb3*. *Rimb3* showed chlorosis phenotype randomly under long-day condition (shown with white arrows) and the shapes of the mature leaves were abnormal. It indicated that the mutant plants were under photooxidative stresses.

The growth of *rimb6* was also severely defective in rosettes diameters. From four weeks onwards under short day conditions, the plants of *rimb6* demonstrated a dwarf stature.

The leaves were narrow and curled due to oxidative stress. Meanwhile the shooting time of the mutant plants were delayed (data not shown). Moreover, it was observed, that in *rimb6* starch and anthocyanins were accumulated (Heiber et al., 2007). Taken together, the mutant phenotype indicated that the antioxidant protection in the plants of *rimb6* was severely disturbed.

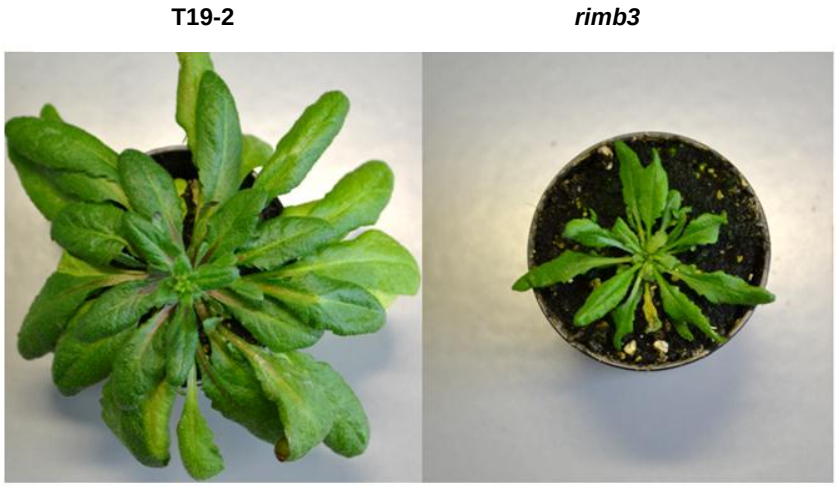

Figure 3-4: Phenotype of *rimb*6. The plants of *rimb*6 demonstrated a dwarf phenotype and narrow and curled leaves under both short- and long-day conditions.

In the previous observation (Hiltscher 2011) the phenotype of *rimb6* was shown to be dependent on the nutrients availability in the soil. In the soil supplemented with high amounts of mineral nutrients, the *rimb6* habitus phenotype was almost lost (Hiltscher, 2011).

A different result was however observed under the growth condition in Berlin: *rimb6* maintained widely the mutant phenotype on nutrient-rich soil, such as clearly stunted growth, narrow and curled leaves *et cetera*, but grew generally faster (Figure 3-5 C). T19-2 grown on nutrient-poor soil did not clearly differ from the T19-2 plants grown nutrient–rich soil in pant growth (Figure 3-5 B and D). However the fresh weights of *rimb6* grown in rich soil were not significantly changed compared to the *rimb6* grown on poor soil, while T19-2 also did not show significant difference in fresh weights of the plants

grown on rich and poor soil but it had generally a clearly higher fresh weight than *rimb6* either on rich or poor soil.

Figure 3-5: Habitus of five week-old *rimb6* on nutrient-poor and -rich soils. The plants were grown for five weeks in a controlled environment. The plants of *rimb6* demonstrated significant variation in rosette diameter on nutrient-poor and -rich soil, whereas the control line T19-2 were not affected by the nutrient content of the soil.

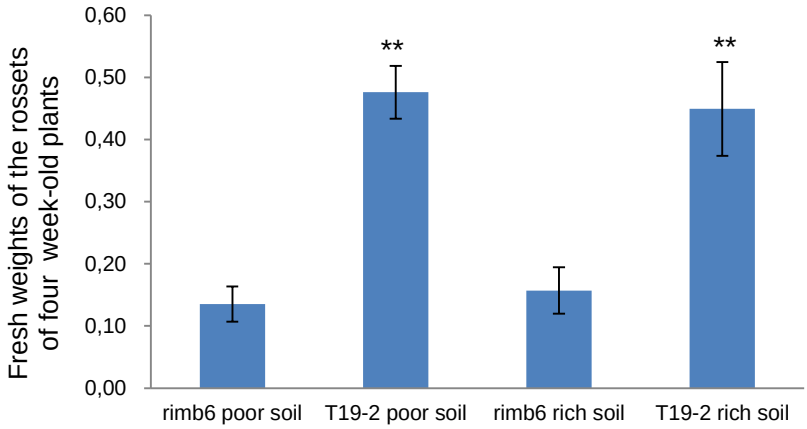

Figure 3-6: Fresh weights of the rosettes of four week-old plants of *rimb6* and T19-2 on nutrient poor soil and rich soils. The T19-2 had generally higher fresh weight than *rimb-6*, while the plants grown on rich- and poor-soil did not show clear difference between in fresh weight. The data are means of 10-12 parallels. ** indicates a significant differences from the value of Col-0 (Student test t-test, P<0.01)

Presumably, it is supposed that the mutant phenotype of *rimb6* correlates to homeostasis of the mineral elements in the plant cell and RIMB6 may be involved in the controlling regulatory network of the transporters and/or channels of the mineral elements on plasma membrane.

3.1.2 Analysis of reporter gene (luciferase) expression

In order to study the activities of 2CPA promoter, the activity of the reporter gene was analyzed *in vivo* by plant imaging system. The analysis of average bio-luminescence of the leaf surface was performed on the plants growing for six weeks under short-day conditions and for four weeks under long day condition (Figure 3-7). In this experiment, wildtype Col-0 and the reporter gene line T19-2 were grown in parallel to the mutant lines *rimb3* and *rimb6* as negative and positive control respectively. The activities of the reporter gene luciferase under control of 2CPA promoter in *rimb3* and *rimb6* were lower than they were in T19-2, indicating the suppression of 2CPA expression in those two mutants. The young leaves displayed higher luciferase-driven fluorescence values than the old leaves, revealing the higher expression of 2CPA in young leave tissues.

To quantify the luciferase-expression level, the plant image system NightSHADE LB 985 (BERTHOLD TECHNOLOGIES GmbH & Co. KG, Bad Wildbad, Germany) was applied. Under long-day conditions, *rimb3* and *rimb6* demonstrated lower luciferase activities (60% and 13% relative to T19-2) in the first two weeks under greenhouse condition (Figure 3-8). From the third week on, the *rimb3* exhibited higher luciferase activity than T19-2, while the *rimb6* always had lower luciferase than T19-2. However, the difference between *rimb6* and T19-2 got smaller after the first two weeks. In the third week for example *rimb6* demonstrated 67% of T19-2 in luciferase activity and in the fourth week it was 62%. Based on this observation it was concluded that RIMB3 acts as a positive regulator of 2CPA expression probably at young developmental stage of Arabidopsis (first two weeks), while RIMB6 probably regulates 2CPA expression positively on all developmental stages. However, in the first two weeks RIMB6 may have a more important function in inducing 2CPA expression than it did later on.

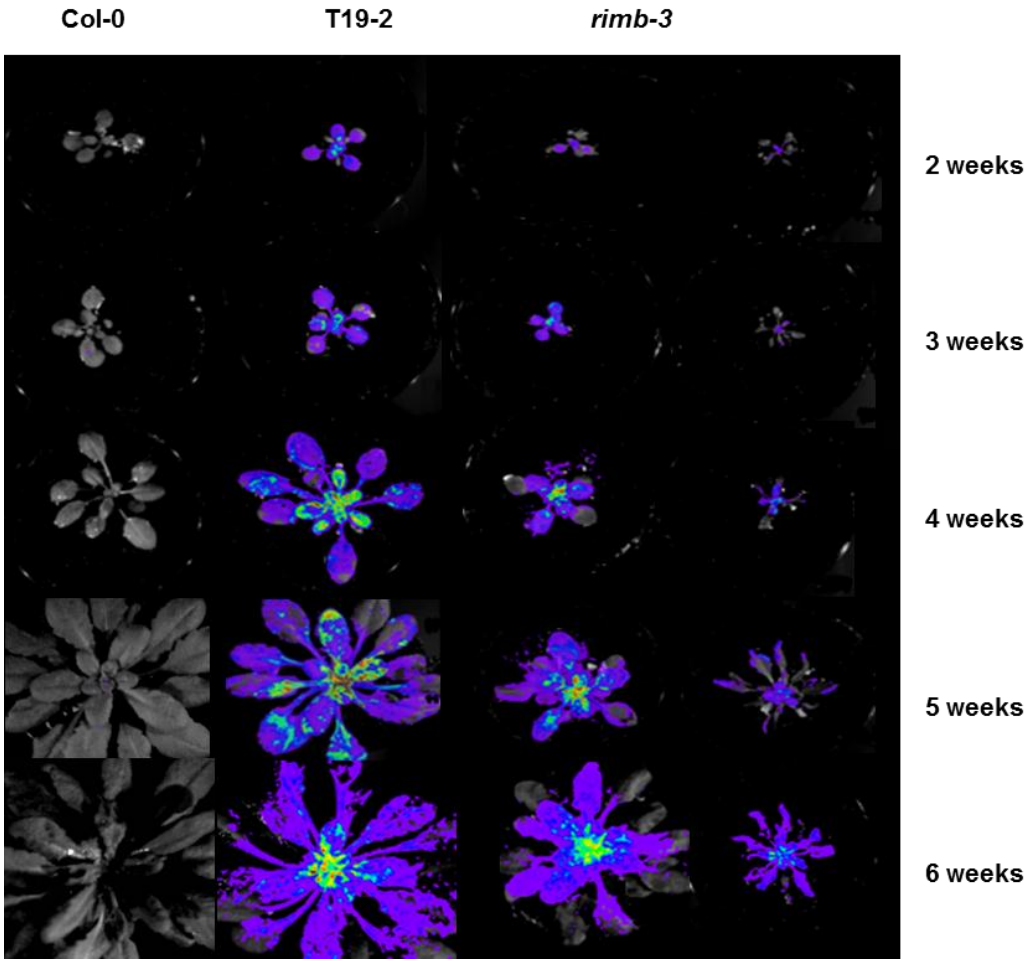

Figure 3-7: Luciferase measurement of Col-0, T19-2, *rimb3*, and *rimb6* with NightSHADE LB 985. The result illustrated the activities of reporter gene luciferase controlled under 2CPA promoter in each line. The *rimb6* had low luciferase activities from seedling to mature stage, while *rimb3* demonstrated low luciferase in comparison to the luciferase control line T19-2 only in the first five weeks.

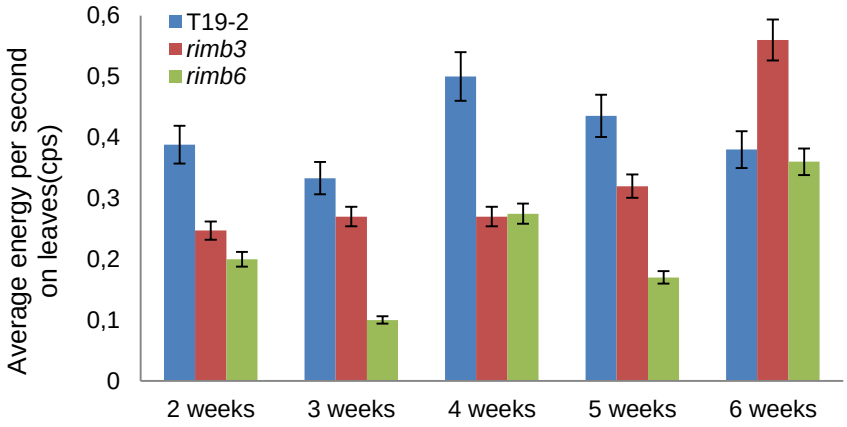

Figure 3-8: Luciferase activities of the plants of *rimb3*, *rimb6* and reporter gene line T19-2 under long-day condition: The luciferase activities were measured with average energy per second on leaves by NightSHADE LB 985. The data are means of 8-10 parallels.

Under short-day conditions, the plants demonstrated the same pattern in terms of plant development. In the first five weeks both of the *rimb* mutants showed lower luciferase activities than T19-2. At six weeks, *rimb3* exhibited even a higher luciferase activity than T19-2. At this stage the inflorescence started to grow. Luciferase activity in *rimb6* was 95% relative to T19-2 (Figure 3-9). Assumedly RIMB3 functions as a positive regulator of 2CPA expression in seedlings, young rosettes, and developed rosettes of Arabidopsis. From the bolting stage (six weeks) onwards, based on the higher luciferase activity in *rimb3* than the activity in the reporter gene line T19-2, it was suggested that RIMB3 could slightly repress 2CPA expression in Arabidopsis wildtype at this developmental stage. Luciferase activity was decreased in *rimb6* plants throughout the entire development process. RIMB6 is therefore assumed to regulate 2CPA expression positively at all the developmental stages of Arabidopsis.

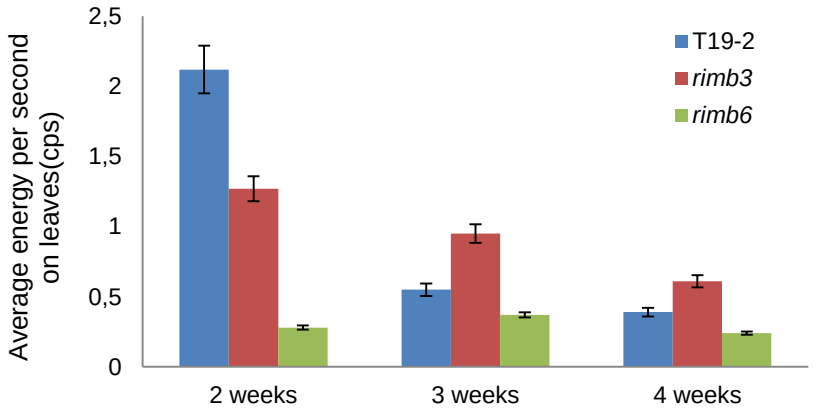

Figure 3-9: Luciferase activities of the plants of *rimb3*, *rimb6* and reporter gene line T19-2 under short-day condition. Average energy per second on leaves indicates the luciferase activities for each line. The reporter gene line T19-2 demonstrated higher luciferase activity than *rimb3* and *rimb6* in the first five weeks. From the sixth week *rimb3* showed higher luciferase activity than T19-2 and *rimb6* did. The data are means of 8-10 parallels.

3.2 Identification and characterization of mutant *rimb6*

3.2.1 The contents of mineral elements in *rimb6* and T19-2

Due to the conditional phenotype of *rimb6* on soil supplemented with different amounts of mineral nutrients (Hiltscher 2011), it was presumed that the contents of the mineral elements of the plants could be also conditional according to the soil types. To study the functions of RIMB6 in homeostasis of the mineral elements in the plant cell, the contents of fifteen elements in *rimb6* and T19-2 were analyzed using ICP-MS.

Significant differences were detected in the contents of the elements Cd, Cr, Cu, Fe, Mn, Mo, Se, Ni and Zn between *rimb6* and T19-2 (Figure 3-10).

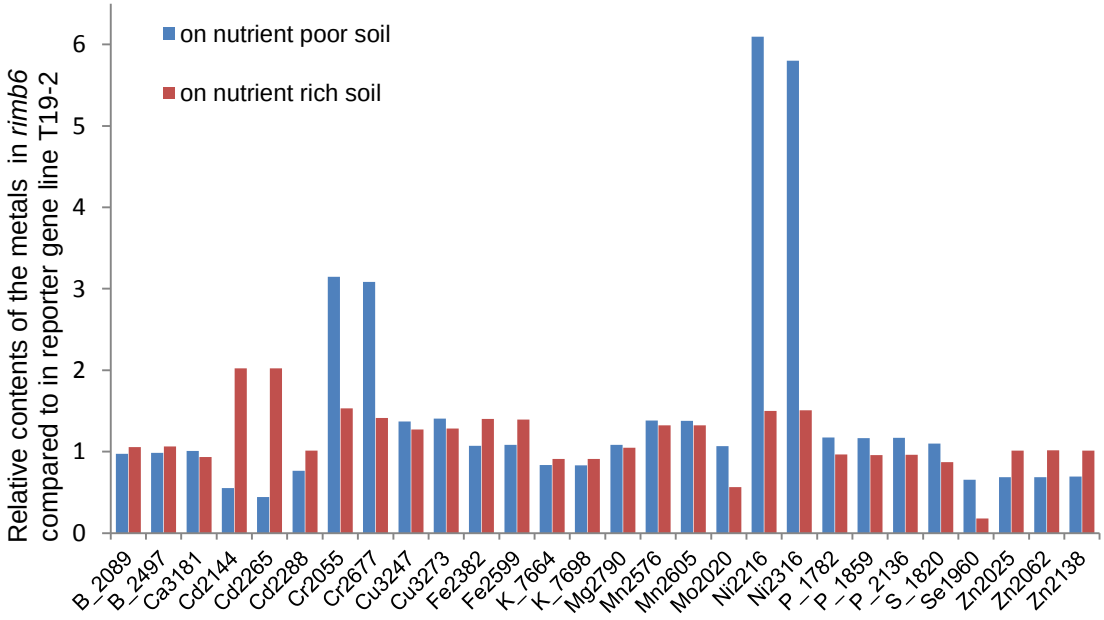

Figure 3-10: The contents of fifteen mineral elements in the five week-old plants of *rimb6* relative to the contents in reporter gene line T19-2. The analysis was performed with ICP-MS. The blue bars showed the mineral element content in the plants grown on nutrient-poor soil and red bars were for the plant grown on nutrient-rich soil. The numbers on x axis stand for the positions of peaks showed in the results of ICP-MS.

On nutrient-poor soil, the contents of Cd, Se and Zn in *rimb6* were clearly decreased, while the contents of Cu, Mn, and especially Cr and Ni were increased in *rimb6* in comparison to T19-2. The contents of Cr and Ni in *rimb6* were 3-fold and 5.8-fold in comparison to T19-2 respectively.

On nutrient-rich soil, the contents of Mo and Se were significantly diminished in *rimb6* plants and contents of Cd, Cr, Cu, Fe, Mn and Ni were increased, compared to their contents in T19-2. The Cd content in *rimb6* was 1- fold higher than its content in T19-2.

3.2.2 Genetic mapping of *rimb6* with next generation sequencing

In a previous part of the project (Hiltscher, 2011), *rimb6* was mapped with SSLP markers to a 201 kb region on the top arm of chromosome IV, in which 57 genes are predicted. Here genetic mapping was continued.

3.2.2.1 Crossing of homozygous *rimb6* to wild type Landsberg *erecta* (L*er*) accession

The mutant line *rimb6* (based on genetic background Col-0) was crossed to the accession Landsberg *erecta* (L*er*) The F1 progeny demonstrated high luciferase activities in comparison to wildtype Col-0 (Figure 3-11), indicating the heterozygosity of the recessive mutant and dominant wildtype suppressor of 2CPA in F1 generation.

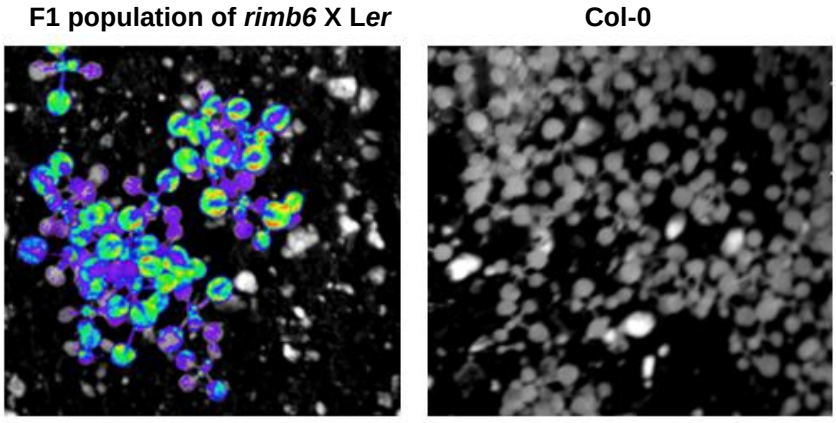

Figure 3-11: F1 of the mapping population: F1 population of *rimb6* X L*er* (left) demonstrated high luciferase activity (imaged by a plant imaging system NightSHADE LB 985) and the wildtype Col-0 (right) did not show any luciferase activity.

3.2.2.2 Selection of the individuals bearing *rimb6* allele in F2 population and isolation of nuclei DNA

More than 1200 plants of the F2 generation of the crossing line *rimb6* x L*er* were grown on nutrient-poor soil under short-day condition. Two weeks after germination, luciferase activities of all the individuals were imaged by a plant imaging system NightSHADE LB 985. All the individuals showing high luciferase activities were excluded from the population, while the others were used for further analysis.

The remaining population with low luciferase activity was further cultivated for another three weeks. 208 individuals with clear *rimb6* mutant phenotype were harvested and pooled into two groups. To avoid the background of plastid DNA in the sequencing step,

DNA was isolated only from nuclei of the two groups. The DNA qualities were verified using a nanophotometer and the DNA qualities were afterwards confirmed on an agarose gel, on which two clear bands with sizes over 10kb were shown (Figure 3-12.)

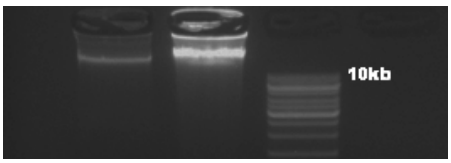

Figure 3-12: Test of DNA qualities of the sequencing samples. The DNA of two groups showed clear bands over 10kb on an agarose gel indicating sufficient qualities of the DNA.

3.2.2.3 One step sequencing with Illumina Hi-Seq 2000 sequencer

The samples were sequenced in 1/4 of a lane on Illumina Hi-Seq 2000 sequencer by Dr. Beth Rowan (Max-Planck-Institut für Entwicklungsbiologie, Tübingen, Germany). The sequencing processes were ended up with over 80 million raw reads for *rimb6.* 57 times coverage of the Arabidopsis genome was achieved. A map of allele frequency of Col-0 alleles across the genome was plotted using SHOREmap_interval.pl with a sliding window size of 200 kb, and the allele frequency across the genome was around 50% everywhere (Figure 3-13).

3.2.2.4 Genetic mapping with the sequencing results

On Chromosome IV, a region was clearly enriched for Col-0 alleles: between 7 and 9 Mb on this chromosome the frequency of the Col-0 allele raised to 0.9 - 0.93 (Figure 3-13). It also looked like there was a drop in frequency of the Col-0 in favor of the L*er* allele on top arm of chromosome I, which demonstrated frequency of the Col-0 up to 0.3. As the *rimb6* is generated with EMS mutagenesis in the accession Col-0, it was concluded that the identified interval on chromosome IV presumably contains the RIMB6 locus.

After removing SNPs from the L*er* parent, the SNPs on the chromosome IV representing mutations in the Col-0 genetic background were analyzed. 12 new SNPs (Table 3-1)

were detected in the coding sequences, in which 11 were synonymous SNPs that gave a rise to amino acid substitutions.

Table 3-1: The 12 SNPs on top arm of chromosome IV. 11 SNPs were nonsynonymous and 1 was synonymous. Apart from the new SNP on 7442672 (introduced a stop codon), all the other nonsynonymous new SNPs caused substitutions of amino acid.

Position	Reference base	Alternate base	Gene	Codon position in gene	Type	Reference aa	New aa
7078331	G	A	AT4G11750	220	Nonsyn	R	C
7442672	G	A	AT4G12560	858	Nonsyn	W	*
8219957	A	-	AT4G14272	214	Nonsyn	K	X
8699123	T	A	AT4G15236	1621	Nonsyn	L	M
8974535	C	-	AT4G15760	14	Nonsyn	G	X
8975844	C	-	AT4G15765	755	Nonsyn	G	X
8976974	A	-	AT4G15765	136	Nonsyn	W	X
8980212	G	-	AT4G15780	540	Nonsyn	T	X
8980214	T	-	AT4G15780	538	Nonsyn	T	X
8989799	C	-	AT4G15810	2060	Nonsyn	G	X
8993849	T	-	AT4G15820	794	Nonsyn	V	X
8126091	G	A	AT4G14096	1296	Syn	R	R

At position 7442672 bp on top arm of chromosome VI in AT4G12560 (Constitutive expresser of PR genes CPR1) a G to A mutation introducing a stop codon in the gene was identified as final candidate mutant locus, as the frequency of the Col-0 allele at this position raised to *ca.* 0.93. The point mutation at position 7442672 bp on top arm of chromosome VI in *rimb6* was verified by PCR and re-sequencing (data not shown). As a control, the parental line T19-2 was also analyzed and the result showed that T19-2 did not contain the point mutation at position 7442672 bp. Additionally, a SSLP marker cer461279, which locates on position 11016373 bp on chromosome 4 near AT4G12560, was applied in a genotyping test of F2 plants *rimb6* x L*er*. The population with mutant phenotype gave a high ration of Col-0 alleles (data not shown).

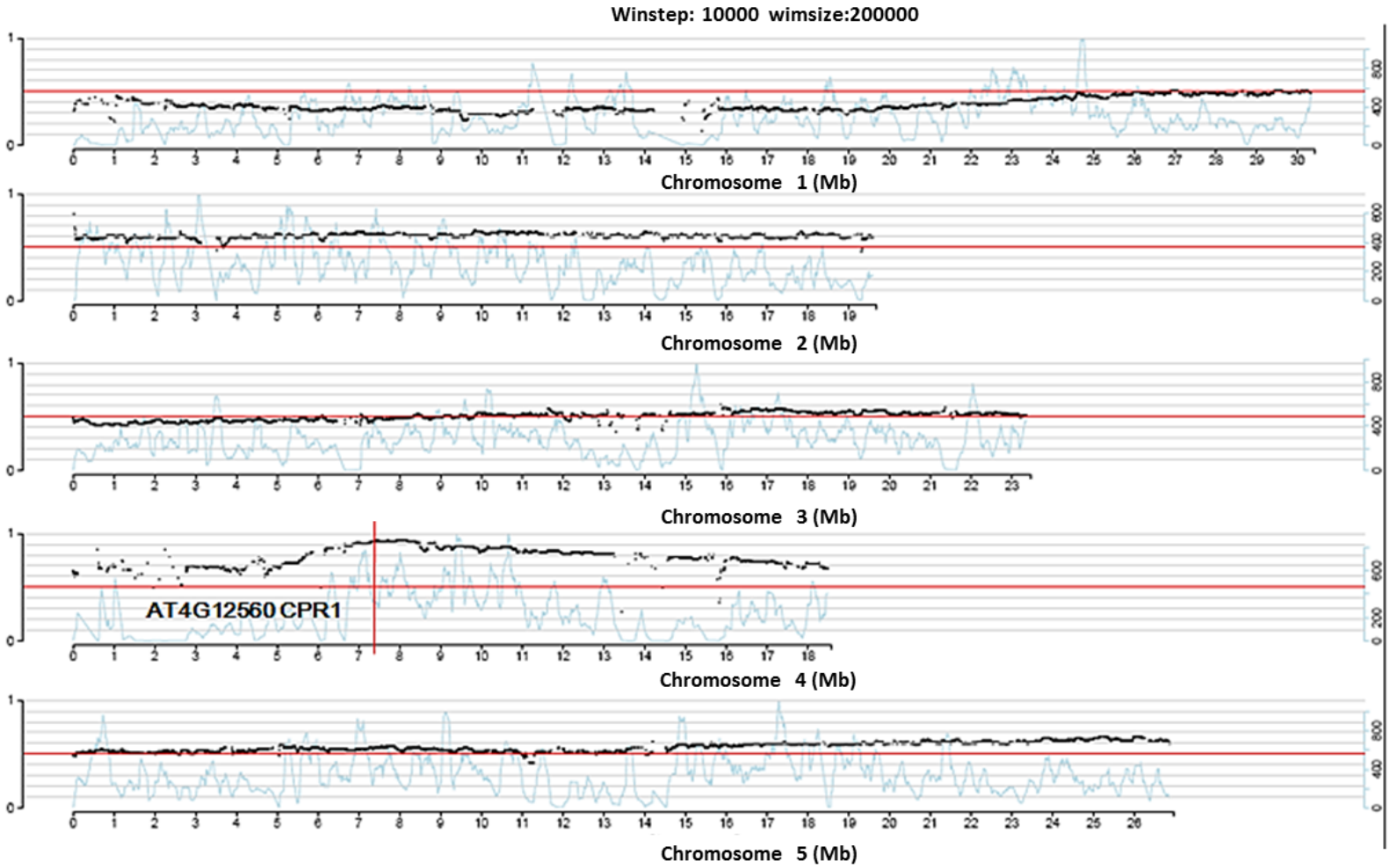

Figure 3-13: Map of Col-0 allele frequency cross the Arabidopsis genome with windows size of 200kb. Apart from chromosome IV the Col-0 allele frequency across the genome was around 50% everywhere. On the chromosome IV it was enriched for Col-0 alleles, especially on the region between 7 and 9 Mb on this chromosome frequency of the Col-0 allele raised up to 0.93. A drop in frequency of the Col-0 in favor of the L*er* allele was also demonstrated on top arm of chromosome I, where the allele frequency of the Col-0 was found to be decreased to 0.3.

3.2.3 Confirmation of the final candidate locus of RIMB6 by transcription analysis using T-DNA knock-out line

The identified candidate locus At4g12560 is being confirmed using transcript analysis of 2CPA in wildtype Col-0 and a homozygous T-DNA insertion line SALK_111420 (Figure 3-14), in which the T-DNA was inserted in the sequence of an F-box associated domain predicted by using CDD database.

Figure 3-14: The T-DNA insertion line SALK_111420. The T-DNA insertion line SALK_111420 was obtained from the Nottingham Arabidopsis Stock Centre (NASC) (http://arabidopsis.info/). The T-DNA of pROK2 was inserted on the position 7742361 bp on chromosome IV (Figure 3-12), in the region of the first exon of locus At4g12560.

3.2.4 At4g12560, the final candidate locus for RIMB6

On the position 858 bp in the coding sequence of the final candidate locus At4g12560 there was a G to A substitution introducing a stop codon (Figure 3-15). At4g12560 encodes CPR1 (Constitutive Expresser of PR Genes 1, also known as CPR30) which is an F-Box containing protein that acts as a negative regulator of defense response and targets resistance proteins (Guo et al., 2009).

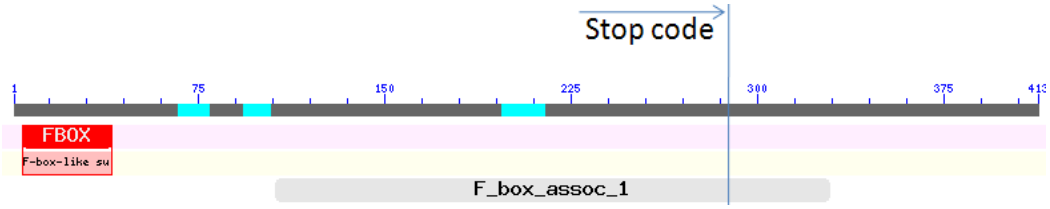

Figure 3-15: The conserved domain of the At4g12560. It has 412 amino acids and might contain an F-box-like domain and an F_box_assoc_1 domain. The stop codon was identified on the F_box_assoc_1 domain.

According to conserve domain database (CDD) on NCBI (http://www.ncbi.nlm.nih.gov/Structure/cdd/cdd.shtml), At4g12560 might contain two

conserved domains: an F-box (a member of F-box-like superfamily, cl02535), which is a receptor for ubiquitination targets; and an F-box associated domain type 1 (F_box_assoc_1, TIGR01640) which is an F-box protein interaction domain on C-terminal region. It contains a motif with 60 amino acids and is involved in ubiquitination as target proteins to mark them for degradation. Yeast-two-hybrid experiments support the idea that most members of F-box protein interaction domain are interchangeable F-box subunits of SCF E3 complexes (Guo et al., 2009).

The stop codon identified in *rimb6* was located on the sequencing region of the F-box protein interaction domain, and that could cause a deactivation of the F-Box protein CPR1.

3.2.5 RIMB6 might be correlated with plasma metal transporters AtIRT1 and AtPDR8

Using Genemaina database (http://www.genemania.org/) based on microarray data, a prediction was performed to check the relationships between RIMB6 and two plasma metal transporters AtIRT1 (AT4G19690) and AtPDR8 (AT1G59870) (Figure 3-16). It is concluded that the RIMB6 (CPR30) may correlate with AtIRT1 via an Arabidopsis- S-phase kinase-associated protein MEO (AT2G20160). The MEO strongly interacts with RIMB6 *in vitro*, proven by yeast-two-hybrid (Guo et al., 2009), while AtIRT1 was shown to coexpress with MEO, according to the microarray data according the microarray data (GEO accession: GSE21611, Moreno-Risueno et al., 2010). The RIMB6 and AtPDR8 expression activities are also not directly correlated. However AtPDR8 contained an ATP-binding cassette (ABC) domain, which is also contained by an ABC transporter G family member PDR11 (AT1G66950). According the microarray data (GEO accession: GSE30223), the PDR11 is predicted to coexpress with ASK16 (AT2G03190, an Arabidopsis S-phase kinase-associated protein 1), which was proven to interact with RIMB6 *in vitro* (Guo et al., 2009). In conclusion, the RIMB6 could correlate with AtPDR8 via ASK16 and AtPDR11.

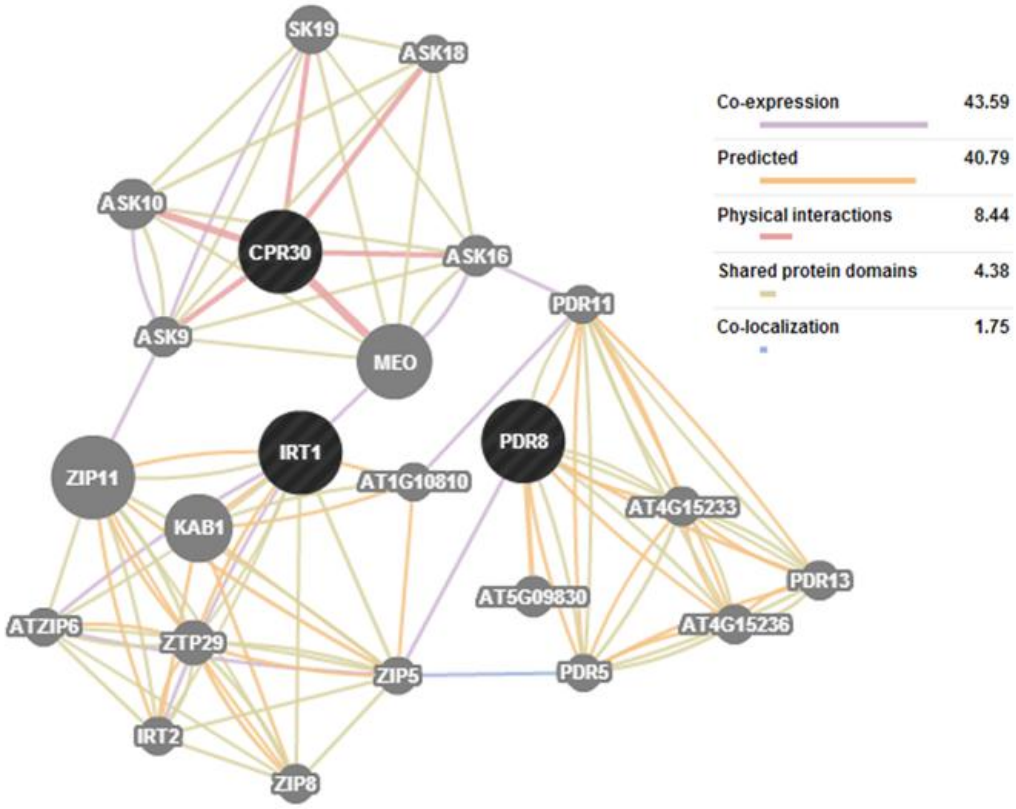

Figure 3-16 Prediction of the relationship between RIMB6 (CPR30) and AtIRT1 and AtPDR8 according to the Genemania database. The RIMB6 (CPR30) is correlated with AtIRT1 via MEO, an Arabidopsis- S-phase kinase-associated protein. The metal transporter AtPDR8 on plasma membrane of Arabidopsis may be correlated with RIMB6 via ASK16 (an Arabidopsis S-phase kinase-associated protein 1) and AtPDR11 (a plasma membrane-localized ABC transporte in Arabidopsis)

3.3 An eQTL of 2CPA regulator between Col-0 and Ler was identified on top arm of chromosome III

3.3.1 Genetic mapping of the rimb3 mutation with SSLP markers

The mutant line *rimb3* (based on genetic background Col-0) was crossed to accession Landsberg *erecta* (Heiber et al., 2007). To select the individuals bearing homozygote recessive repressors of 2CPA expression, the plants in the segregating F2 population were screened for low luciferase activity which was 15 - 35% relative to the parental line T19-2. In this way a mapping population was generated and the SSLP mapping was performed to identify the locus of recessive mutation in Arabidopsis genome.

3.3.2 An eQTL of 2CPA was identified based on L*er* genetic background

To cover the five chromosomes of Arabidopsis, 29 SSLP markers (Figure 3-17) were selected to design primers for the mapping PCRs. From the mapping population (F2 population of *rimb3* X L*er*), 43 lines with low luciferase were chosen to isolate genomic DNA as templates in the mapping PCR. In addition, PCR with a pair of specific primers binding to luciferase sequence was performed to confirm the presence of the luciferase construct in the selected lines.

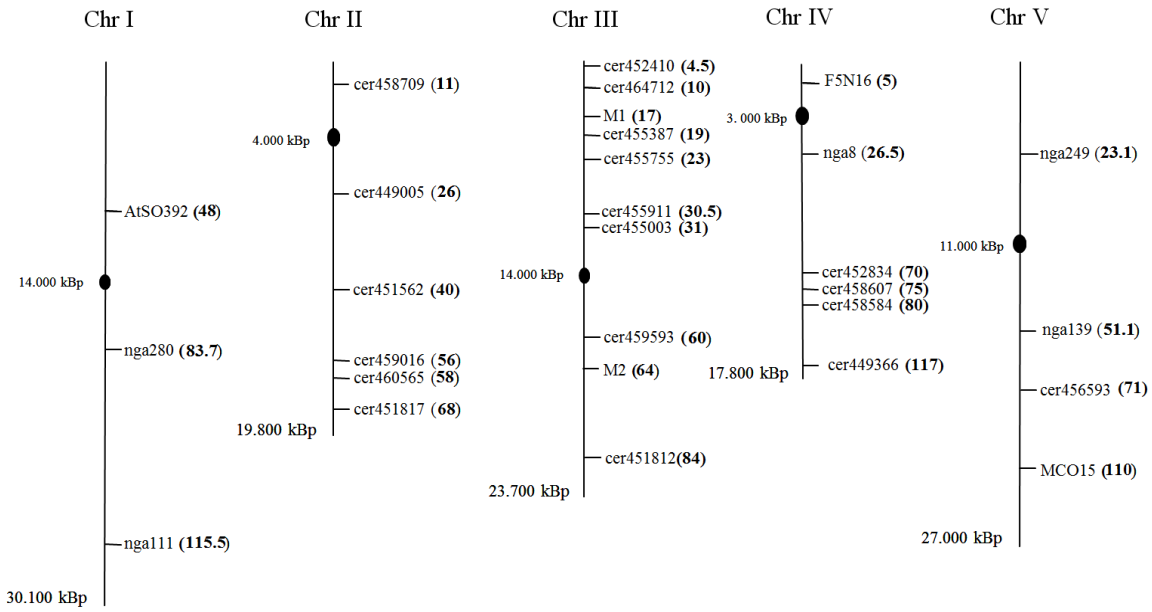

Figure 3-17: Overview of the applied SSLP markers on the Arabidopsis genome. The Map was designed by Heiber (2007) and the information of the markers was from the database of the Cereon/ Monsanto Arabidopsis Polymorphism Collections (http://www.arabidopsis.org /browse/Cereon/).

The genetic mapping was aimed to genotype the mapping population for homozygous Col-0 allele at a marker on the candidate locus of RIMB3. Interestingly, at marker M1, which is located on the position 4208576 bp on the top arm of chromosome III, the genotyping analysis demonstrated a relative high frequency of L*er* alleles. The value of recombination frequency R was up to 72% (Figure 3-18) indicating a L*er*-specific recessive repressor or Col-0 specific inducer of 2CPA on chromosome III near the position of marker M1.

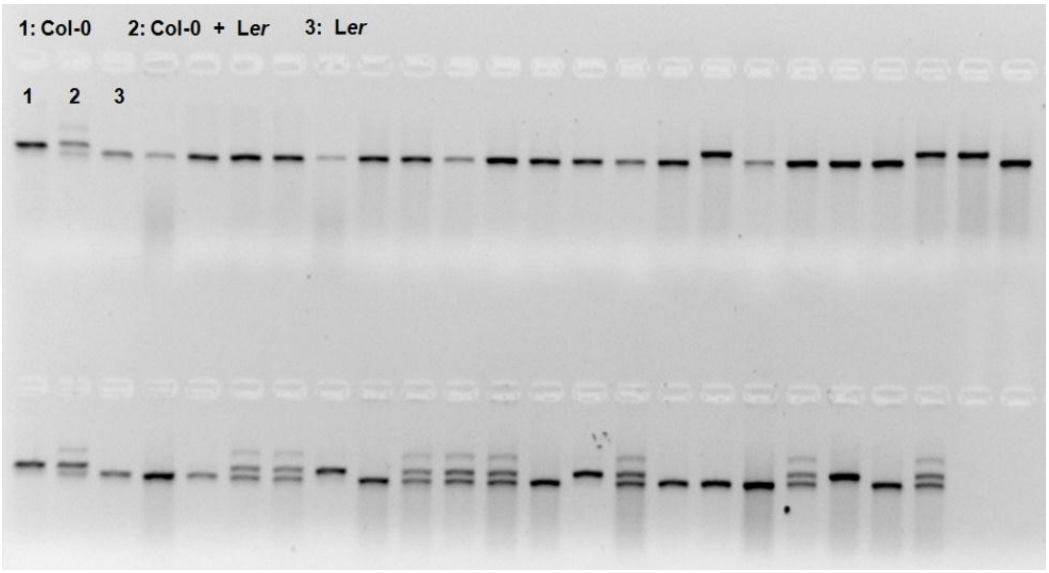

Figure 3-18: An electrophoresis displayed high frequency of PCR products of L*er* genetic background on the position of marker M1 (on Chr III). The value of recombination frequency R was 71.97%. The picture demonstrated the bands of the PCR products on a 4% agarose gel, on which the upper bands stand for the Col-0 genetic background (1), lower bands represented L*er* background (3) and the double bans indicted heterozygote on the position of M1 (2).

It is assumed that a locus near the marker M1 could be an expression quantitative trait locus (eQTL) regulating expression of 2CPA in Arabidopsis. Additionally, a rescreening of seedlings of the F3 progeny showed low luciferase activities of all seedlings tested.

3.3.3 Confirmation of the eQTL

The eQTL was confirmed with F3 progeny of the mapping F2 population. While 19 F3 plants, whose genetic background were confirmed as L*er* on top arm of chromosome III, were selected and cultivated on MS medium, another 20 lines showing Col-0 genetic background on top arm of Chromosome III were chosen for the further analysis. Quantification of 2CPA-promoter driven luciferase activity was performed at the 10 day-old F3 seedlings, in which 89% of the seedlings with L*er* background on chromosome III top arm had lower than 10% luciferase activity relative to T19-2, whereas most of the seedlings (85%) with Col-0 background on chromosome III showed relative high luciferase activity (over 30% relative to T19-2, Figure 3-19).The previous hypothesis was therefore confirmed: the eQTL and low luciferase activities correlate in the mapping population.

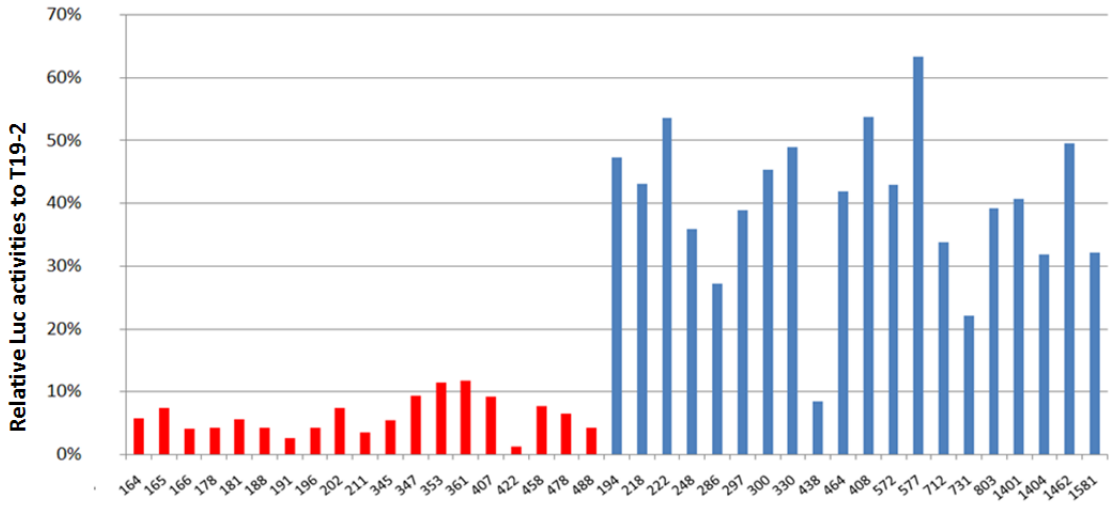

Figure 3-19: F3 progenies of the mapping population were screened for luciferase activities. The samples with Ler genetic background on chromosome III top arm were labeled as red and the samples with Col-0 as blue. The result confirmed the eQTL on the top arm of chromosome III.

3.3.4 Genetic mapping of the eQTL with SSLP

About 10000 plants of the F2 population of *rimb3* X L*er* were screened at an age of 10 days for low luciferase activity. 2000 lines showing 10-50% (relative to the parental line T19-2) luciferase activity controlled under 2CPA promoter were determined as individuals bearing the homozygous eQTL alleles and they were selected for further genetic mapping with SSLP markers. Fine mapping was performed according to Jander et al., (2002), in which 420 lines of low luciferase activity were included and 15 SSLP markers (Figure 3-20) targeting to the region near M1 on top arm of chromosome III were applied. The candidate locus was finally determined on a 77 kb region on chromosome III between the markers cer455911 on BAC MIL23 and cer457003 on BAC MSD21 (Figures 3-20 and 3-21). The candidate region encodes 23 genes, which were screened for the SNPs and Indels variation in their promoter- and coding sequence according to the Monsanto Arabidopsis Polymorphism and L*er* Sequence Collections (http://www.arabidopsis.org/browse/Cereon/index.jsp). Finally, four from the 23 candidate genes were determined as candidates containing natural variations of amino acid between accessions Col-0 and L*er* (Figure 3-20, Table 3-1).

cer 464712	M1	Cer464886 MRP15	cer 455755	cer457441 MVE11	cer456185 MLD14	cer 456690 MPN9	cer 464893 MSA6	cer457693 MXL8	cer473958 MHC9	CER455911 MIL23	CER455923 MIL23	cer 457003 MSD21	cer455243 MCB17	cer457602 MXC7
10	17	18	23	26.3	27.6	28.2	30.3	30.5	30.7	31	31.1	31.2	31.3	33.5
	4208576	4402690	5633957	6465401	6748166	6901588	7410876	7441952	7504049	7573149	7626624	7649939	7912818	8234742
8	8	8	16	15	15			18						17
56.25	62.50	68.75	78.13	80.00	86.67			91.67						70.59
2	2	3	3	3	3			3						
1	2	2	3	3	3	3		3					3	3
2	2	2	2	3	3			3					3	3
2	2	2	2	2	3			3						3
			2	2	3			3						2
			2	2	2	2	2	3				3	3	3
2	2	2	2	2	2	2	3	3				3	3	3
			2	2	2			2	2	2	2	2	3	3
2	2	2	2	2	2			2	2	2	3	3	3	3
3	3	3	3	3	3			3	3	3	3	3	2	2
			3	3	3	3		3	3	3	3	2	2	2
			3	3		3		3	3	3	3	3	2	2
			3	3	3	3		3	3	3	3	2	2	2
			3	3	3	3		3	3	3	2	2	2	2
			3		3	3		3	3	3	3	3	2	2
								3	3	3	3	3	2	2

Figure 3-20: Detailed PCR results of SSLP mapping of the eQTL on the top arm of chromosome III. The applied markers are displayed on the top of the table, together with their positions and BACs. Each line from left to right describes the mapping results of one individual from the mapping population. The number ‘‘1” represents the PCR result of Col-0 genetic background of a mapping sample with a specific marker; “2’’ represents a heterozygote of Col-0 and L*er*, and “3’’ represents L*er* genetic background. The short red lines demonstrate recombinant to L*er* alleles. The green colored PCR results demonstrate a trend: the closer the position is to the region between cer455923 and cer457003, the more alleles with L*er* genetic background are shown according to the SSLP mapping. This trend indicates that on this region a locus from L*er* caused a similar mutant phenotype (low luciferase activity) of all the mapping individuals.

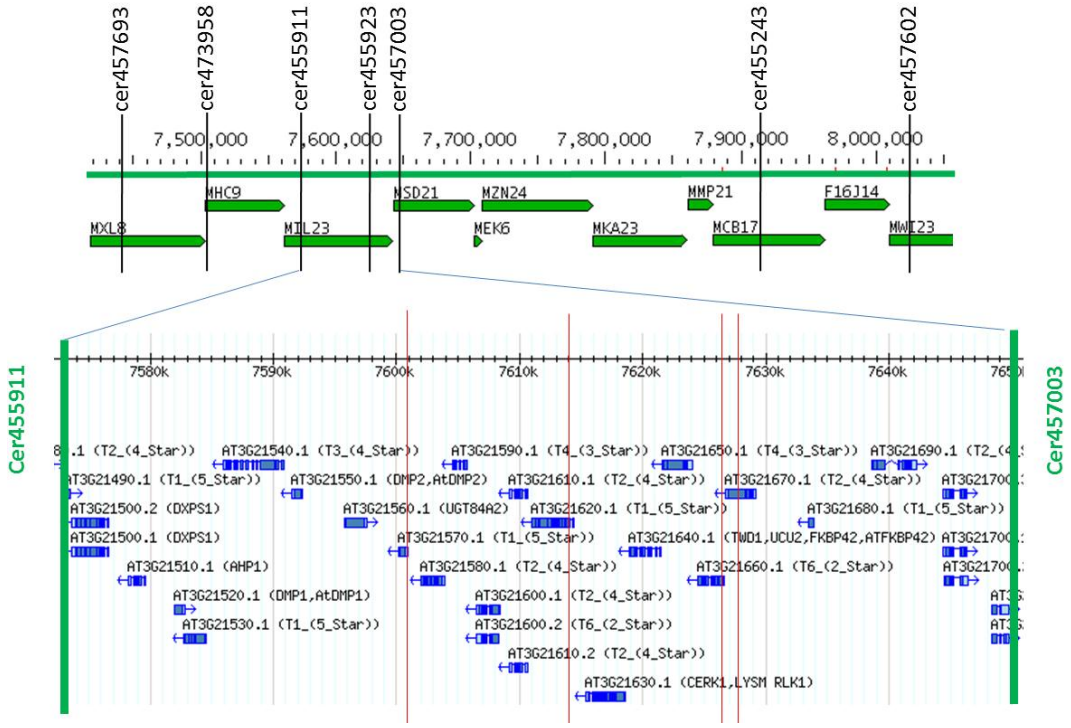

Figure 3-21: Overview of the eQTL mapping. The mapping of eQTL was finished on a region between marker cer455911 and cer457003, where 23 loci were located on, among which only 4 loci had polymorphism between Col-0 and L*er* in their coding sequence. The four loci were marked with a red line.

Table 3-2: Four candidate loci for the eQTL. Between markers cer455911 and cer457003 on chromosome III, four loci could be identified to show polymorphisms in amino acids between accession Col-0 and L*er*. AT3G21570, AT3G21660 and AT3G21670 have substitutions in amino acid sequences. AT3G21660 contains a 25 bp insertion in L*er.*

Gene	Locus	Variation beteewn Col-0 and L*er*	Position	DNA	Amino Acid
AT3G21570	unknown protein	Substitute	7600366	A->T	V->D
AT3G21620	ERD (early-responsive to dehydration stress) family protein	Substitute	7612481	A->G	Y->H
AT3G21660	UBX domain-containing protein	insertion	7626624	25bp in Ler	
AT3G21670	Major facilitator super-family protein	Substitute	7628822	T->A	Y->F

3.3.5 Transcription analysis of the candidate genes of the eQTL using T-DNA knock-out line

For the transcription analysis of 2CPA, T-DNA insertion lines were obtained for all four candidate genes of interest, in which the T-DNA were inserted in coding sequence (Figure 3-22). After genotyping, the homozygote T-DNA insertion lines and wild types were distinguished and selected for the further analysis. In order to establish the same genetic background of the plants, only the wildtypes obtained from the seeds of T-DNA Insertion lines were applied as control lines of wildtype.

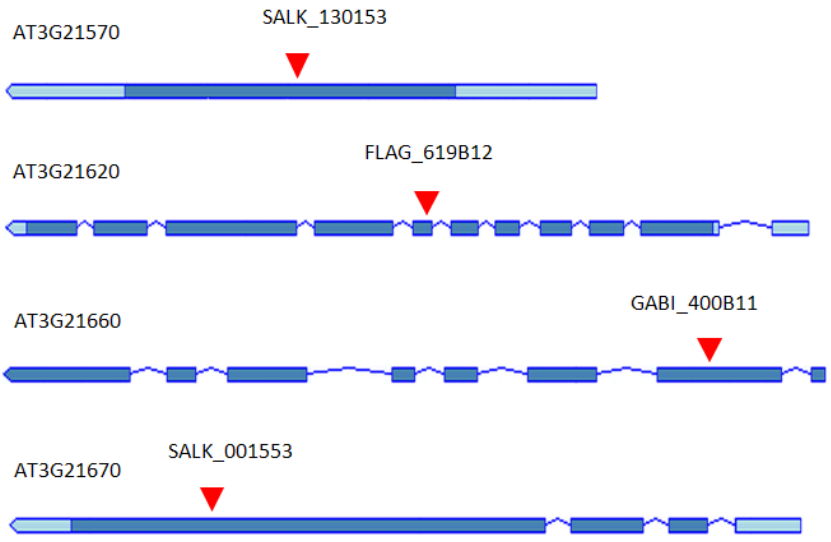

Figure 3-22: T-DNA insertion lines were applied to check the effects of knock-out of the 4 candidates of the eQTL. All T-DNA lines contained an insertion over 10 kb in the coding sequences, which could knock down the locus in the plants. The plants with loss of function of each candidate locus for the eQTL were further analyzed with transcript analysis of 2CPA.

The T-DNA insertion lines were grown in parallel to wildtype Col-0 on MS medium under short-day condition in controlled environment and the 10 day-old seedling were harvested for analysis of 2CPA transcript level of 2CPA. The transcript levels of 2CPA in the T-DNA insertion lines were evaluated relative to the housekeeping gene *Actin7*. The transcript levels were compared to the 2CPA expression in wildtypes. The result of the transcript analysis of the four candidate loci is shown below (Figure 3-23). Among the four final candidates, only the T-DNA insertion line for locus At3g21660 showed a significant

reduction of 2CPA expression (67% relative to 2CPA expression level in Col-0). The knock-out line of the locus At3g21570 demonstrated slight up-regulation (103% relative to 2CPA expression level in Col-0), while the 2CPA expression in the knock-out lines of At3g21620 and At3g21670 were insignificantly down-regulated (94%).

As conclusion, At3g21660 was considered as the final candidate of the eQTL, which may function as a Col-0-specific positive regulator or L*er*-specific repressor of 2CPA expression in Arabidopsis. The eQTL could also be one of the reasons of natural variation in expression of 2CPA in accessions of *Arabidopsis thaliana* (Juszczak et al., 2012). In the comparison of 2CPA expression in seven *Arabidopsis thaliana* accessions, the 2CPA transcript level in accession Col-0 is higher than it is in accession L*er*).

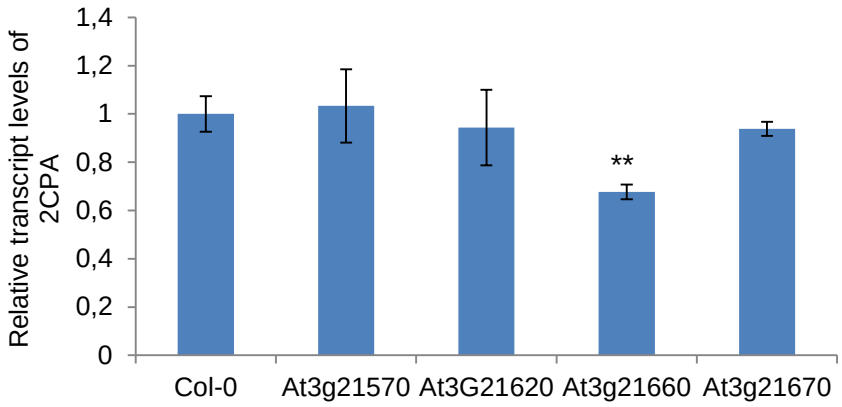

Figure 3-23: Relative transcript level of 2CPA in homozygous knock-out line of the final 4 candidate loci of the eQTL. The transcript level of 2CPA in wildtype Col-0 was set as 100%. The data are means of 7-10 samples (± SD) grown in three independent experiments. ** indicates a significant differences from the value of Col-0 (Student test t-test, P<0.01)

3.3.6 Natural variation of At3g21660 between Col-0 and L*er*

In the first exon at the position 33 of the gene At3g21660, a sequence of 25 bp (ATTGATCAGCTCCTTTATTGAGGTC) is inserted in the genome of L*er* (Figure 3-24).

Figure 3-24: In the first exon of At3g21660, an insertion with 25 bp as natural variation between Arabidopsis accession Col-0 and L*er* was identified. The data of the inserted sequence was obtained from database of 1001 Genomes Project and verified by Sanger sequencing.

In addition to 8 extra codons it introduced a frame shift in L*er* genome and caused a complete loss-of-function of this locus. The insertion was verified by PCR together with other four accessions with marker cer455923 (Figure 3-25). The results of PCR were according to the Arabidopsis SNP Sequence Viewer (http://natural.salk.edu/cgi-bin/snp.cgi), in which Bay-0, Van-0, Cvi-0 and L*er* contained an insertion on the position of marker cer455923, while C24 and Col-0 did not.

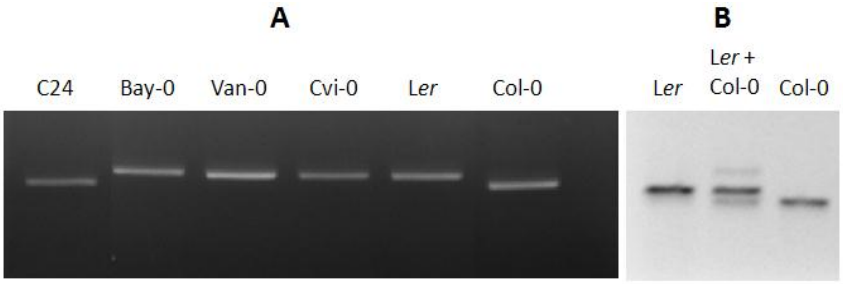

Figure 3-25: Confirmations of the insertion of the eQTL in different Arabidopsis accessions. Genomic DNA of different Arabidopsis accessions were used as DNA templates in a PCR with SSLP marker cer455923, which locates on the flaking sequence of the eQTL insertion, the lower bands indicated the PCR without the insertion. A: The PCR with six different Arabidopsis accessions showed, that C24 and Col-0 do not contain the eQTL insertion, whereas Bay-0, Van-0, Cvi-0 and L*er* contain an insertion in the position of marker cer455923. B: Using marker cer455923, three PCRs were performed with the genomic DNA of L*er*, the mixture of L*er* and Col-0, and Col-0 as DNA templates. The upper bands, which were the PCR products of L*er*, Indicated that Ler contain a insertion on the position of marker cer45923 while Col-0 did not.

3.3.7 Prediction of protein At3g21660 with Conserved Domain Database of NCBI

The locus At3g21660 encodes a UBX domain-containing protein with 435 amino acids containing 2 SEP superfamily domains (74 and 29 amino acids respectively) and an UBQ superfamily domain (76 amino acids) at the C-terminal region of the amino acid sequencing (Figures 3-26 and 3-27).

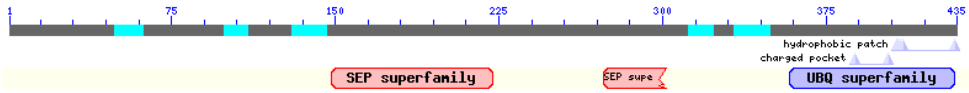

Figure 3-26: The structure and predicted conserved domains of At3g21660. It contains two SEP superfamily domains in the middle of the protein and an UBQ superfamily domain at N-terminal.

```
                      10        20        30        40        50        60        70
                ....*....|....*....|....*....|....*....|....*....|....*....|....*....|....*....
gi 332643014 358 AAPTTSIQLILADSTRIVTQFNTHHTIRDIRCFIDTSRP-DGSKDYQLliMGSPPT-PLSDFDQTIEKAGIANSVLVQK 434
Cdd:cd01770    1 LEPTTSIQIRLADGKRLVQKFNSSHRVSDVRDFIVNARPeFAARPFTL--MTAFPVkELSDESLTLKEANLLNAVIVQR 77
```

Figure 3-27: The UBQ superfamily domain predicted in At3g21660 by CDD NCBI has high similarity to the subfamily sd01770 (gi 332643014).

According to the prediction of Conserved Domain Database (CDD) on NCBI (http://www.ncbi.nlm.nih.gov/Structure/cdd/cdd.shtml), the UBQ domain is highly conserved to the subfamily cd01770, a p47_UBX domain member, which belongs to the cd01767 UBX family (Figure 3-28). Moreover, the sub-family ubiquitin domain cd01803 is classified under cd01769 UBL family, which is near the cd01767 UBX family according to the sequence clustering. Cd01769 and cd01767 are both classified under superfamily cl00155 ubiquitin-like proteins.

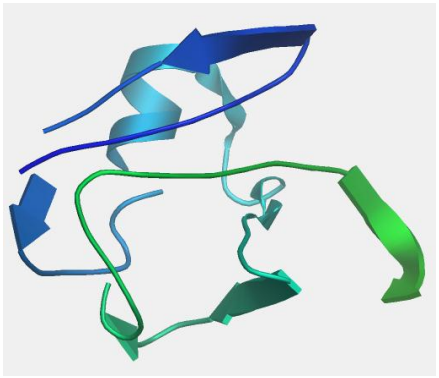

Figure 3-28: 3D structure of the UBQ superfamily domain in At3g21660. The modeling result demonstrated that the conserved domain UBQ contains one α-helix and seven β-sheets. The amino acid sequences were submitted to the online alignment-based modeling tool SWISS-MODEL (http://swissmodel.expasy.org) and the structure was displayed by using the Swiss-pdbViewer DeepView 4.1 (http://swissmodel.expasy.org/spdbv)

3.3.8 At3g21660 positively regulates the 2CPA and 2CPB

A transcription analysis was performed with the T-DNA insertion line GABI_400B11 to check the function of the eQTL At3g21660 in antioxidant defense system of plant cells. 2-Cys peroxiredoxin A (2CPA, At3g11630), 2-Cys peroxiredoxin B (2CPB, At5g06290), stromal ascorbate peroxidase (sAPx, At4g08390) and thylakoid ascorbate peroxidase (tAPx, At1g77490) were studied in this analysis (Figure 3-29). Expression levels of 2CPA, 2CPB, sAPx and tAPx relative to the housekeeping gene *Actin7* in the eQTL knock-out line and wildtype Col-0 were analyzed in 10 day-old seedlings.

In the eQTL knock-out line the expression levels of 2CPA and 2CPB were significantly decreased: in comparison to wildtype Col-0, the relative expression levels of 2CPA and 2CPB were 68% and 76% in the knock-out line. No significant change in the expression of sAPx and tAPx was observed: their relative expression levels to the levels in wildtype were 99% and 93% respectively. It is presumed that the eQTL regulates the expression of 2-cys-peroxiredoxin specifically

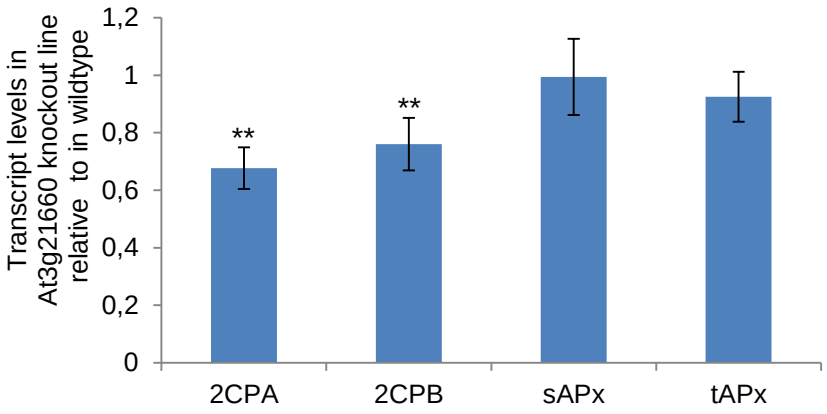

Figure 3-29: Transcript levels of 2CPA, 2CPB, sAPx and tAPx in homozygous T-DNA knock-out lines of At3g21660 relative to their levels in wildtype Col-0. The data are means of 7-10 samples (± SD) grown in three independent experiments. ** indicate significant differences from the transcript value in Col-0 (t-test, P<0.01)

3.3.9 Test for the polymorphism in promoter of Col-0 and L*er*

According to the Cereon database (http://www.arabidopsis.org/browse/Cereon/), on position 3672064 bp of chromosome III, one substitution G to A between Arabidopsis accession Col-0 and L*er* was found, that is indicated by marker cer464400. To test effect of this substitution on 2CPA expression, a transient gene expression was performed with plasmids expressing luciferase under control of Col-0 promoter and L*er* promoter. Two groups of 10 day-old Arabidopsis seedlings (Col-0) were infiltrated respectively with the Agrobacterium expressing luciferase under control of 2CPA promoter of Col-0 (p2CPA-Col:Luc) and the Agrobacterium expressing luciferase under control of 2CPA promoter of L*er* (p2CPA-L*er*:Luc). The luciferase reporter line T19-2 was used as positive control. After an infiltration in luciferin, the 2CPA promoter activities were checked by measurement of the luciferase activities. The activities of the promoters of Col-0 and L*er* did not show significant difference (Figure 3-30), indicating that the polymorphism of 2CPA expression between Col-0 and L*er* is not caused by the G to A substitution in the promoter region of 2CPA of Col-0 and L*er*.

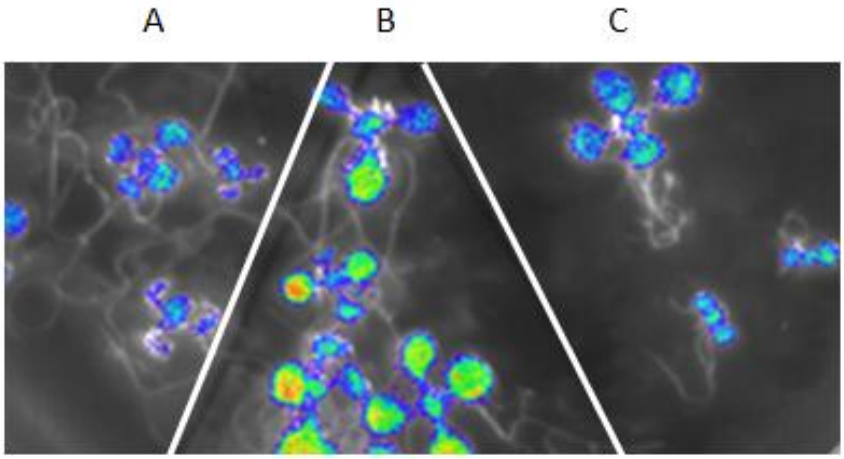

Figure 3-30: Transient gene expression of 2CPA promoters of Col-0 and L*er*. A: Col-0 infiltrated with Agrobacteria expressing luciferase under control of the 2CPA promoter of Col-0 (p2CPA-Col:Luc). **B**: luciferase gene reporter line T19-2. **C**: Col-0 infiltrated with Agrobacterium expressing luciferase under control of plasmid with 2CPA promoter of L*er* (p2CPA-L*er*::Luc). The picture was taken from same plate.

3.3.10 Prediction of the function network of At3g21660

Based on the microarray data of transcriptome analysis of *Arabidopsis thaliana*, the online software of gene function predictions Genemaina predicted a possible network of all the eQTL's partners of interactions, coexpression, co-localization and protein with similar domains (Figure 3-31).

The analysis predicted a functional correlation between the eQTL (AT3G21660) and three CDC48 proteins and furthermore it demonstrated 12 proteins sharing an UBX domain with the eQTL. Among the 12 UBX domain-containing proteins, five PUX proteins (PUX1 to PUX5) have strong physical interaction with ATCDC48, which functions as an important motor and regulator for the turnover of ubiquitylated proteins (Buchberger, 2010).

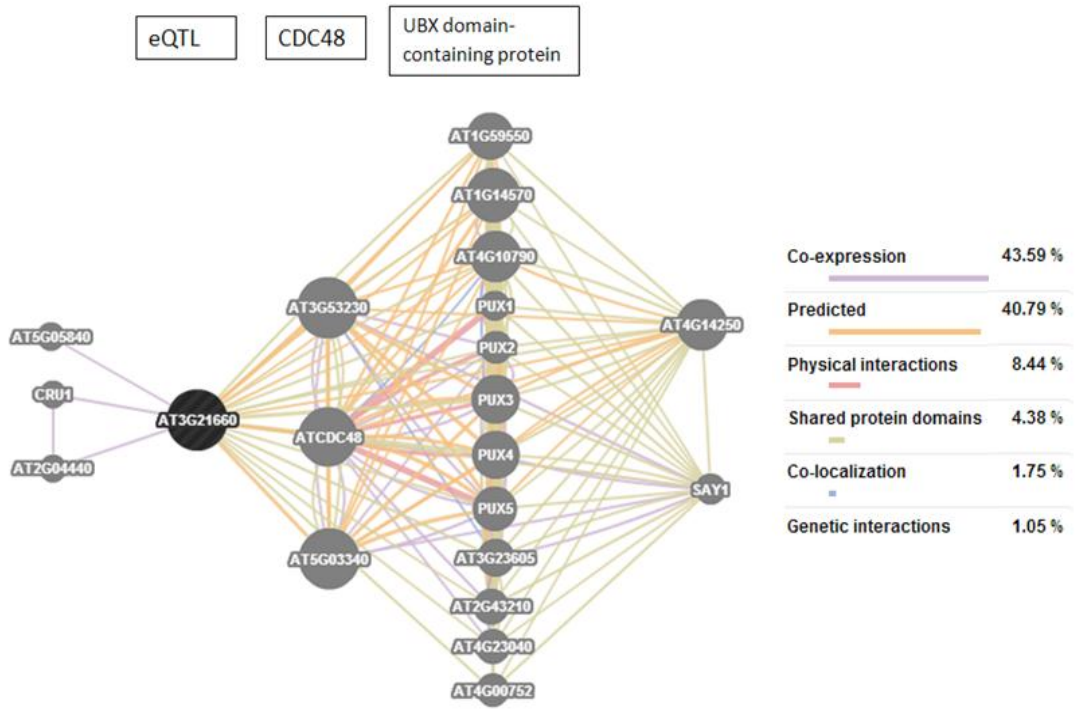

Figure 3-31: Prediction of function's network of At3g21660 with Genemania database. The results demonstrated strong prediction between the eQTL At3g21660 and 3 CDC48 proteins. According to the database 11 UBX proteins have physical interaction with CDC48, especially the ATCDC48. Furthermore, the eQTL shared the UBX domain with all the UBX protein.

3.3.11 Coexpression analysis of Ubox protein with CDC48, PUX2 and 2CPA

Since the eQTL contains a UBX domain, it is assumed that the eQTL might have a similar function to other UBX-containing proteins and interact with CDC48, the interacting partners of PUX proteins. Coexpression analysis was performed to confirm the hypothesis using bioinformatical database Genevestigator (https://www.genevestigator.com). In all the analysis the P value was set to 0.05.

3.3.11.1 The eQTL (AT3G21660) and PUX2 might have a negative correlation

According to the data of expression pattern under different conditions, the eQTL and the most well studied UBX containing proteins PUX2 (AT2G01650), which is concerned as a positive regulator of CDC48, are negatively correlated (Figure 3-32).

The PUX2 was down-regulated under cold, heat, circadian change and germination/stratification and iron deficiency condition as well, whereas the expression of the eQTL was not much changed or even increased. Under hypoxia, high/low nitrogen treatment conditions and in mock treated roots as well as desiccated seed samples, the PUX2 was up-regulated, while the eQTL was down in most of the cases.

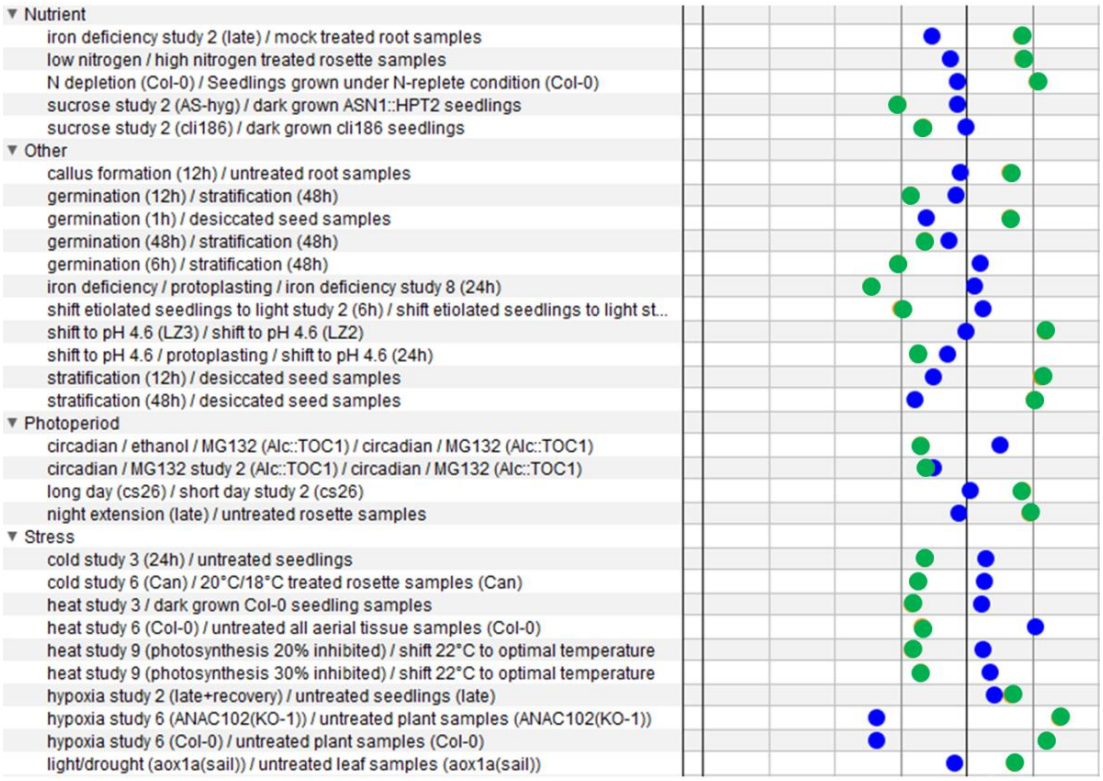

Figure 3-32: The result of coexpression analysis of the eQTL and PUX2 with Genevestigator. The blue dots stand for the PUX2 and the green dots stand for the eQTL. The eQTL and PUX2 protein were negatively correlated under different nutrients condition, germination and pH conditions, photoperiod conditions and several different stresses. The direction to the left stands for down-regulation, and to the right represents up-regulation.

3.3.11.2 2CPA negatively correlated with ATCDC48

Under biotic, chemical, drought stress and UV treatment, the 2CPA was down-regulated but the CDC48 was up-regulated (Figure 3-33). The CDC48 was down-regulated under iron deficiency and methyl jasmonate (MeJa) treatment, while 2CPA was up-regulated.

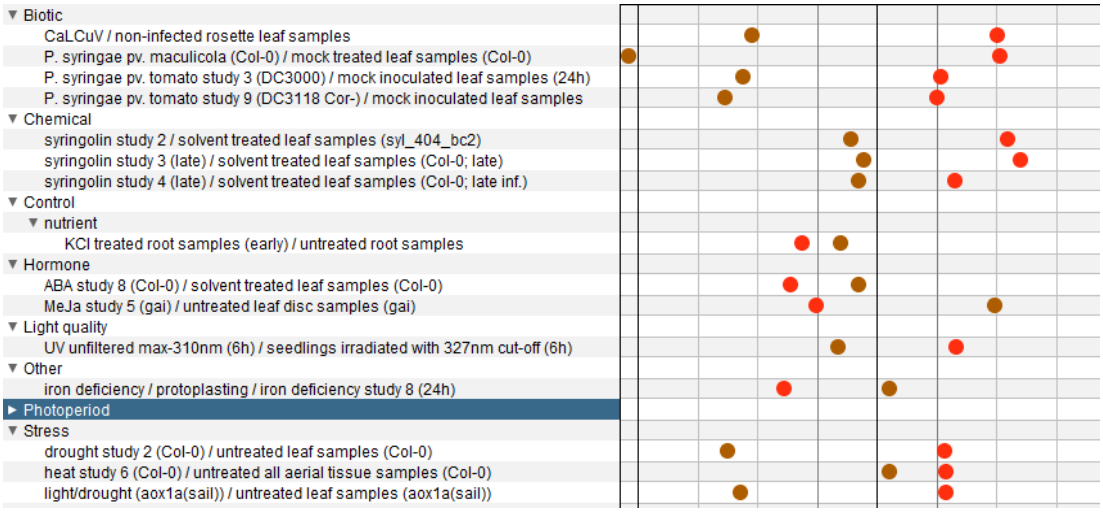

Figure 3-33: The result of coexpression analysis of the 2CPA and ATCDC48 with Genevestigator. The brown color represents 2CPA and light red color is for ATCDC48. The 2CPA and ATCDC48 were negatively correlated under different biotic and abiotic stresses syringlolin, MeJa and ABA treatments. The direction to the left stands for down-regulation, and to the right represents up-regulation.

3.3.11.3 PUX2 is positively correlated with ATCDC48

The expression of PUX2 and CDC48 showed the same trend (Figure 3-34). During biotic, chemical and UV treatment both were highly expressed whereas under KCL, ABA, MeJa and iron deficiency treatment, the two genes were both down-regulated. The most changes were over 1-fold.

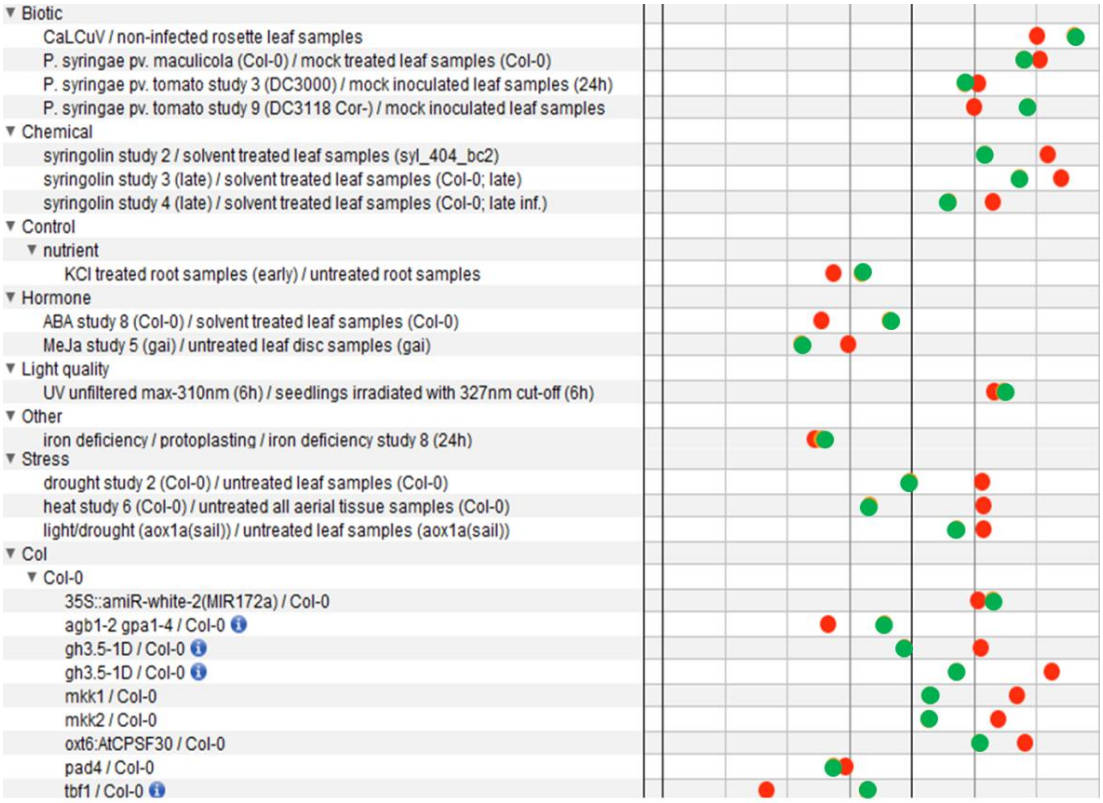

Figure 3-34: The result of coexpression's analysis of the PUX2 and ATCDC48 according to the Genevestigator. Green color stands for PUX2, red color represents ATCDC48. The PUX2 protein positively correlated with ATCDC48 under different biotic stresses (CalCuV and P.Syringae treatments), abiotic stresses (UV, drought, and light), in syringolin and KCl study, ABA, MeJa and iron deficiency studies. The direction to the left stands for down-regulation, and to the right represents up-regulation.

3.3.11.4 PUX2 is negatively correlated with 2CPA

The microarray data of the expression of PUX2 and 2CPA demonstrated opposite trend (Figure 3-35) under many conditions except cold and heat treatment. In the red/blue light study and sucrose study, under germination with different stratification time as well as circadian changes as well, the expression of PUX2 was repressed while 2CPA was highly expressed. Under nitrogen treatment, night extension, hypoxia and light/drought as well as osmotic stress, the PUX2 was up-regulated while 2CPA level was decreasing.

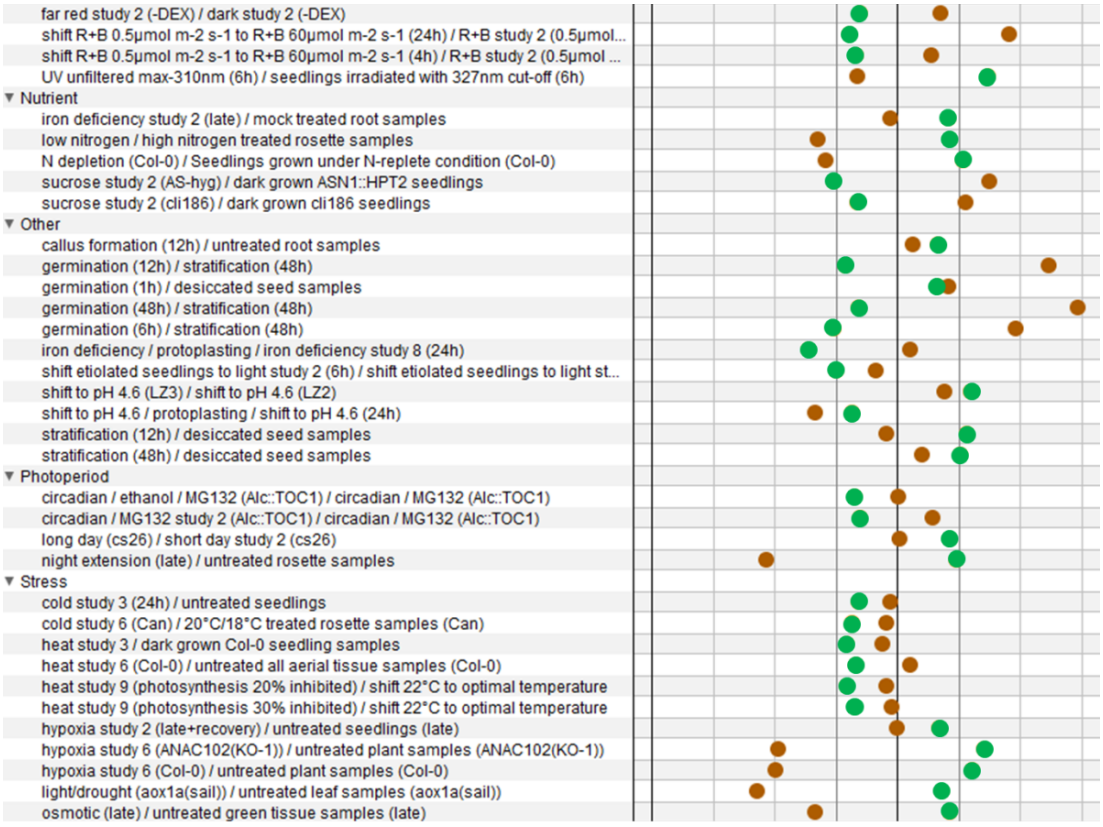

Figure 3-35: The result of coexpression's analysis of the 2CPA (brown) and PUX2 (Green) according to the Genevestigator. The 2CPA and PUX2 were negatively correlated under different abiotic stresses (cold, heat, hypoxia, drought and osmotic), different nutrient treatments, in different light qualities, photoperiod and germination studies. The direction to the left stands for down-regulation, and to the right represents up-regulation.

3.3.12 The eQTL and RIMB6 might be correlated via ASK9 and ASK16

Because the eQTL and the RIMBs have similar functions in regulating 2CPA expression, they might be involved in a same regulating network in the plant cell. A prediction of the relationships of the eQTL and all the RIMBs was given by using Genemaina database. Interestingly, the eQTL and RIMB6 was correlated via ASK9 (ARABIDOPSIS SKP1-LIKE 9) and ASK16 (ARABIDOPSIS SKP1-LIKE 9) (Figure 3-36).

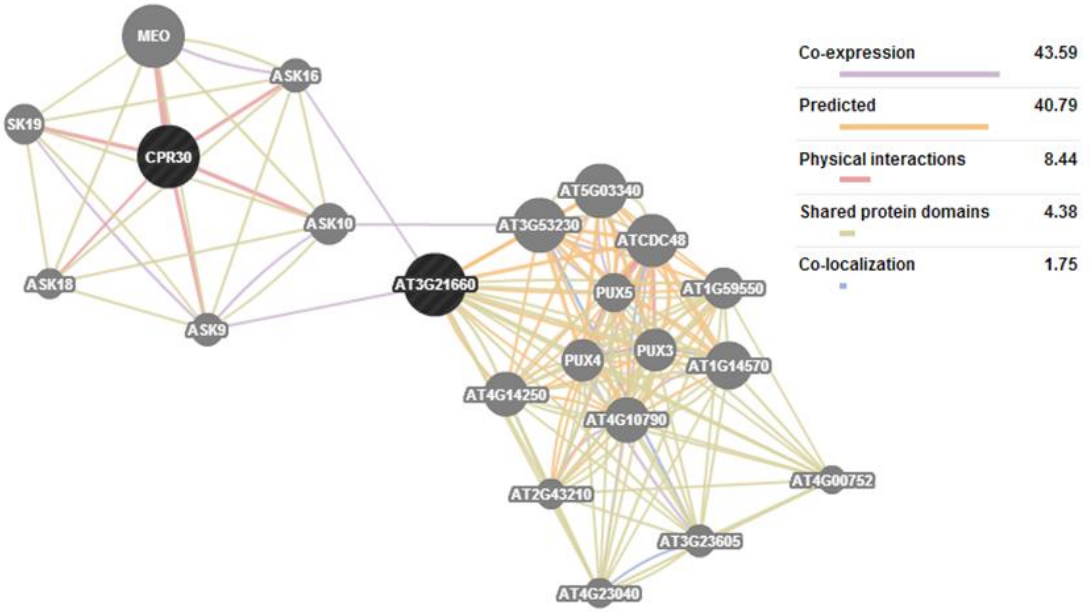

Figure 3-36: Prediction of the relationship of the eQTL (At3g21660) and RIMB6 (CPR30) according to the Genemania database (GEO accession: GSE15617). The CPR30 physically interacted with 6 S-phase kinase-associated proteins (SKP), among which ASK9 and ASK16 were coexpressed with the eQTL (At3g21660).

RIMB6 (CPR30) was already known to interact with ASK9 and ASK16 physically, which was proved by yeast-two-hybrid (Guo et al., 2009). In addition, according to the result of the microarray data the expression of germinating Arabidopsis seeds (GEO accession: GSE30223) the eQTL is coexpressed with ASK9 (Narsai et al., 2009). Furthermore according to the microarray data GSE15617 on GEO, the eQTL is also coexpressed with ASK16 (Kram et al., 2009).

The coexpression of the eQTL, ASK9 and ASK16 was further confirmed by using response viewer of genevestigator database. At all the developmental stages the eQTL, ASK9 and ASK16 were expressed on a low level, all levels of expression (signal intensity on 22k array) were below 9.0 (Figure 3-37). All the three genes have highest expression at the mature siliques stage (8.0, 8.1 and 8.7 respectively).

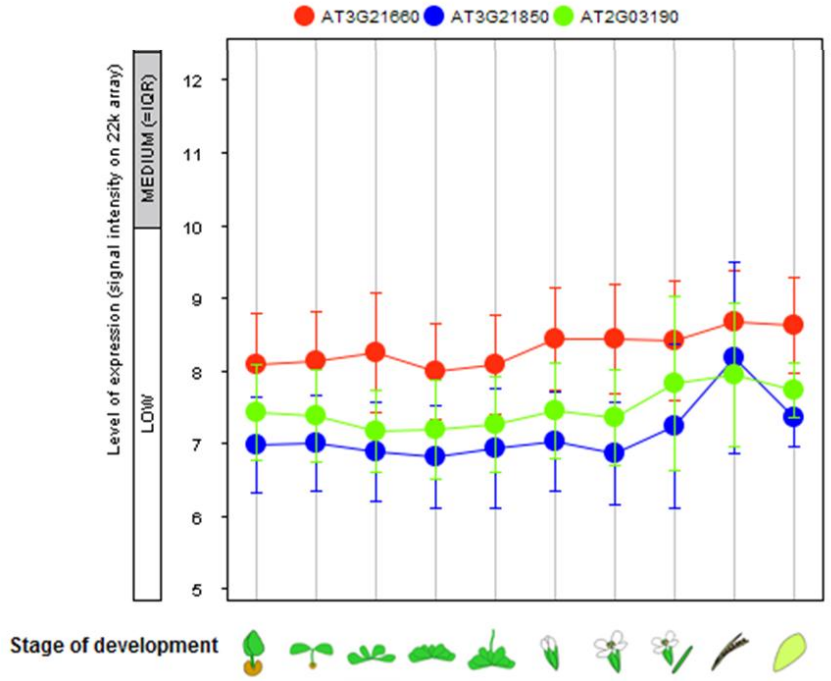

Figure 3-37: The eQTL (red, At3g21660), ASK9 (blue, At3g21850) and ASK16 (green, At2g03190) are coexpressed at all stages of development according to the analysis of genevestigator. The 3 genes are expressed on a low level at the stages of germinated seed, seedling, young rosette, developed rosette stage, bolting stage, young flow stage, developed flower stage, flower and siliques, mature siliques stage, and senescence stage. At mature siliques stage, the eQTL, ASK9 and ASK16 express at highest level.

The microarray data of the expression of the eQTL, ASK9 and ASK16 on Genevestigator was displayed across different samples and experiments, and exhibited coexpression of the three genes (Figure 3-38). In most experiments the eQTL, ASK9 and ASK16 were expressed on low levels, which was set as lower than 10 of the signal intensity on 22k array. However the ASK16 had much higher expression levels than the eQTL and ASK9 in the embryo and endosperm studies. For instance, in suspensor of embryo and chalazal endosperm the expression level of ASK16 were up to 13 and 14 respectively (the medium level was set up to 12.3), while the levels of the eQTL and ASK9 were lower than 9.

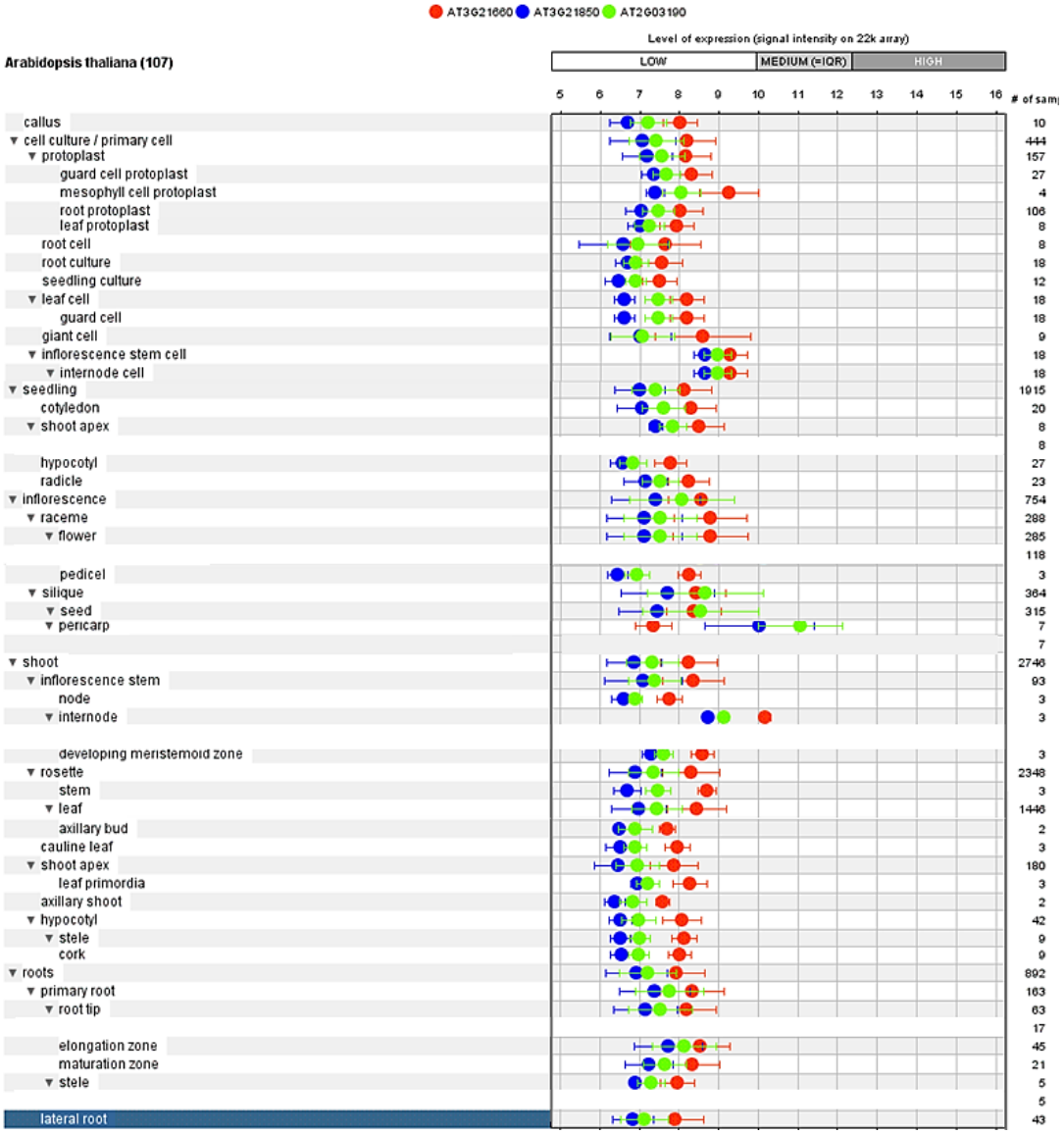

Figure 3-38: The expression levels of the eQTL (red, At3g21660), ASK9 (blue, At3g21850) and ASK16 (green, At2g03190) across selected samples and experiments on Genevestigator. The signal intensity was set according on a 22k array. In most samples the 3 genes were expressed on similar levels and they showed a same trend across different parts and developmental stages of plant.

3.4 Identification and characterization of mutant *rimb3*

3.4.1 Co-segregation analysis of low luciferase and chlorosis phenotype

The *rimb3* mutant line (Col-0 background) was crossed to the accession L*er*. A co-segregation analysis was subsequently performed with a population of 700 F2 plant of *rimb3* x L*er*. In this population 563 plants were wildtype like, whilst 137 displayed defective growth, which according to the Mendelian ratio in 3:1. It was therefore verified that the mutation inherited as a single recessive locus.

20 plants demonstrating chlorosis phenotype and 40 wildtype like plants were selected and their seeds were cultivated on MS medium in 96 wells microtiter plats. Quantification of luciferase activity was performed in 10 day-old seedlings. From the 20 lines of chlorosis plants (Figure 3-39), all the offspring demonstrated low luciferase activity (30 - 50% relative to T19-2), while about 20% offspring of the 40 wildtype like plants showed low luciferase activity. The co-segregation of low luciferase and chlorosis phenotype was confirmed.

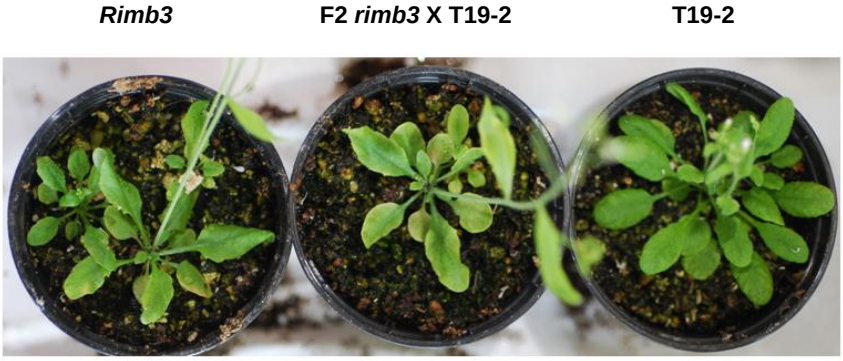

Figure 3-39: An example of co-segregated F2 plant of *rimb3* X T19-2. The plants in the middle were from the F2 generation of *rimb3* X T19-2. It demonstrated a typical phenotype of *rimb3* : abnormal leaves and chlorosis. About 20% of the F2 plants were phenotypically like *rimb3.*

3.4.2 Genetic mapping of *rimb3* with next generation sequencing

3.4.2.1 Selection of the individuals bearing *rimb3* allele

Since the phenotype of the mutant line *rimb3* was not sufficient to distinguish the mutant-phenotypical plants in the F2 Population and the eQTL also disturbed the mapping of *rimb3*, a rescreening of F3 population for low luciferace activity was performed to ensure that all plants in the mapping population were bearing the mutant allele and therefore the plants of F3 generation was used for the one step genomic sequencing. 200 lines with low luciferase activity in F2 population were selected. Each line was checked with a SSLP marker (cer455923) representing the eQTL on top arm of chromosome III, and only the lines with pure Col-0 genetic background on the eQTL position were selected.

In addition, PCR with a pair of specific primers binding to luciferase sequence was performed to confirm that all the samples contain the luciferase reporter gene. Their low luciferase activities were decided by the homozygous recessive mutant locus.

3.4.2.2 Isolation of nuclei DNA

From each line approximately 30 F3 plants were grown in poor-soil. At an age of four weeks the plants were harvested and pooled into 5 groups according to the capacity of nuclei DNA isolation method. DNA isolation was performed via nuclei isolation to avoid the noise of plastid DNA. The quality was verified using nanophotometer and electrophoresis on an agarose gel, on which eight clear bands with sizes over 10 kb were shown (Figure 3-40).

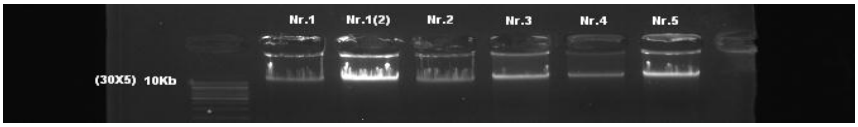

Figure 3-40: Test of DNA qualities of the sequencing samples. The DNA of 5 samples showed clear bands over 10 kb on agarose 1.2% gel indicating sufficient qualities of the DNA.

3.4.3 One step sequencing with Illumina G2 Analyzer

All the samples from 5 groups were pooled equally for sequencing, from which 1.6 ug of DNA were taken for sequencing with an Illumina G2 Analyzer by Dr. Rowan Beth (Max-Planck-Institut für Entwicklungsbiologie, Tübingen, Germany). After aligning the reads to the Col-0 reference sequence with SHORE map flowcell, the sequencing processes were accomplished with over 30 million raw reads, which were averagely 100 bp long. Consequently the data of the sequencing results covered 19x of the Arabidopsis genome.

3.4.3.1 Genetic mapping with the sequencing results

The polymorphisms (SNPs and Indels) were analyzed, through that a consensus list was finished. (See appendix) With the consensus subset of marker positions between the mapping population and L*er* marker list, the allele frequency of Col-0 alleles was plotted across the genome by SHOREmap_interval.pl. The Col-0 allele frequency was plotted on a map with windows size of 200kb, in which the allele frequency across the genome was around 50% everywhere (Figure 3-41).

On chromosome I, the centromere region between 14 and 15 Mb was enriched for Col-0 alleles. Similarly, the frequencies of Col-0 alleles were also slightly higher than L*er* alleles on the centromere regions 14 Mb and 3 Mb of on chromosome III and IV. All the data on centromere regions were excluded from the further analysis.

On chromosome IV, 5 regions (around 0.1 Mb, 0.5Mb, 1Mb, 4.5Mb and 6Mb) seemed to be enriched for Col-0 alleles (Figure 3-41). It was assumed that these 5 regions on chromosome IV could be the candidate regions of RIMB3.

SNPs from the L*er* parent were removed, and the new SNPs and Indel polymorphism on the chromosome IV were analyzed (Table 3-3). 62 new non-synonymous SNPs were

discovered in coding sequences, among which five SNPs were located near the five candidate regions (Table 3-4).

Table 3-3: New SNPs on chromosome IV. The detected nonsynonymous new SNPs for mapping RIMB3 were displayed till 7Mb on chromosome IV. 62 new nonsynonymous SNPs were discovered in the mapping population, among which 12 new SNPs were within the candidate region of RIMB3.

Position	Reference base	Alternate base	Gene	Reference aa	New aa
539608	G	A	AT4G01290	P	L
561780	T	G	AT4G01350	C	G
875169	C	A	AT4G02000	L	I
1399785	C	T	AT4G03165	E	K
1662039	T	G	AT4G03740	N	H
2580327	T	C	AT4G05040	F	S
3318702	C	T	AT4G06526	R	Q
5388336	T	C	AT4G08480	T	A
5389422	T	C	AT4G08480	I	V
5389437	T	G	AT4G08480	I	L
6025041	T	C	AT4G09520	R	G
7395435	A	C	AT4G12460	I	L

Table 3-4: Five candidate SNPs on chromosome IV. Five SNPs were detected near the five candidate regions enriched for Col-0 alleles. They were considered as candidate loci of RIMB3. Besides AT4G08480, which showed 3 amino acid substations in the sequencing result, all 3 candidates contained only one amino acid substitution.

Gene	Position	na mutant		aa mutant		code
AT4G01290	539608	G	A	P	L	AAC
AT4G01350	561780	T	G	C	G	GGC
AT4G03165	1399785	C	T	E	K	AGG
AT4G08480	5388336	T	C	T	A	ACA
	5389422	T	C	I	V	CAA
	5389437	T	G	I	L	AAC
AT4G09520	6025041	T	C	R	G	GAA

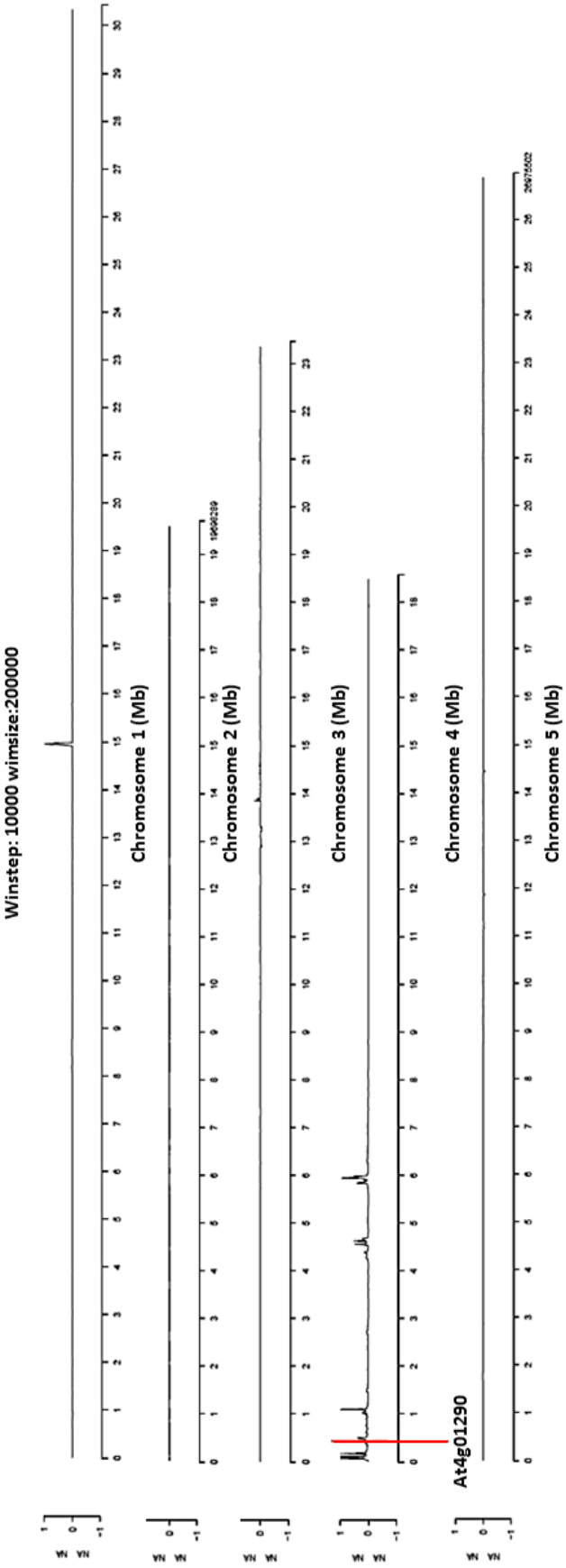

Figure 3-41: Map of Col-0 allele frequency cross the Arabidopsis genome with windows size of 200kb. Besides the top arm of chromosome IV the Col-0 allele frequency across the genome was around 50% everywhere. On the chromosome IV there were 5 regions indicated by peaks (at the position around 0.1 Mb, 0.5Mb, 1Mb, 4.5Mb and 6Mb), where it enriched for Col-0 alleles.

3.4.3.1 Identification of final candidate locus with resequencing of all the candidate loci

In order to check, whether the SNPs exist also in T19-2, all the candidates genes were re-sequenced with genomic DNA of the mutant line rimb3 and the parental line T19-2.

The re-sequencing results showed that in *rimb3*, only the locus AT4G01290 contains a new SNP, which introduced a G to A substitution leading a P to L amino acid substitution (Figures 3-42 and 3-43). It was assumed that the G to A substitution is the point mutation generated by EMS mutagenesis (Heiber et al., 2007) and that this substitution is reason of photooxidative damage and the chlorosis phenotype of rimb3 mutants.

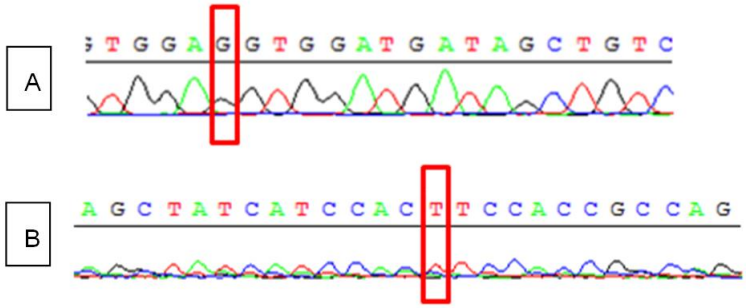

Figure 3-42: The G to A substitution in AT4G01290 in *rimb3* was verified with re-sequencing. A: Result of forward sequencing of AT4G01290 in T19-2 showed the sequence according to wildtype Col-0. B: Result of reverse sequencing of AT4G01290 in rimb3 demonstrated a T on the position of 539608 on top arm of chromosome IV. This substitution was considered as the point mutation introduced by EMS mutagenesis in rimb3.

Figure 3-43: A G to A substitution was introduced in *rimb3* at the position 539608 on top arm of chromosome VI. The substitution introduced a amino acid exchange from proline to leucine.

The gene At4g01290 encodes an unknown protein in *Arabidopsis thaliana*. According to the prediction with Conserved Domain Database of NCBI, this protein may contain a

domain: topoisomorase II-associated protein domain (PAT1), which is necessary for accurate chromosome transmission during cell division. The position of the possible PAT1 domain is about 1350 bp after the G to A substitution to C-terminal (Figure 3-44).

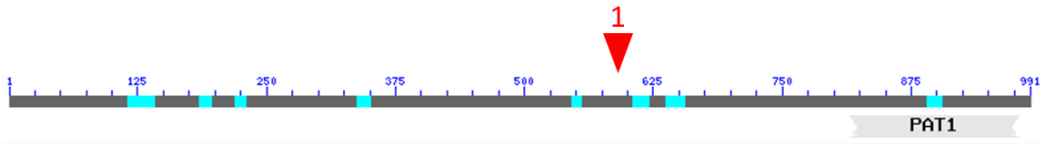

Figure 3-44: The predicted structure and conserved domain of AT4G01290. There might be a PAT1 domain at end of the sequence. The P to L substitution was occurred at the position 580.

3.4.4 Transcript abundance analysis of RIMB3 and 2CPA

The T-DNA insertion line SALK_038452 was obtained from the Nottinghan Arabidopsis Stock Centre NASC (http://arabidopsis.info/). In this line the T-DNA of pROK2 was inserted on the position 539670 bp on chromosome IV, which is in the longest exon of locus At4g01290 (Figure 3-45). This insertion was supposed to stop the expression before the PAT1 domain.

Figure 3-45: The T-DNA line SALK_038452. in the T-DNA line SALK_038452 the T-DNA was inserted in the largest exon before the PAT1 domain. The function of the locus AT4G01290 was disturbed in this line.

After genotyping, the homozygote T-DNA insertion lines and wildtype were distinguished and separated. The selected wildtype was used as positive control in further analyses. A transcript analysis of 2CPA was performed in wildtype and in the At4g01290 knock-out line SALK_038452. *Actin7* was used as housekeeping gene (Figure 3-46). The transcript level of 2CPA was detected to be clearly decreased (75%) in the knock-out line compared to its level in the wildtype. The result indicated that the candidate locus At4g01290 could act as positive regulator of 2CPA expression in Arabidopsis. Together with the re-

sults of genetic mapping by sequencing, it is concluded that in *rimb3* the locus At4g01290 was mutagenized by EMS and contains a G to A substitution.

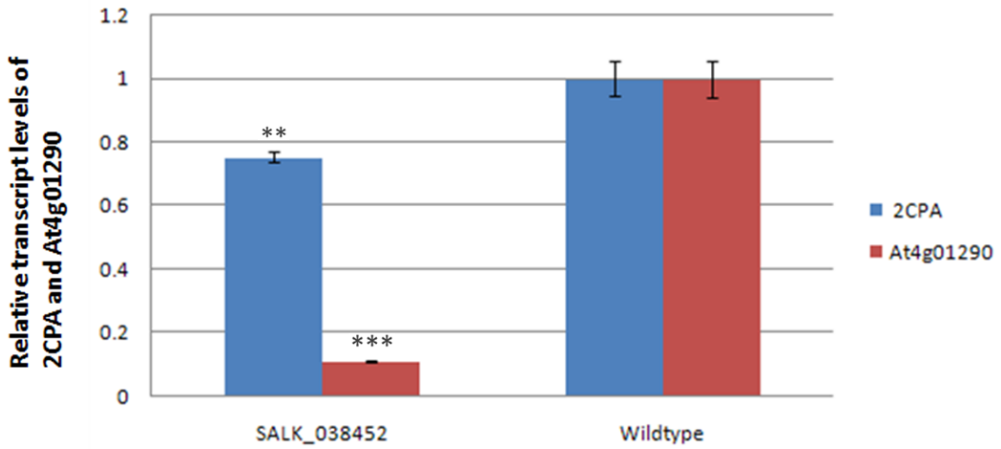

Figure 3-46: Relative transcript analysis of 2CPA and At4g01290 in wildtype Col-0 and the At4g01290 knock-out line SALK_038452. In the knock-out line 2CPA expression was down-regulate on 75% relative to its expression in wildtype. The data are means of 7-10 samples (± SD) grown in three independent experiments. **and *** indicate significant differences from the value of wildtype Col-0 (t-test), ** represents the significant difference P<0.01 and ***represents the significant difference P<0.001.

3.4.5 Coexpression analysis of RIMB3 and RIMB1 (RCD1)

The expression pattern of RIMB3 (At4g01290) and the previously identified RIMB1 (RCD1, At1g32230, Hiltscher, 2011) was analyzed using response viewer of Genevestigator database. At the stages of germinated seed, seedling, young rosette, developed rosette stage, bolting stage, young flow stage, developed flower stage, flower and siliques, mature siliques stage, and senescence stage both of REMB3 and RIMB1 were highly expressed, and the all levels of expression (signal intensity on 22k array) were over 12.5 (Figure 3-47). Both of RIMB3 and RIMB1 have highest expression at the senescence stage (13.2 and 14.1 respectively).

Under various stress treatments the RIMB1 and RIMB3 seemed to be coexpressed (Figure 3-48). Under cold, drought and light/drought stresses, the expressions of RIMB3 and RIMB1 were induced, while heat stress represses the expression of the both genes.

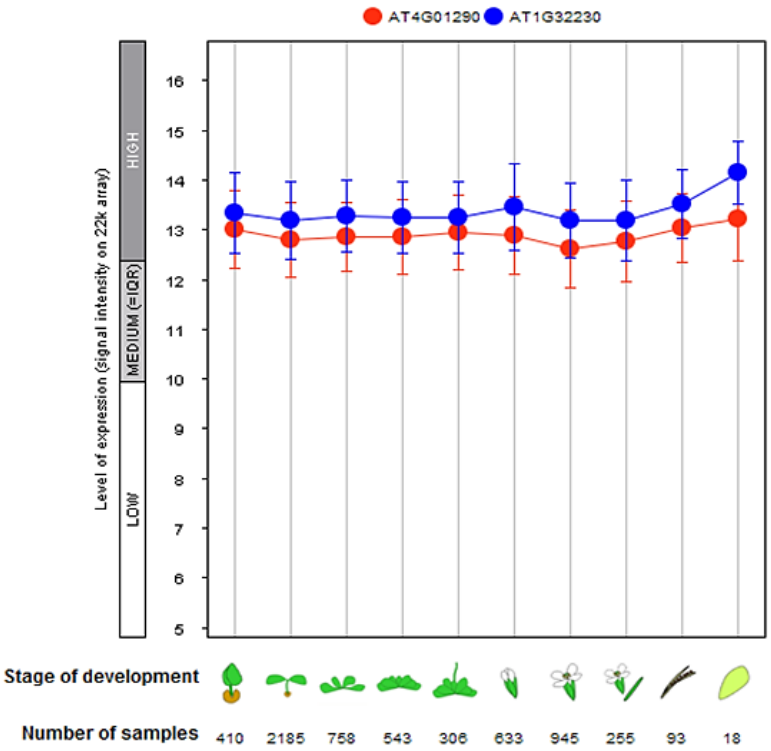

Figure 3-47: RIMB1 and RIMB3 are coexpressed at all stages of development according to the analysis of genevestigator. The microarray data showed the expression levels of RIMB1 and RIMB3 around 13. At senescence stage, RIMB1 and RIMB3 are expressed at highest level.

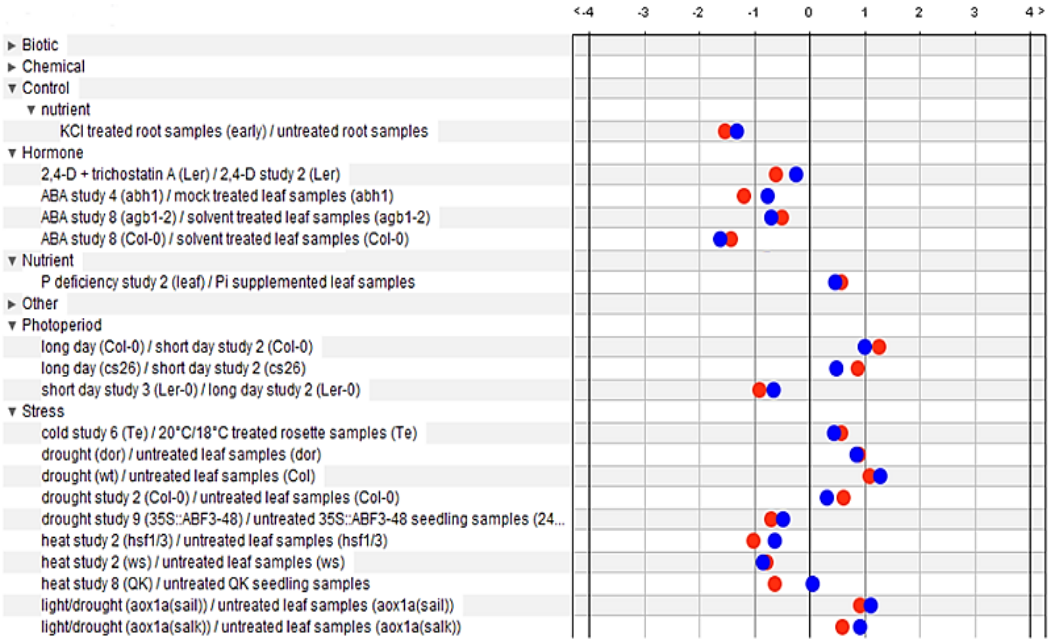

Figure 3-48: RIMB1 and RIMB3 are clearly coexpressed: at KCl treatment, ABA treatment, different photoperiod treatments, cold stress, drought, heat and light stresses. The analysis was performed with the database Genevestigator. The direction to the left stands for down-regulation, and to the right represents up-regulation.

By using the online database Genemania, the relationship of RIMB1 (RCD1, At1g32230) and RIMB3 (At4g01290) was predicted. As a result, the RIMB1 and RIMB3 are coexpressed with a weight of 1.2 (Figure 3-49). The data was collected from GEO accession GSE19520.

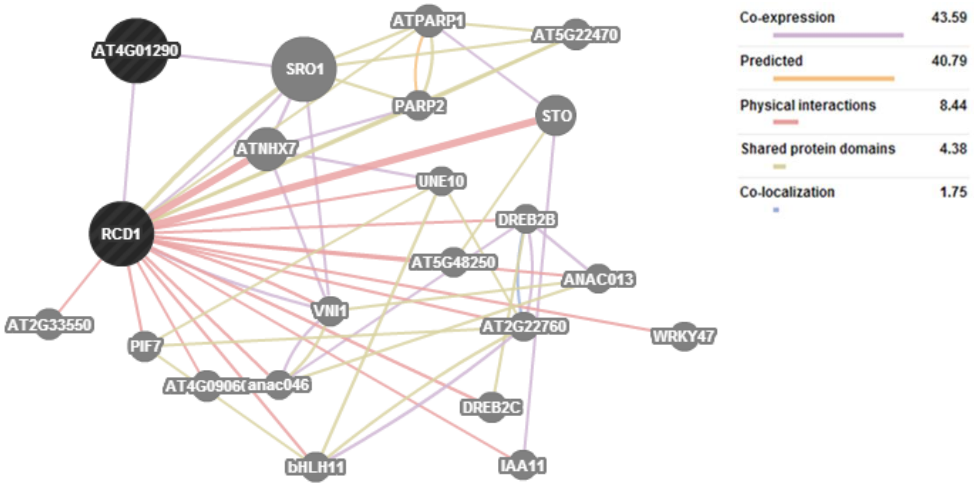

Figure 3-49: According to the analysis of Genemania (http://www.genemania.org/), RIMB1 (RCD1) and RIMB3 (At4g01290) are directly coexpressed. The data was collected from GEO accession GSE19520.

To check the relative expression level of RIMB3 in *rimb1* and rcd1, a transcript analysis was performed (Figure 3-50), while the relative expression level of RIMB1 was checked in *rimb3* (Figure 3-51). The expression of RIMB3 in *rcd1* was increased clearly: the relative transcript level of RIMB3 was up to 122% compared to wildtype Col-0, while the transcript level of RIMB3 in *rimb1* did not clearly differ from the transcript level of RIMB3 in Col-0 (Figure 3-51). In transcript analysis of RIMB1, the relative transcript level of RIMB1 in *rimb3* was significantly decreased (79%) in comparison to its level in Col-0 (Figure 3-52), suggesting that RIMB3 is an upstream regulator of RIMB1.

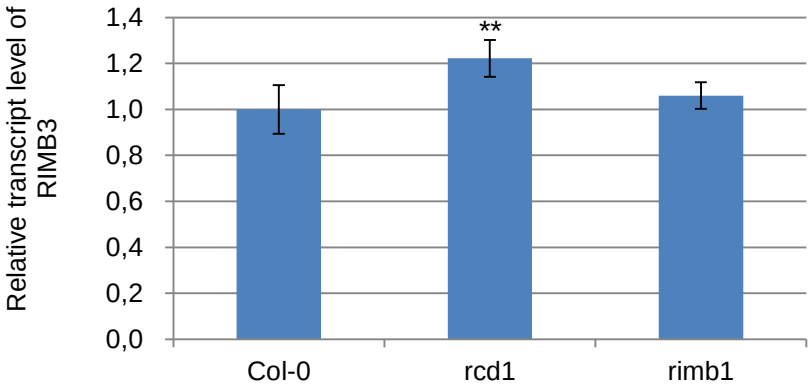

Figure 3-50: Relative transcript level of At4g01290 in wildtype, rimb1 and rcd1. The relative transcript level of At4g01290 in wildtype Col-0 was set as 100%. In the RCD knock-out line rcd1 the relative expression level of At4g01290 was clearly increased (122% relative to Col-0), while in the RIMB1 knock-out line rimb1 the At4g01290 expression did not show significant increase in comparison to in Col-0. The data are means of 7-10 samples (± SD) grown in three independent experiments. ** indicates significant differences from the transcript value in Col-0. (t-test, P<0.01)

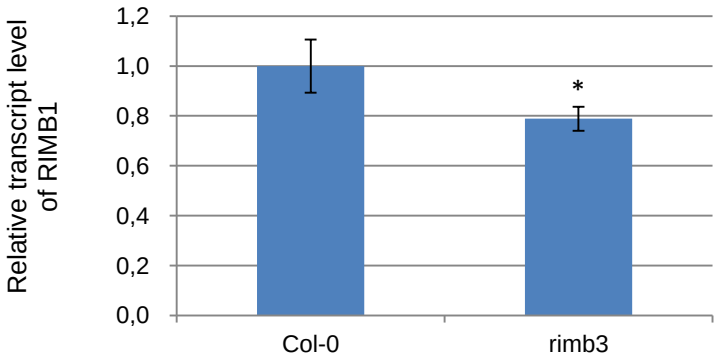

Figure 3-51: Relative transcript level of RIMB1 in wildtype and rimb3. The relative transcript level of RIMB1 in wildtype Col-0 was set as 100%. The relative transcript level of RIMB1 in rimb3 was dropped on 79% compared to its level in Col-0. The data are means of 7-10 samples (± SD) grown in three independent experiments. * represents significant differences from the transcript value in Col-0 (t-test, P<0.05)

3.4.6 Coexpression analysis of RIMB3 and ATCDC48

An coexpression analysis was performed with Genemania (http://www.genemania.org/) , to test the level of coexpression of RIMB3 and ATCDC48 (Figure 3-52). The microarray data of GEO accession GSE30223 was used in this analysis. The prediction demonstrated that RIMB3 (At4g01290) is coexpressed with ATCDC48, which physically interacts with PUX proteins.

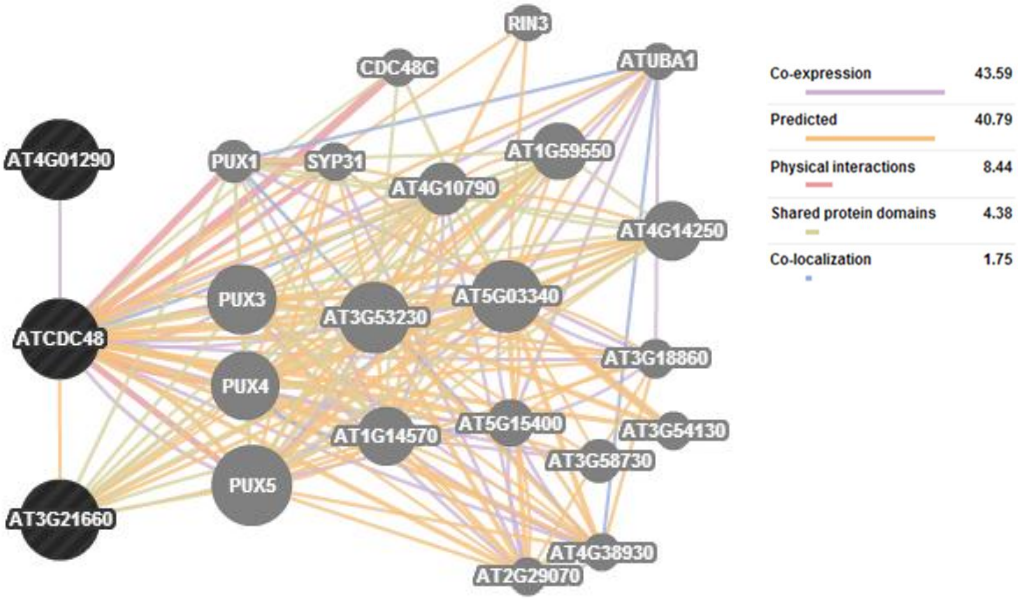

Figure 3-52: RIMB3 (At4g01290) is coexpressed with ATCDC48 (At3g09840) according to the analysis of the Genemania (http://www.genemania.org/). The analysis was based on the microarray data of GEO accession GSE277.

4 Discussion

4.1 Genetic mapping of loci RIMB3, RIMB6 and the eQTL of 2CPA

In this project, the loci of RIMB3, RIMB6 and an eQTL between the Arabidopsis accessions Col-0 and L*er* were mapped based on their effect on 2CPA promoter regulation.

The eQTL was the first locus mapped in this project. It followed the previous RIMB3 project, and was mapped with SSLP markers according to Jander et al., (2002). The initial mapping process was achieved with 29 SSLP markers (Figure 3-17). The final candidate region was determined on a 77 kb region on chromosome IV. Since there was no suitable SSLP marker to apply, the candidate loci were tested for amino acid polymorphisms between the Arabidopsis accessions Col-0 and L*er* using the genomic sequence information provided by the Cereon/Monsanto Arabidopsis Polymorphism Collections (http://www.arabidopsis.org/browse/Cereon/). Four final candidate loci were identified. T-DNA knock-down line for the loci was obtained by transcript analysis of 2CPA. The locus AT3G21660 correlated with decreased 2CPA expression and, therefore, eQTL locus was identified to regulate 2CPA expression. It encodes a PUX-like protein (Figure 3-26).

Additionally, the mutation of *rimb6* was mapped by next generation sequencing. The plants of *rimb6* showed a very clear and unique mutant phenotype (Figure 3-1), which made it possible to select the individuals from F2 generation bearing homozygote mutant locus in the genome and to apply the selected F2 plants directly to genetic mapping of one step sequencing with Illumina HiSeq 2000 analyzer. The coverage of 57x of the Arabidopsis genome ensured that a single final candidate of the mutant locus can be di-

rectly identified with the sequencing result. As a result the AT4G12560 was identified as final candidate of RIMB6. It encodes a constitutive expresser of PR genes CPR30.

By next generation sequencing RIMB3 was identified (Figure 3-41). As the mutant phenotype of *rimb3* was not sufficient to surely pick up the individuals from F2 generation (Figure 3-1), the next generation of the selected individuals, which was F3 generation of *rimb3* X L*er*, was rescreened with luciferase assay. About 30 F3 plants of each line, which were confirmed to have low luciferase activity, were harvested and sequenced to map the mutant locus. Coverage of 19 x of the Arabidopsis genome was achieved, which demonstrated five candidate regions on chromosome IV. The loci, which were near the candidate regions and had new SNP in Col-0 genetic background, were re-sequenced in *rimb3* and its parental line T19-2 to confirm the new SNP. As final result, At4g01290 was identified to contain a new SNP that was introduced in T19-2 using EMS mutagenesis. In conclusion the AT4G01290 was considered as final candidate of RIMB3.

4.2 RIMB6

In the mutant *rimb6* the gene regulation is severely defected in the central chloroplast-to-nucleus signaling pathway (Heiber et al., 2007). RIMB6 activates 2CPA at the highest level on young developmental stages (Figures 3-8 and 3-9). However the mutant plant *rimb6* demonstrated more severely defected growth at mature stage (Figures 3-1 and 3-2). It is assumed that RIMB6 may negatively regulate an unknown factor, which defects the plant growth of Arabidopsis. The increasing defective effect on *rimb6* may be caused by the accumulation of this unknown factor. In this project the locus AT4G12560 (CPR30) was identified as final candidate of RIMB6, according to the mapping by one step genomic sequencing with the one step Illumina HiSeq 2000 (Figure 3-13).

In the previous study (Heiber et al., 2007), the abnormal shape of the leaves and increased ascorbate level, as well as accumulation of starch and anthocyanins in *rimb*6 were observed. It was concluded that RIMB6 is a general regulator of nuclear encoded chloroplast proteins.

In a previous part of the project, the leaf shape of *rimb6* was determined as a conditional phenotype depending on the soil supplemented with different amounts of mineral nutrients. On nutrient-rich soil, *rimb6* looked almost like wildtype, whereas on nutrient-poor soil it developed severe phenotype in the rosette stage (Hiltscher, 2011).

The conditional phenotype of *rimb6* under the growth condition in Berlin was confirmed. However on the nutrient-rich soil the *rimb6* also demonstrated a slight mutant phenotype of the leaves on rosette stage. This might indicate that the RIMB6 is a constitutive activator of 2CPA expression.

4.2.1 RIMB6 (CPR30) is a negative regulator of plant defense response system

The constitutive expresser of PR genes 30 (CPR30) was studied and designated by Guo et al., (2009). It was concluded that CPR30 negatively regulates both SA-dependent and SA-independent defense signaling in the plant cell.

Guo et al., (2009) concluded that enhanced disease susceptibility 1 (EDS1), phytoalexin deficient 4 (PAD4) and non-race-specific disease resistance 1 (NDR1), which are the key regulators of plant defense response in Arabidopsis, are directly or indirectly repressed by CPR30 (Gou et al., 2009). In *cpr30* mutant plants EDS1, PAD4 and NDR1 are activated. They consequently lead to the activation of both the basal and R-gene-mediated resistances. In addition, CPR30 regulates plant growth and disease resistance, via a PAD4-, EDS1- and NDR1-dependent, but SA-independent pathway (Guo et al., 2009). Furthermore, part of the SID2-mediated SA synthesis is also involved in the cpr30-activated disease resistance (Guo et al., 2009). Pathogen resistance response

consumes large amounts of energy in plant cells. It is repressed during normal growth and development conditions and in the absence of pathogens. In contrast, the pathogen resistance response is constitutively activated in the mutant line *cpr30*. This autoimmunity could be part of the reason of the typical *rimb6* phenotype like narrow leaves, stunted growth *et cetera* (Figure 3-1).

RIMB6 (also known as CPR1/CPR30) is an F-box protein containing two different F-box motifs which are needed for binding Arabidopsis-S-phase kinase-associated protein 1 (SKP1)-like proteins (ASK). It has be proven in *vivo* that CPR30 interacts with 11 ASK proteins (Guo et al., 2009).

In the SKP1-CULLIN1-F-box complex, F-box protein functions for the specificity of the complex, which is a multi-protein E3 ubiquitin ligase complex and catalyzes the ubiquitination of proteins destined for proteasomal degradation. F-box protein aggregates to target proteins independently of the SCF complex and binds to the SKP1 component, which is the bridging the proteins Cullin1 (Cul1) and RING-box protein 1 (Rbx1) (Willems et al., 2004). A horseshoe-shaped complex (Morgan, 2007), which is a multi-protein E3 ubiquitin ligase complex, is formed by F-box protein, SKP1, Cul1 and Rbx1. It allows the protein to be brought into proximity with the functional E2 protein. In addition, the F-box is also essential in regulating SCF activity during the process of the cell-cycle. Therefore, SCF levels are thought to remain constant throughout the cell-cycle.

As component of SCF complex, the CPR30 was also reported to control the stability of the nucleotide-binding domain and leucine-rich repeats containing proteins (NLRs) functioning as immune receptors in animals and plants. It is suggested that SCF complex-mediated stability control of plant NLR proteins is an important mechanism of regulating their protein levels and preventing autoimmunity (Cheng et al., 2011).

The further study on CPR30 concluded that with the form of SCF complex CPR30 negatively regulates accumulation of disease resistance (R) protein SNC1 (suppressor of

npr1-1 constitutive 1) by protein degradation in the absence of pathogen. The regulation of SNC1 by CPR30 is dependent on the 26S proteasome. This is proven with a protease inhibitor MG132 which stabilizes SNC1 and counteracts the implication of CPR1 on SNC1 (Gou et al., 2012).

It is concluded that RIMB6 (CPR30) positively regulates the expression of 2CPA, which plays an important role to scavenge the ROS in plant cell (Baier et al., 1997). As ROS are known to be involved in plant defense response system as second messenger, it is suggested that the RIMB6 (CPR30) may repress the plant defense response system also via decreased ROS level in plant cell. It is further assumed that RIMB6 controls the stability of an unknown repressor of 2CPA mediated by SCF complex.

4.2.2 RIMB6 is involved in cross-talk between redox signaling and plant defense response

Here, it can be concluded that the RIMB6 serves as sensor of fluctuating redox state of the electron acceptors of PSI and triggers a retrograde signal from chloroplast to nucleus in order to coordinate the nucleus and chloroplast. At the same time, RIMB6 is also a constitutive negative regulator of plant defense response, which requires a complex network of signaling, including calcium signaling. Calcium signaling is already reported to be involved in cross-talk with protein phosphorylation at the thylakoid (Stael et al., 2012), which may be connected to the chloroplast redox retrograde signaling. Since RIMB6 plays important roles both in redox signaling and plant defense response, it could be therefore a central factor of the cross-talk between these two systems.

4.2.3 RIMB6 is involved in the metal homeostasis system in plant cell

The *rimb6* displayed mutant phenotype was more severe on nutrient-poor soil than it did on nutrient–rich soil (Hiltscher, 2011). This indicated that mineral content in *rimb6* could affect its phenotype. Therefore, ICP-MS was applied to check the contents of mineral elements in the rosettes of *rimb6* plants, grown on both soil types. The results illustrated

clear variation of the contents of Cd, Cr, Cu, Fe, Mn, Mo, Se, Ni and Zn in the plant tissue.

Fe, Cu, Zn, and Ni are known as essential micronutrients at certain concentrations. They are involved in the functional activities of many proteins involved in keeping growth and development of living organisms. However, at excess concentrations, these metal ions can be detrimental to plants (Choudhuryl, 2005).

Among the heavy metals tested in this project, Cr, Cu and Fe are redox active, while Cd, Zn and Ni are redox inactive heavy metals (Hossain M. A., 2012). The redox active heavy metals Cu, Fe and Cr are directly involved in the redox reaction in cells and result in the formation of $O_2^{\bullet -}$, and subsequently in H_2O_2 and $^{\bullet}OH$ production, via the Haber-Weiss and Fenton reactions (Schutzendubel and Polle, 2002). In *rimb6* plants growing on nutrient-poor soil the Cr content was 2-fold higher than it was in the control line T19-2, suggesting that Cr caused high level of ROS in *rimb6*. On contrary, high contents of redox inactive heavy metals, such as Cd and Ni in this study, also result in oxidative stress through indirect mechanisms such as interaction with the antioxidant defense system, disturbing effect on the electron transport chain, and initiation of lipid peroxidation (Hall, 2002; Dal Corso et al., 2005). The Ni content in *rimb6* was six times as it was in T19-2, which could introduce severe disruption to the electron transport chain and further may cause a redox imbalance in the plant cell. The significant mutant phenotype of *rimb6* could be partially due to the heavy metal stresses in the plant cell.

It is suggested that metal homeostasis is changed by the disruption in regulation of metal transporters, antiporters or channels on plasma membrane, for instance AtPDR8 (AT1G59870), AtIRT1 (AT4G19690) and CNG channels.

4.2.4 AtPDR8 may be repressed in *rimb6*

The ATP-binding cassette (ABC) transporter AtPDR8, a Cd transporter on plasma membrane, was determined as a Cd extrusion pump conferring heavy metal resistance in

Arabidopsis (Kim et al., 2007). Interestingly, if AtPDR8 was knocked out, the plants showed hypersensitive cell death upon pathogen infection. This may be connected to the plant defense system, and the AtPDR8 could be also correlated with RIMB6, as RIMB6 is a constitutive repressor of plant defense system. The contents of Cd in the plants of *rimb6* grown on nutrient-poor and nutrient-rich soil illustrated diverse directions: on the poor soil the *rimb6* plant contained less Cd in comparison to T19-2 plant, whereas on soil supplemented with normal amount of mineral nutrients *rimb6* had much higher Cd content than T19-2. The data suggested that AtPDR8 was up-regulated on nutrient-poor condition and repressed in nutrient-rich condition in *rimb6*. High expression of the defense response genes, PR-1, PR-2 for instance, was observed in the *atpdr8* mutants within 10 h after infection with the virulent bacterial pathogen, *Pseudomonas syringae* (Kim et al., 2007). AtPDR8 is considered then as a key factor triggering cell death in the defense response and suggested that AtPDR8 transports some substance which is closely related to the response of plants to pathogens (Kobae et al., 2006).

It is concluded that RIMB6 responds to different nutrient conditions and it may be negatively correlated with AtPDR8. RIMB6 may indirectly repress AtPDR8 expression or AtPDR8 activity under nutrient-poor condition and activate the AtPDR8 expression or protein activity under normal (nutrient-rich) condition. Furthermore AtPDR8 represses PR genes which are constitutively repressed by RIMB6 and activates the plant defense system (Figure 4-1). Summarized, RIMB6 might be a negative regulator of plant defense system mediated by AtPDR8.

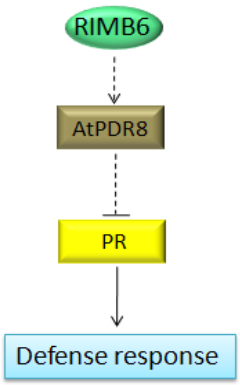

Figure 4-1: Under nutrient-rich condition, RIMB6 represses the plant defense system. RIMB6 could positively correlate with AtPDR8 which constitutively suppresses PR1 and PR2, the activators of plant defense system.

4.2.5 AtIRT1 and CNG channels might be disturbed in *rimb6*

Apart from Cd, some other metals, for instance Cr, Cu, Fe, Mn, Mo, Se, Ni and Zn, also showed significant variations between *rimb6* and T19-2 (Figure 3-10). This indicated, not only AtPDR8 was disturbed, the function of other metal transporters in *rimb6* were also changed.

In addition to AtPDR8, Iron-Regulated Transporter 1 (AtIRT1), a member of the Zrt/Irt-like protein (ZIP) family of transporters (Vert et al., 2002), was reported as a primary iron uptaking transporter in the root, and to mediate Ni accumulation in Arabidopsis (Nishida et al., 2011). The specificity of AtIRTs are broad for divalent heavy metals, which mediate the accumulation of Zn, Mn, Cd and Co under Fe-deficient conditions (Vert et al., 2009). Competition between Fe^{2+} and Ni^{2+} occurs often within membrane transport systems (Gendre et al., 2007). According to results of the ICP-MS, the plants of *rimb6* grown on poor soil contained Ni about 5-fold higher than the plants of T19-2. It is suggested that a Ni transporter AtIRT1 on plasma membrane was probably repressed in *rimb6*. Therefore, RIMB6 is suggested to repressed indirectly the AtIRT1. Loss of RIMB6 may activate Fe and Ni transporter AtIRT1 and may have caused high accumulation of Ni in *rimb6*.

Additionally to metal transporter on the plasma membrane of plants, some cyclic nucleotide-gated ion channels (CNG channels) have been identified to keep metal homeostasis in plant cells (Schuurink et al., 1998; Arazi et al., 1999; Kohler et al., 1999). These channels appear to be plasma membrane-located and non-selective, and they are permeable to both monovalent and divalent cations (Schuurink et al., 1998, Arazi et al., 1999). They may also be affected by the loss of RIMB6, and it may consequently cause changes of metal contents nonspecifically.

Up to now, no direct connection could be found between 2CPA, AtIRT1 and CNG channels. It is assumed that RIMB6 might trigger a regulating network, in which 2CPA, AtIRT1 and proteins of CNG channels are all involved.

To confirm this hypothesis, analyses of coexpression and in *vivo* interaction between RIMB6 and AtPDR8, AtIRT1 and the proteins of CNG channels need to be performed.

4.2.6 Possible regulation network of RIMB6 with eQTL

It is summarized that RIMB6 triggers a retrograde signal to nucleus in a development-dependent way, to regulate the 2CPA expression in responses to the changes of redox state of the electron acceptors of PSI caused by environmental stimulus. In parallel, RIMB6 also regulates the plant defense system and the metal homeostasis in plant cell (Figure 4-2). RIMB6 may up-regulate the expression of the Cr transporter AtPDR8 which constitutively represses the PR genes. Furthermore, RIMB6 interacts with SKP1 and forms a SCF complex together with SKP1 and Cullin1. By protein degradation, RIMB6 negatively regulates accumulation of R protein SNC1 with the form of SCF complex in the absence of pathogen. The expression of 2CPA is positively regulated by RIMB6 via unknown 2CPA repressor which is negatively regulated by RIMB6. Therefore, RIMB6 activates the 2CPA expression in plant cells to detoxify the ROS which is a second messenger to activate the plant defense system. Together with negative regulation to the R protein SNC1 and PR genes, RIMB6 is a constitutive repressor of plant autoimmunity. In addition, RIMB6 is involved in metal homeostasis in plant cell, in which RIMB6 may repress the AtIRT1 and CNG channels besides AtPDR8. The presented data proposed a cross-talk between chloroplast retrograde signaling, regulation of plant defense response and metal homeostasis in plant cells is established mediated by RIMB6.

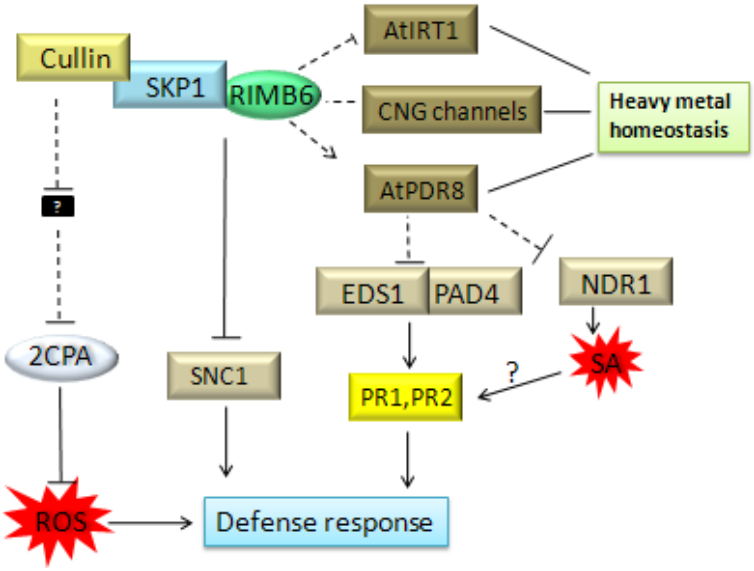

Figure 4-2: The hypothesis of regulation network of RIMB6. Together with Cullin and SKP1, RIMB6 forms a SCF complex. The SCF complex activates 2CPA expression via an unknown repressor of 2CPA, and 2CPA detoxifies the ROS that acts as second messenger to activate plant defense response. The SCF complex might activate the expression of the Cd transporter AtPDR8, which represses PR genes via a PAD4-, EDS1- and NDR1-dependent pathway. The SCF complex also represses an R protein SNC1. Through repression to SNC1 and PR genes, RIMB6 constitutively represses plant defense response. In addition, RIMB6 might negatively regulate AtIRT1 and maybe interact with CNG channels. Together with up-regulation to AtPDR8, RIMB6 is involved in regulation of metal homeostasis in plant cell.

4.3 The eQTL in 2CPA regulation

Using the F2 of the cross *rimb3* x L*er*, an expression quantitative locus (eQTL) At3g21660 was identified based on natural variation between the Arabidopsis accessions Col-0 and L*er*. The homozygote eQTL on L*er* background caused low expression of the reporter gene luciferase in the mapping population with F2 plant of the *rimb3* x L*er*. However, the plants bearing homozygote L*er* background on the position of the eQTL did not exhibit any visible phenotype, thus rescreening of the luciferase activities in the population of next generation was often performed during the SSLP mapping. The transcript analysis of 2CPA in the T-DNA knock-out line of the eQTL confirmed the positive regulation of the eQTL to 2CPA in Col-0.

4.3.1 Natural variation of At3g21660

Compared to the sequence of At3g21660 in Col-0, a short sequence of 25 bp is inserted at position 33 of the gene At3g21660 in L*er*. In the sequence of At3g21660, natural variation occurs often between different accessions according to Arabidopsis SNP Sequence Viewer (http://natural.salk.edu/cgi-bin/snp.cgi). Juszczak et al. studied recently the natural variation in chloroplasts antioxidant protection system, and observed variation of 2CPA expression in different Arabidopsis accessions (Juszczak et al., 2012). The 2CPA expression in L*er* was 45% relative to Col-0 in the study. The 25 bp short insertion was inserted at the position 33 of the sequence of the eQTL in L*er* (Figure 3-24). This insertion introduced a frameshift at beginning of the gene, therefore a Col-0 specific 2CPA inducer could be deactivated in L*er* or a L*er* specific 2CPA repressor might be deactivated in Col-0.

4.3.2 The eQTL positively regulates 2-Cys-peroxiredoxin expression

The transcript analysis in the eQTL knock-down line showed a significantly lower level of 2CPA and 2CPB expression compared with the wildtype Col-0, while the transcript levels of sAPx and tAPx were similar to the transcript level in wild type Col-0. This could prove that the eQTL is a Col-0 specific positive regulator of 2-Cys-peroxiredoxins but it has no regulating effect on ascorbate peroxidase expression (Figure 4-3). Furthermore, the effect of the eQTL on expressions of other antioxidant enzymes need to be checked to determine the role of the eQTL in the antioxidant system of plant cells, for example copper/zinc superoxide dismutase (Csd2), peroxiredoxin Q, type II peroxiredoxin E and glutathione peroxidase 1.

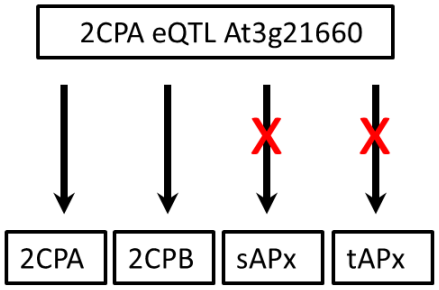

Figure 4-3: The eQTL specifically activates expression of peroxiredoxins. There was no effect of the eQTL to transcript levels of ascorbate peroxidases sAPx and tAPx.

4.3.3 The eQTL belongs to UBX containing protein family that physically interacts with CDC48

The protein structure was analyzed and predicted with Conserved Domain Database on NCBI (http://www.ncbi.nlm.nih.gov/Structure/cdd/cdd.shtml). The prediction illustrated three possible domains of At3g21660: two SEP super family domains and a UBQ super family domain.

The SEP domain is named after *Saccharomyces cerevisiae* Shp1, *Drosophila melanogaster* eyes closed gene (eyc) and vertebrate p47 (Yuan et al., 2004). In p47, the SEP domain has been shown to bind to and then inhibit the cysteine protease cathepsin L (Soukenik et al., 2004). Most SEP domains are succeeded closely by a UBX domain (Yuan et al., 2004). The UBQ super family domain in At3g21660 is an ubiquitin homolog. The UBQ super family domain includes ubiquitin and ubiquitin-like proteins. Ubiquitin-mediated proteolysis is involved in the regulated turnover of proteins required to control cell cycle progression. Other family members are protein modifiers with numerous functions.

Furthermore, according to the prediction about the interaction network of At3g21660 with genemania database (http://www.genemania.org/), the eQTL is predicted to interact with CDC48 (also known as p97/VCP) protein, which physically interacts with five PUX (plant UBX-domain containing) proteins. The analysis also showed that the eQTL At3g21660

shared a UBX-domain with the five PUX proteins, among which the PUX3, PUX4 and PUX5 also contain a SEP superfamily domain.

CDC48 is a conserved and essential hexameric AAA-ATPase that plays a role as a molecular chaperone in many different cellular activities (Rancour et al., 2002). CDC48 activity is needed for specific functions through its interaction with adapter proteins.

There are over ten members of the PUX protein family in Arabidopsis (Rancour et al., 2004). Some data in non-plant systems suggested a role for the UBX-domain, an ubiquitin-like protein fold, as a specific interaction domain for CDC48. Physical interactions of five PUX proteins (1-4 and 11) with AtCDC48 in Arabidopsis were proven in *vivo*, suggesting that the PUX protein family is a class of AtCDC48 regulators (Rancour et al., 2004).

4.3.4 PUX2 is a positive regulator of CDC48 and negatively correlates with the eQTL

The coexpression analysis of PUXs and the eQTL with Genevestigator demonstrated that the transcript levels of PUX2 and eQTL are negatively correlated. It is reported that PUX2 is a peripheral membrane protein which interacts with AtCDC48 in *vitro* and co-fractionates with membrane-associated but not soluble AtCDC48 in *vivo* (Rancour et al., 2005). It is further concluded that PUG domain in PUX2, which is a protein domain found in protein kinases, N-glycanases and other proteins with nuclear localization, is required for interaction with AtCDC48. Biochemical reconstitution and immunolocalization data suggest that PUX2 facilitates the interaction of AtCDC48, thereby regulating an AtCDC48 membrane-associated function (Park et al., 2008).

4.3.5 The eQTL is coexpressed with ASK9 and ASK16

The coexpression analysis with Genemania database (http://www.genemania.org/) (Figure 3-36) demonstrated that eQTL coexpresses with ASK9 and ASK16 (Arabidopsis

Skp1 protein), which functions as bridging protein and together with cullin forms part of the horseshoe-shaped SCF complex which plays an important role in protein degradation. The ASKs are essential in the recognition and binding of the F-box.

As previously discussed, RIMB6, an F-Box containing protein, is proven to interact physically with ASK9 and ASK16. It constitutively represses the plant defense system mediated by repressing the accumulation of R protein and PR protein (Gou et al., 2009; Cheng et al., 2011; Gou et al., 2012), and activating 2CPA expression as well.

The analysis supports a hypothesis that the eQTL and RIMB-6 are involved in same redox retrograde signaling network and they regulate 2CPA expression by protein degradation.

4.3.6 Hypothesis of two possible models of eQTL regulation network

With the data presented in this study it can be suggested that the eQTL and RIMB6 sense the fluctuation of redox state of the electron acceptors of PSI under environmental stimulus and function as chloroplast retrograde signals in a complex network. By protein degradation the network activates 2CPA expression to detoxify the excess ROS and keep the redox status balanced. The UBX domain contained in the eQTL indicates that the regulation of ubiquitination may be involved in the chloroplast redox retrograde signaling. The analysis further allows the shaping of two possible models of the regulation network of the eQTL to 2CPA (Figure 4-4). The eQTL functions as repressor PUX2 or it directly competes with PUX2 binding to CDC48, which negatively regulates an unknown positive regulator of peroxiredoxins mediated by protein degradation. The eQTL is functionally related to RIMB6 via ASK9 and ASK16. Further tests for the physical interactions between the eQTL, PUX2 and CDC48 still need to be finished. To confirm the upstream regulating function of the eQTL to CDC48s, transcript analysis should be performed with lines of loss of function mutants of the eQTL and CDC48 in the future.

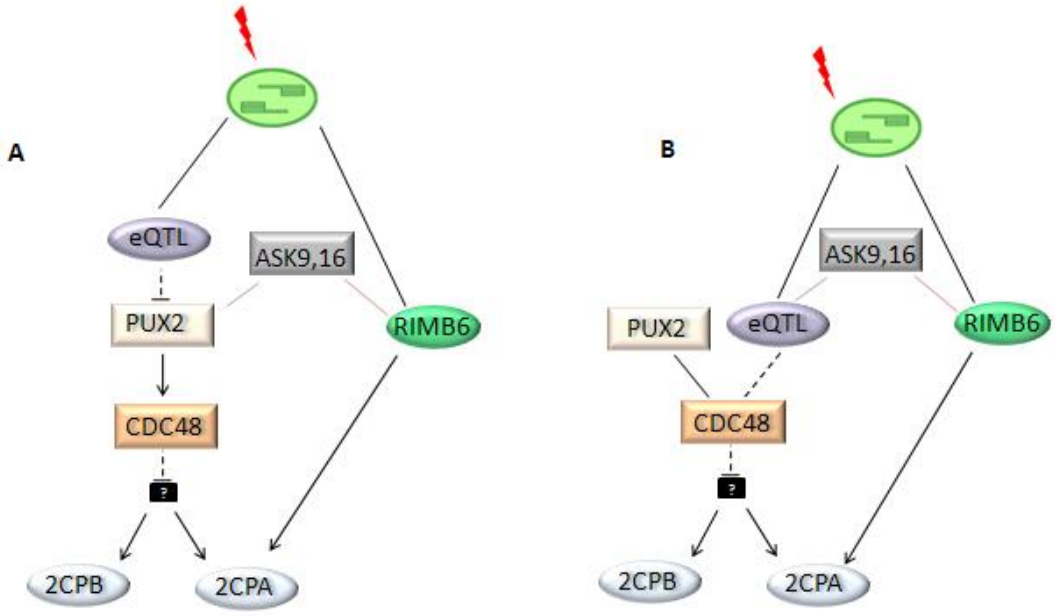

Figure 4-4: Two possible models of the regulatory network of the eQTL. The eQTL responses to the fluctuation of redox state of the electron acceptors of PSI and activates the 2CPA expression via CDC48 and unknown regulator of 2CPA. A: The eQTL may repress PUX2 and further positively control CDC48. B: The may repress CDC48 directly and compete with PUX2.

4.3.7 An alternative approach to discover the new regulator using the natural variation recourses of *Arabidopsis thaliana*

Though the eQTL was mapped by a crossing a mutant line (mutagenized on T19-2) and another accession (*rimb3* x L*er*), mapping of the eQTL is actually based on natural variation. It is assumed, directly with a crossing line of a reporter gene line T19-2 (Col-0 background) and another accession L*er* (T19-2 x L*er*), the eQTL could be still mapped on the same position with the same mapping strategy. The mapping process could be accelerated by this method, as the mutant locus, a potential disturber of the analysis, is missing when using this method. The process of mapping the eQTL may be applied as new approach to discover new regulators in Arabidopsis with the recourses of natural genetic variation.

Instead of using mutant lines, different accessions can be applied to map an unknown regulator in the new approach. A reporter gene line needs to be at first generated with one accession, in which the reporter gene is controlled under the promoter of interest.

Second accession will be selected to cross with the reporter gene line. In the F2 generation, in which alleles segregate, some individuals may have higher or lower reporter gene activities in comparison to the reporter gene line. In those lines with higher reporter gene activities, there might be a positive regulator of the promoter of interest, which is based on the second accession. Such positive regulator is specifically active in the second accession, but is deactivated in the first accession (with reporter gene) due to a kind of natural mutation. On the other hand, reporter gene tests need to be done in the line of low reporter gene activities to ensure that phenotype of low reporter gene activities is not due to the absence of the reporter gene. In the line with reporter gene but showing low reporter gene activity, a repressor of the promoter of interest must exist in the second accession. But in the first accession the positive regulator is deactivated. Such F2-individuals with high or low reporter gene activities can be selected followed by a genetic mapping either with SSLP or next generation sequencing. Those loci, which are determined with genetic mapping, could be unknown regulators of the promoter of interest. In this way regulators can be identified without additional step of mutagenesis.

Since genomes of the most ecotypes of Arabidopsis are already sequenced (Cao et al., 2011), large amount of the polymorphisms between different ecotypes were discovered. For instance, Lu et al. detected 349,171 Single Nucleotide Polymorphisms (SNPs), 58,085 small and 2315 large insertions/deletions (Indels) in sequences of Col-0 and L*er* (Lu et al., 2012). The genetic variation of Arabidopsis already became the most important basic resource for plant biology to study the plant genome (Alonso-Blanco and Koornneef, 2000). Furthermore, among Arabidopsis accessions from different geographical regions, a great number of genetic variations have been discovered (Alonso-Blanco and Koornneef, 2000). Various adaptive traits were reported in different Arabidopsis ecotypes, such as tolerance to freezing (Hannah et al., 2006), disease resistance (Kunkel, 1996), circadian rhythms (Swarup et al., 1999) and the chloroplast antioxidant system (Juszczak et al., 2012). As result of whole genome sequencing of many Arabidopsis accessions, the natural genetic variation in the Arabidopsis chloroplast antioxidant system

can nowadays be used as an alternative resource to discover novel regulators in this system, based on the available data of a great number of the polymorphisms between genomes of different ecotypes. In this project, the eQTL is an example, which was identified using the genetic variation of Arabidopsis.

4.4 RIMB3

The mutant *rimb3* is affected in the central chloroplast-to-nucleus signaling. RIMB3 integrates light intensity dependent signals in the regulation of nuclear encoded antioxidant enzymes (Heiber et al., 2007). At the young stages of the mutant plant *rimb3*, plant image system NightSHADE LB 985 displayed low reporter gene activity which is under control of 2CPA promoter and confirmed that RIMB3 is an activator of 2CPA expression at young stages (Figures 3-7, 3-8 and 3-9). However at the mature stages of Arabidopsis RIMB3 regulatory network seems to slightly repress 2CPA expression. This indicates that the regulatory network of RIMB3 is developmentally regulated. The growth of *rimb3* plants was defective of all the developmental stages (Figure 3-2). This indicates a systematic effect of loss of RIMB3 function on plant development.

With next generation sequencing the locus At4g01290, an unknown protein, was determined as RIMB3. The result was confirmed with transcript analysis of 2CPA in T-DNA insertion line (Figure 3-46).

4.4.1 The predicted structure and functions of RIMB3

After an analysis with CDD database on NCBI a conserved domain topoisomerase II-associated protein (PAT1) was predicted at the C-terminal region of the protein. The PAT1 domain was studied in yeast and animals, but up to now there is no report about the function of PAT1 domain protein published in plant.

The PAT1 proteins are conserved across eukaryotes (yeast, Drosophila, *Caenorhabditis elegans* and human) (Marnef and Standart, 2010) and during cell division, it is necessary for accurate chromosome transmission (Wang et al., 1996). Involvement of PAT1 was observed protein in mRNA degradation in yeast (Bouveret et al., 2000). In Drosophila and human cells, PAT1 proteins also play conserved roles in the 5'→3' mRNA decay pathway. Based on the studies in the past 15 years it is suggested that PAT1 proteins serve as scaffold proteins, with which the repression and decay factors and sequentially bind on mRNPs, and eventually lead to degradation of mRNPs (Marnef and Standart 2010).

4.4.2 RIMB3 coexpresses with ATCDC48

Interestingly, bioinformatical analysis with Genevestigator demonstrated coexpression of RIMB3 and ATCDC48, according to the microarray data Series GSE277 on GEO of NCBI (Figure 3-52). Both of the genes are involved in controlling mechanism during cell division: ATCDC48, cell division protein 48 (CDC48), is involved pathways that operate at the division plane to mediate plant cytokinesis (Rancour et al., 2002). In addition, due to its UBX domain the 2CPA eQTL was also predicted to physically interact with ATCDC48 (Figure 3-30). Taken together, the data supported the following hypothesis: RIMB3 and the 2CPA eQTL may be involved in the same network, and together they activate 2CPA expression.

4.4.3 RIMB3 positively correlates with RIMB1 and functions upstream of RIMB1

With help of Genevestigator, the coexpression analysis also demonstrated a positive correlation between RIMB3 and RIMB1 (CEO1). A transcript analysis was performed to check expression level of RIMB3 in *rimb1* and expression level of RIMB1 in *rimb3*. The result showed that RIMB3 functions in upstream of RIMB1 (Figures 3-50 and 3-51). It is suggested that RIMB1 and RIMB3 can both response to the fluctuation of redox state of

the electron acceptors of PSI and triggers a network of signaling to nucleus. RIMB1 can also sense the upstream signal from RIMB3 and further regulate Rap2.4a, which regulates 2CPA expression in a redox dependent manner (Shaikhali et al., 2008).

4.4.4 Possible regulation network of RIMB3

The presented data suggested a regulating network of RIMB3 (Figure 4-5), which also involves RIMB1 and the eQTL. The RIMB3 plays a role in plant cells as sensor in response to biotic or abiotic stresses and activates the expression of 2CPA in a development-dependent manner. In parallel, RIMB3 coexpresses with RIMB1 that binds to Rap2.4a and acts as upstream factor of RIMB1 in one of the possible signaling pathways of RIMB1. It is not yet proven, whether RIMB3 also interacts with Rap2.4a. In addition, RIMB3 coexpresses with CDC48, which may interact with the 2CPA eQTL and positively regulates the expression of 2CPA and 2CPB via an unknown regulator. In this network, the 2CPA regulators, RIMB1, RIMB3 and the eQTL, may directly response to stresses or indirectly sense the stimulus via an unknown common upstream factor.

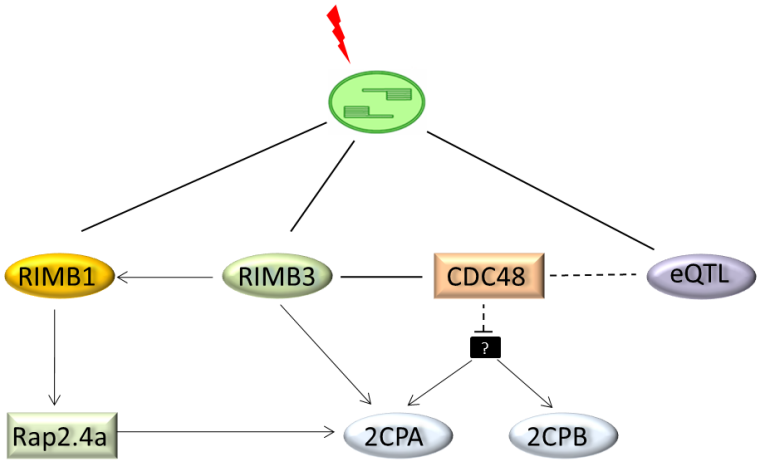

Figure 4-5: Possible regulatory network of RIMB3. In parallel to RIMB1, RIMB6 and the eQTL, RIMB3 senses the redox stimulus and activates the 2CPA expression. RIMB3 also functions in a pathway in upstream of RIMB1 and positively regulates RIMB1. In addition, RIMB3 is coexpressed with CDC48, which may physically interact with the 2CPA eQTL and affect the expression of 2CPA and 2CPB via an unknown factor.

4.5 Conclusion

This project was focused on discriminating retrograde redox signaling from chloroplasts to the nucleus by identifying and characterizing RIMBs, which act as regulators of 2-Cys-Peroxiredoxin A transcription in *Arabidopsis thaliana.*

RIMB3 (At4g01290) may function in a pathway upstream of RIMB1 and activate 2CPA expression directly or via Rap2.4a or CDC48 in a development-dependent manner (Shaikhali et al., 2008). RIMB6 (At4g12560) negatively regulates the plant defense system by constitutive repression of PR and SCN1 genes. RIMB6 may activate 2CPA expression by repression of an unknown negative regulator of 2CPA. Furthermore RIMB6 is also involved in regulatory system of metal homeostasis, in which metal channels and/or transporters are regulated. The eQTL (At3g21660) may physically interact with CDC48. The eQTL positively regulates expression of 2CPA and 2CPB. It is proposed to acts via CDC48 and an unknown positive regulator of 2CPA downstream of CDC48. The eQTL coexpresses with ASK9 and ASK16, which physically interact with RIMB6 (Figure 4-6).

RIMB3, RIMB6 and eQTL may play important roles in the network of redox retrograde signaling pathway from chloroplast to nucleus. The network of the 2CPA regulators may contribute to the understanding of cross-talk between retrograde signaling, ubiquitination, plant defense responses and metal homeostasis in plant cells.

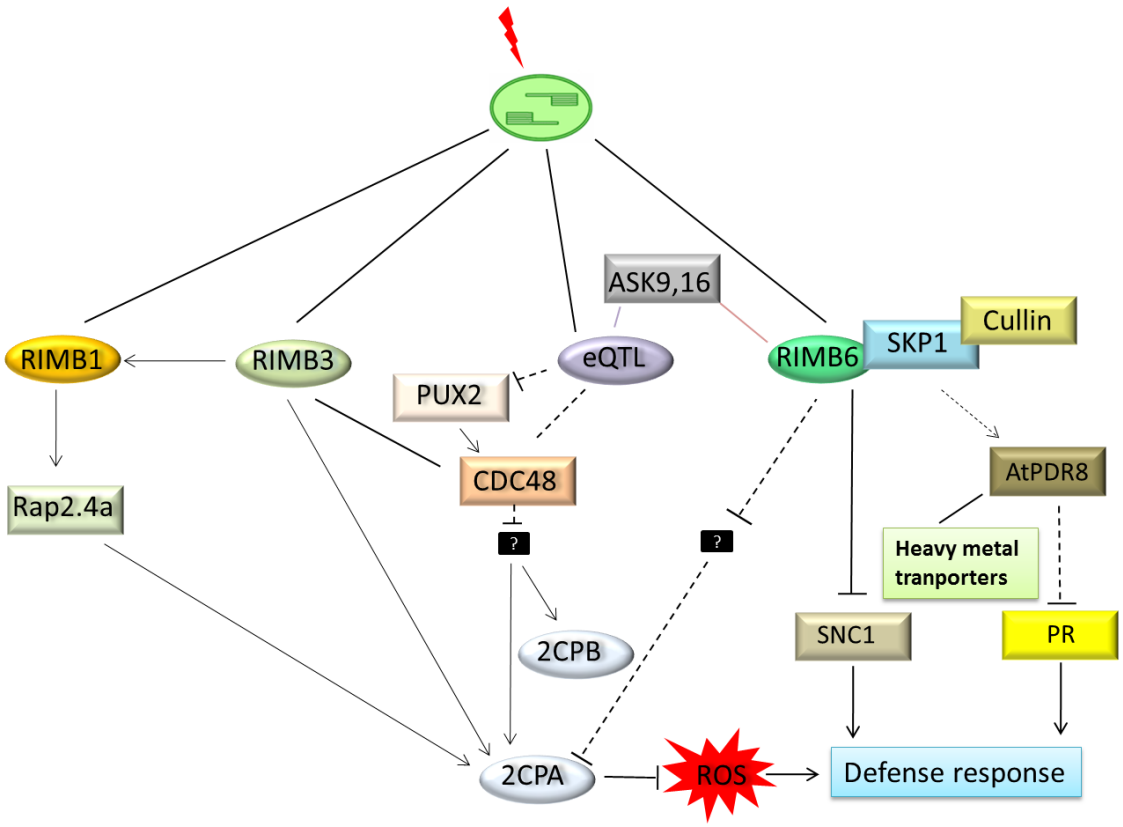

Figure 4-6: The regulatory network of RIMBs and the eQTL. Responding to the environmental stimuli, the RIMB1, RIMB3, eQTL and RIMB6 mediate the chloroplast retrograde signaling to nucleus, and positively regulate the 2CPA expression. The RIMB1 positively regulates Rap2.4a (Hiltscher, 2011), which actives the 2CPA expression in a redox dependent manner (Shaikhali et al., 2008). RIMB3 positively regulates the 2CPA expression either directly, or via RIMB1 pathway or CDC48 pathway. The eQTL may act as a negative regulator of CDC48 via repression of PUX2, which interacts with CDC48 as a positive regulator. CDC48 suppresses expression of 2CPA and 2CPB via an unknown positive regulator of 2CPA and 2CPB. The RIMB6 activates 2CPA expression via an unknown repressor of 2CPA. The RIMB6 correlates with the eQTL through ASK9 and ASK16. On the other hand, RIMB6 is involved in regulation of plant defense reaction in form of SCF, which plays an important role in regulation of metal homeostasis of plant cell.

5 References

Abe, H., Yamaguchi-Shinozaki, K., Urao, T., Iwasaki, T., Hosokawa, D., and Shinozaki, K. (1997). Role of arabidopsis MYC and MYB homologs in drought- and abscisic acid-regulated gene expression. The plant cell **9,** 1859-1868.

Abuharbeid, S., Apel, J., Sander, M., Fiedler, B., Langer, M., Zuzarte, M.L., Czubayko, F., and Aigner, A. (2004). Cytotoxicity of the novel anti-cancer drug rViscumin depends on HER-2 levels in SKOV-3 cells. Biochemical and Biophysical Research Communications **321,** 403-412.

Adams, M.R., Aid, S., Anthony, P.L., Baker, M.D., Bartlett, J.F., et al. (1990). A Spectrometer for Muon Scattering at the Tevatron-E665 Collaboration. Nuclear Instruments and Methods in Physics Research A **291,** 533-551.

Ahlfors, R., Lang, S., Overmyer, K., Jaspers, P., Brosche, M., Taurianinen, A., Kollist, H., Tuominen, H., Belles-Boix, E., Piippo, M., Inze, D., Palva, E.T., and Kangasjarvi, J. (2004). Arabidopsis radical-induced cell death1 belongs to the WWE protein-protein interaction domain protein family and modulates abscisic acid, ethylene, and methyl jasmonate responses. The plant cell **16,** 1925-1937.

Alonso-Blanco, C., and Koornneef, M. (2000). Naturally occurring variation in Arabidopsis: an underexploited resource for plant genetics. Trends in Plant Science **5,** 22-29.

Apel, K., and Hirt, H. (2004). Reactive oxygen species: metabolism, oxidative stress, and signal transduction. Annual Review of Plant Biology **55,** 373-399.

Aravind, L. (2001). The WWE domain: a common interaction module in protein ubiquitination and ADP ribosylation. Trends in Biochemical Sciences **26,** 273-275.

Arazi, T., Sunkar, R., Kaplan, B., and Fromm, H. (1999). A tobacco plasma membrane calmodulin-binding transporter confers Ni^{2+} tolerance and Pb^{2+} hypersensitivity in transgenic plants. The Plant Journal **20,** 171-182.

Arnold, K., Bordoli, L., Kopp, J., and Schwede, T. (2006). The SWISS-MODEL workspace: a web-based environment for protein structure homology modelling. Bioinformatics **22,** 195-201.

Arsova, B., Hoja, U., Wimmelbacher, M., Greiner, E., Ustun, S., Melzer, M., Petersen, K., Lein, W., and Bornke, F. (2010). Plastidial Thioredoxin z Interacts with Two Fructokinase-Like Proteins in a Thiol-Dependent Manner: Evidence for an Essential Role in Chloroplast Development in Arabidopsis and Nicotiana benthamiana. The plant cell **22,** 1498-1515.

Asada, K. (1999). The water-water cycle in chloroplasts: Scavenging of active oxygens and dissipation of excess photons. Annual Review of Plant Physiologyogy and Plant Molecular Biology **50,** 601-639.

Asada, K. (2000). The water-water cycle as alternative photon and electron sinks. Philosophical transactions of the Royal Society of London. Series B, Biological Sciences **355,** 1419-1431.

Baier, M., and Dietz, K.J. (1996). Primary structure and expression of plant homologues of animal and fungal thioredoxin-dependent peroxide reductases and bacterial alkyl hydroperoxide reductases. Plant Molecular Biology **31,** 553-564.

Baier, M., and Dietz, K.J. (1997). The plant 2-Cys peroxiredoxin BAS1 is a nuclear-encoded chloroplast protein: its expressional regulation, phylogenetic origin, and implications for its specific physiological function in plants. The Plant Journal **12,** 179-190.

Baier, M., and Dietz, K.J. (1999). Protective function of chloroplast 2-cysteine peroxiredoxin in photosynthesis. Evidence from transgenic Arabidopsis. The Plant Physiologyogy **119,** 1407-1414.

Baier, M., Stroher, E., and Dietz, K.J. (2004). The acceptor availability at photosystem I and ABA control nuclear expression of 2-cys peroxiredoxin-alpha in *Arabidopsis thaliana*. Plant and Cell Physiology **45,** 997-1006.

Baier, M., Pitsch, N.T., Mellenthin, M., and Guo, W. (2010). Regulation of Genes Encoding Chloroplast Antioxidant Enzymes in Comparison to Regulation of the Extra-plastidic Antioxidant Defense System. Ascorbate-Glutathione Pathway and Stress Tolerance in Plants**,** 337-386.

Baptista, P., Martins, A., Pais, M.S., Tavares, R.M., and Lino-Neto, T. (2007). Involvement of reactive oxygen species during early stages of ectomycorrhiza establishment between Castanea sativa and Pisolithus tinctorius. Mycorrhiza **17,** 185-193.

Baruah, A., Simkova, K., Apel, K., and Laloi, C. (2009). Arabidopsis mutants reveal multiple singlet oxygen signaling pathways involved in stress response and development. Plant Molecular Biology **70,** 547-563.

Bellafiore, S., Barneche, F., Peltier, G., and Rochaix, J.D. (2005). State transitions and light adaptation require chloroplast thylakoid protein kinase STN7. Nature **433,** 892-895.

Bienert, G.P., Schjoerring, J.K., and Jahn, T.P. (2006). Membrane transport of hydrogen peroxide. BBA-Biomembranes **1758,** 994-1003.

Bonardi, V., Pesaresi, P., Becker, T., Schleiff, E., Wagner, R., Pfannschmidt, T., Jahns, P., and Leister, D. (2005). Photosystem II core phosphorylation and photosynthetic acclimation require two different protein kinases. Nature **437,** 1179-1182.

Bouveret, E., Rigaut, G., Shevchenko, A., Wilm, M., and Seraphin, B. (2000). A Sm-like protein complex that participates in mRNA degradation. EMBO Journal **19,** 1661-1671.

Bouvier, F., Isner, J.C., Dogbo, O., and Camara, B. (2005). Oxidative tailoring of carotenoids: a prospect towards novel functions in plants. Trends in Plant Science **10,** 187-194.

Bowler, C., Vanmontagu, M., and Inze, D. (1992). Superoxide-dismutase and stress solerance. Annual review of Plant Physiologyogy and Plant Molecular Biology **43,** 83-116.

Brautigam, K., Dietzel, L., Kleine, T., Stroher, E., Wormuth, D., Dietz, K.J., Radke, D., Wirtz, M., Hell, R., Dormann, P., Nunes-Nesi, A., Schauer, N., Fernie, A.R., Oliver, S.N., Geigenberger, P., Leister, D., and Pfannschmidt, T. (2009). Dynamic plastid redox Ssgnals integrate gene expression and metabolism to induce distinct metabolic states in photosynthetic acclimation in arabidopsis. The plant cell **21,** 2715-2732.

Buchberger, A. (2010). Control of ubiquitin conjugation by cdc48 and its cofactors. Subcellular Biochemistry **54,** 17-30.

Cao, J., Schneeberger, K., Ossowski, S., Gunther, T., Bender, S., Fitz, J., Koenig, D., Lanz, C., Stegle, O., Lippert, C., Wang, X., Ott, F., Muller, J., Alonso-Blanco, C., Borgwardt, K., Schmid, K.J., and Weigel, D. (2011). Whole-genome sequencing of multiple *Arabidopsis thaliana* populations. Nature Genetics **43,** 956-U960.

Chae, H.Z., Chung, S.J., and Rhee, S.G. (1994). Thioredoxin-dependent peroxide reductase from yeast. The Journal of Biological Chemistry **269,** 27670-27678.

Chan, C.S., Guo, L., and Shih, M.C. (2001). Promoter analysis of the nuclear gene encoding the chloroplast glyceraldehyde-3-phosphate dehydrogenase B subunit of *Arabidopsis thaliana*. Plant Molecular Biology **46,** 131-141.

Cheng, Y.T., Li, Y.Z., Huang, S.A., Huang, Y., Dong, X.N., Zhang, Y.L., and Li, X. (2011). Stability of plant immune-receptor resistance proteins is controlled by SKP1-CULLIN1-F-box (SCF)-mediated protein degradation. Proceedings of the National Academy of Sciences USA **108,** 14694-14699.

Chew, O., Whelan, J., and Millar, A.H. (2003). Molecular definition of the ascorbate-glutathione cycle in Arabidopsis mitochondria reveals dual targeting of antioxidant defenses in plants. Journal of Biological Chemistry **278,** 46869-46877.

Choudhuryl, S.K.P.S. (2005). Chromium stress in plants. Brazilian Journal of Plant Physiologyogy **17**.

Coll, N.S., Danon, A., Meurer, J., Cho, W.K., and Apel, K. (2009). Characterization of *soldat8*, a suppressor of singlet oxygen-induced cell death in Arabidopsis seedlings. Plant and Cell Physiology **50,** 707-718.

Corpet, F. (1988). Multiple sequence alignment with hierarchical-clustering. Nucleic Acids Research **16,** 10881-10890.

Dal Corso, G., Borgato, L., and Furini, A. (2005). In vitro plant regeneration of the heavy metal tolerant and hyperaccumulator Arabidopsis halleri (Brassicaceae). Plant Cell Tissue and Organ Culture **82,** 267-270.

Demmig-Adams, B., Gilmore, A.M., and Adams, W.W., 3rd. (1996). Carotenoids 3: in vivo function of carotenoids in higher plants. The FASEB Journal **10,** 403-412.

Desikan, R., Reynolds, A., Hancock, J.T., and Neill, S.J. (1998). Harpin and hydrogen peroxide both initiate programmed cell death but have differential effects on defence gene expression in Arabidopsis suspension cultures. The Biochemical Journal **330 (Pt 1),** 115-120.

Doke, N. (1985). NADPH-dependent O_2^- generation in membrane-fractions isolated from wounded potato-tubers inoculated with phytophthora-infestans. Physiological Plant Pathology **27,** 311-322.

Doke, N., Miura, Y., Sanchez, L.M., Park, H.J., Noritake, T., Yoshioka, H., and Kawakita, K. (1996). The oxidative burst protects plants against pathogen attack: mechanism and role as an emergency signal for plant bio-defence--a review. Gene **179,** 45-51.

Donald, R.G.K., and Cashmore, A.R. (1990). Mutation of either G-Box or I-Box sequences profoundly affects expression from the Arabidopsis Rbcs-1a promoter. EMBO Journal **9,** 1717-1726.

Dyall, S.D., Brown, M.T., and Johnson, P.J. (2004). Ancient invasions: from endosymbionts to organelles. Science **304,** 253-257.

Elstner, E.F. (1991). Oxygen radicals - biochemical basis for their efficacy. Wiener klinische Wochenschrift **69,** 949-956.

Escoubas, J.M., Lomas, M., Laroche, J., and Falkowski, P.G. (1995). Light-Intensity regulation of CAB gene-transcription is signaled by the redox state of the plastoquinone pool. Proceedings of the National Academy of Sciences USA **92,** 10237-10241.

Estavillo, G.M., Crisp, P.A., Pornsiriwong, W., Wirtz, M., Collinge, D., Carrie, C., Giraud, E., Whelan, J., David, P., Javot, H., Brearley, C., Hell, R., Marin, E., and Pogson, B.J. (2011). Evidence for a SAL1-PAP chloroplast retrograde pathway that functions in drought and high light signaling in Arabidopsis. The plant cell **23,** 3992-4012.

Fester, T., and Hause, G. (2005). Accumulation of reactive oxygen species in arbuscular mycorrhizal roots. Mycorrhiza **15,** 373-379.

Foreman, J., Demidchik, V., Bothwell, J.H.F., Mylona, P., Miedema, H., Torres, M.A., Linstead, P., Costa, S., Brownlee, C., Jones, J.D.G., Davies, J.M., and Dolan, L. (2003). Reactive oxygen species produced by NADPH oxidase regulate plant cell growth. Nature **422,** 442-446.

Forsburg, S.L., and Guarente, L. (1989). Communication between mitochondria and the nucleus in regulation of cytochrome genes in the yeast Saccharomyces cerevisiae. Annual Review of Cell Biology **5,** 153-180.

Foyer, C.H., and Noctor, G. (2000). Oxygen processing in photosynthesis: regulation and signalling. New Phytologist **146,** 359-388.

Foyer, C.H., and Noctor, G. (2003). Redox sensing and signalling associated with reactive oxygen in chloroplasts, peroxisomes and mitochondria. Physiologia Plantarum **119,** 355-364.

Foyer, C.H., and Noctor, G. (2005). Redox homeostasis and antioxidant signaling: A metabolic interface between stress perception and physiological responses. The plant cell **17,** 1866-1875.

Foyer, C.H., LopezDelgado, H., Dat, J.F., and Scott, I.M. (1997). Hydrogen peroxide- and glutathione-associated mechanisms of acclimatory stress tolerance and signalling. Physiologia Plantarum **100,** 241-254.

Galvez-Valdivieso, G., and Mullineaux, P.M. (2010). The role of reactive oxygen species in signalling from chloroplasts to the nucleus. Physiologia Plantarum **138,** 430-439.

Gechev, T.S., and Hille, J. (2005). Hydrogen peroxide as a signal controlling plant programmed cell death. The Journal of Cell Biology **168,** 17-20.

Gendre, D., Czernic, P., Conejero, G., Pianelli, K., Briat, J.F., Lebrun, M., and Mari, S. (2007). TcYSL3, a member of the YSL gene family from the hyper-accumulator Thlaspi caerulescens, encodes a nicotianamine-Ni/Fe transporter. The Plant Journal **49,** 1-15.

Gorman, A.A., and Rodgers, M.A.J. (1992). Current perspectives of singlet oxygen detection in biological environments. Journal of Photochemistry and Photobiology B **14,** 159-176.

Gou, M., Su, N., Zheng, J., Huai, J., Wu, G., Zhao, J., He, J., Tang, D., Yang, S., and Wang, G. (2009). An F-box gene, CPR30, functions as a negative regulator of the defense response in Arabidopsis. The Plant Journal: for cell and molecular biology **60,** 757-770.

Gou, M.Y., Shi, Z.Y., Zhu, Y., Bao, Z.L., Wang, G.Y., and Hua, J. (2012). The F-box protein CPR1/CPR30 negatively regulates R protein SNC1 accumulation. The Plant Journal **69,** 411-420.

Goujon, M., McWilliam, H., Li, W.Z., Valentin, F., Squizzato, S., Paern, J., and Lopez, R. (2010). A new bioinformatics analysis tools framework at EMBL-EBI. Nucleic Acids Research **38,** W695-W699.

Green, B.R. (2011). Chloroplast genomes of photosynthetic eukaryotes. The Plant Journal **66,** 34-44.

Guan, L., Polidoros, A.N., and Scandalios, J.G. (1996). Isolation, characterization and expression of the maize Cat2 catalase gene. Plant Molecular Biology **30,** 913-924.

Guex, N., and Peitsch, M.C. (1997). SWISS-MODEL and the Swiss-PdbViewer: an environment for comparative protein modeling. Electrophoresis **18,** 2714-2723.

Guttman, H.N., and Vitetta, E.S. (1967). Endosymbiosis: infection and cure. The Yale Journal of Biology and Medicine **40,** 183-191.

Hall, J.L. (2002). Cellular mechanisms for heavy metal detoxification and tolerance. Journal of Experimental Botany **53,** 1-11.

Halliwell B, G.J. (1989). Free Radicals in Biology and Medicine. (Oxford University Press).

Hannah, M.A., Wiese, D., Freund, S., Fiehn, O., Heyer, A.G., and Hincha, D.K. (2006). Natural genetic variation of freezing tolerance in arabidopsis. Plant Physiologyogy **142,** 98-112.

Heiber, I., Stroher, E., Raatz, B., Busse, I., Kahmann, U., Bevan, M.W., Dietz, K.J., and Baier, M. (2007). The redox imbalanced mutants of Arabidopsis differentiate signaling pathways for redox regulation of chloroplast antioxidant enzymes. Plant Physiologyogy **143,** 1774-1788.

Hiltscher, H. (2011). Identifizierung und Charakterisierung von Signaltransduktionselementen der 2‐Cys‐Peroxiredoxin A Regulation in *Arabidopsis thaliana* (Heinrich-Heine-Universität Düsseldorf).

Hofmann, B., Hecht, H.J., and Flohe, L. (2002). Peroxiredoxins. Biological Chemistry **383,** 347-364.

Horling, F., Baier, M., and Dietz, K.J. (2001). Redox-regulation of the expression of the peroxide-detoxifying chloroplast 2-cys peroxiredoxin in the liverwort Riccia fluitans. Planta **214,** 304-313.

Horling, F., Lamkemeyer, P., Konig, J., Finkemeier, I., Kandlbinder, A., Baier, M., and Dietz, K.J. (2003). Divergent light-, ascorbate-, and oxidative stress-dependent regulation of

expression of the peroxiredoxin gene family in Arabidopsis. Plant Physiology **131,** 317-325.

Hossain M. A., P.P., Jaime A. Teixeira da Silva, and Masayuki Fujita. (2012). Molecular mechanism of heavy metal toxicity and tolerance in plants: central role of glutathione in detoxification of reactive oxygen species and methylglyoxal and in heavy metal chelation. Journal of Botany **2012,** 37.

Isemer, R., Mulisch, M., Schafer, A., Kirchner, S., Koop, H.U., and Krupinska, K. (2012). Recombinant Whirly1 translocates from transplastomic chloroplasts to the nucleus. FEBS Letters **586,** 85-88.

Jander, G., Norris, S.R., Rounsley, S.D., Bush, D.F., Levin, I.M., and Last, R.L. (2002). Arabidopsis map-based cloning in the post-genome era. Plant Physiology **129,** 440-450.

Jeong, W., Cha, M.K., and Kim, I.H. (2000). Thioredoxin-dependent hydroperoxide peroxidase activity of bacterioferritin comigratory protein (BCP) as a new member of the thiol-specific antioxidant protein (TSA)/Alkyl hydroperoxide peroxidase C (AhpC) family. The Journal of Biological Chemistry **275,** 2924-2930.

Juszczak, I., Rudnik, R., Pietzenuk, B., and Baier, M. (2012). Natural genetic variation in the expression regulation of the chloroplast antioxidant system among *Arabidopsis thaliana* accessions. Physiologia Plantarum **146,** 53-70.

Kangasjarvi, S., Lepisto, A., Hannikainen, K., Piippo, M., Luomala, E.M., Aro, E.M., and Rintamaki, E. (2008). Diverse roles for chloroplast stromal and thylakoid-bound ascorbate peroxidases in plant stress responses. Biochemical Journal **412,** 275-285.

Karimi, M., Inze, D., and Depicker, A. (2002). GATEWAY^{TM} vectors for Agrobacterium-mediated plant transformation. Trends in Plant Science **7,** 193-195.

Karpinski, S., Escobar, C., Karpinska, B., Creissen, G., and Mullineaux, P.M. (1997). Photosynthetic electron transport regulates the expression of cytosolic ascorbate peroxidase genes in Arabidopsis during excess light stress. The plant cell **9,** 627-640.

Karpinski, S., Reynolds, H., Karpinska, B., Wingsle, G., Creissen, G., and Mullineaux, P. (1999). Systemic signaling and acclimation in response to excess excitation energy in Arabidopsis. Science **284,** 654-657.

Kiddle, G., Pastori, G.M., Bernard, S., Pignocchi, C., Antoniw, J., Verrier, P.J., and Foyer, C.H. (2003). Effects of leaf ascorbate content on defense and photosynthesis gene expression in *Arabidopsis thaliana*. Antioxidants & Redox Signaling **5,** 23-32.

Kiefer, F., Arnold, K., Kunzli, M., Bordoli, L., and Schwede, T. (2009). The SWISS-MODEL Repository and associated resources. Nucleic Acids Research **37,** D387-D392.

Kilian, J., Whitehead, D., Horak, J., Wanke, D., Weinl, S., Batistic, O., D'Angelo, C., Bornberg-Bauer, E., Kudla, J., and Harter, K. (2007). The AtGenExpress global stress expression data set: protocols, evaluation and model data analysis of UV-B light, drought and cold stress responses. The Plant Journal **50,** 347-363.

Kim, D.Y., Bovet, L., Maeshima, M., Martinoia, E., and Lee, Y. (2007). The ABC transporter AtPDR8 is a cadmium extrusion pump conferring heavy metal resistance. The Plant Journal **50,** 207-218.

Kindgren, P., Noren, L., Lopez Jde, D., Shaikhali, J., and Strand, A. (2012a). Interplay between Heat Shock Protein 90 and HY5 controls PhANG expression in response to the GUN5 plastid signal. Molecular Plant **5,** 901-913.

Kindgren, P., Eriksson, M.J., Benedict, C., Mohapatra, A., Gough, S.P., Hansson, M., Kieselbach, T., and Strand, A. (2011). A novel proteomic approach reveals a role for Mg-protoporphyrin IX in response to oxidative stress. Physiologia Plantarum **141,** 310-320.

Kindgren, P., Kremnev, D., Blanco, N.E., de Dios Barajas Lopez, J., Fernandez, A.P., Tellgren-Roth, C., Kleine, T., Small, I., and Strand, A. (2012b). The plastid redox insensitive 2 mutant of Arabidopsis is impaired in PEP activity and high light-dependent plastid redox signalling to the nucleus. The Plant Journal: for cell and molecular biology **70,** 279-291.

Klein, P., Seidel, T., Stocker, B., and Dietz, K.J. (2012). The membrane-tethered transcription factor ANAC089 serves as redox-dependent suppressor of stromal ascorbate peroxidase gene expression. Frontiers in Plant Science **3,** 247.

Kliebenstein, D.J., Monde, R.A., and Last, R.L. (1998). Superoxide dismutase in Arabidopsis: An eclectic enzyme family with disparate regulation and protein localization. Plant Physiology **118,** 637-650.

Kobae, Y., Sekino, T., Yoshioka, H., Nakagawa, T., Martinoia, E., and Maeshima, M. (2006). Loss of AtPDR8, a plasma membrane ABC transporter of *Arabidopsis thaliana*, causes hypersensitive cell death upon pathogen infection. Plant and Cell Physiology **47,** 309-318.

Kohler, C., Merkle, T., and Neuhaus, G. (1999). Characterisation of a novel gene family of putative cyclic nucleotide- and calmodulin-regulated ion channels in *Arabidopsis thaliana*. The Plant Journal **18,** 97-104.

Koussevitzky, S. (2007). Signals from chloroplasts converge to regulate nuclear gene expression (vol 316, pg 715, 2007). Science **316,** 1698-1698.

Kram, B.W., Xu, W.W., and Carter, C.J. (2009). Uncovering the *Arabidopsis thaliana* nectary transcriptome: investigation of differential gene expression in floral nectariferous tissues. BMC Plant Biology **9**.

Kruk, J., Hollander-Czytko, H., Oettmeier, W., and Trebst, A. (2005). Tocopherol as singlet oxygen scavenger in photosystem II. Journal of Plant Physiology **162,** 749-757.

Kunkel, B.N. (1996). A useful weed put to work: Genetic analysis of disease resistance in *Arabidopsis thaliana.* Trends in Genetics **12,** 63-69.

Lamkemeyer, P., Laxa, M., Collin, V., Li, W., Finkemeier, I., Schottler, M.A., Holtkamp, V., Tognetti, V.B., Issakidis-Bourguet, E., Kandlbinder, A., Weis, E., Miginiac-Maslow, M., and Dietz, K.J. (2006). Peroxiredoxin Q of *Arabidopsis thaliana* is attached to the thylakoids and functions in context of photosynthesis. The Plant Journal **45,** 968-981.

Larkin, R.M., Alonso, J.M., Ecker, J.R., and Chory, J. (2003). GUN4, a regulator of chlorophyll synthesis and intracellular signaling. Science **299,** 902-906.

Laule, O., Hirsch-Hoffmann, M., Hruz, T., Gruissem, W., and Zimmermann, P. (2006). Web-based analysis of the mouse transcriptome using Genevestigator. BMC Bioinformatics **7**.

Lee, K.P., Kim, C., Landgraf, F., and Apel, K. (2007). EXECUTER1- and EXECUTER2-dependent transfer of stress-related signals from the plastid to the nucleus of *Arabidopsis thaliana*. Proceedings of the National Academy of Sciences USA **104,** 10270-10275.

Levine, A., Tenhaken, R., Dixon, R., and Lamb, C. (1994). H_2O_2 from the oxidative burst orchestrates the plant hypersensitive disease resistance response. Cell **79,** 583-593.

Low, P.S., and Merida, J.R. (1996). The oxidative burst in plant defense: Function and signal transduction. Physiologia Plantarum **96,** 533-542.

Lu, P.L., Han, X.W., Qi, J., Yang, J.G., Wijeratne, A.J., Li, T., and Ma, H. (2012). Analysis of Arabidopsis genome-wide variations before and after meiosis and meiotic recombination by resequencing Landsberg erecta and all four products of a single meiosis. Genome Res **22,** 508-518.

Marchler-Bauer, A., Zheng, C.J., Chitsaz, F., Derbyshire, M.K., Geer, L.Y., Geer, R.C., Gonzales, N.R., Gwadz, M., Hurwitz, D.I., Lanczycki, C.J., Lu, F., Lu, S.N., Marchler, G.H., Song, J.S., Thanki, N., Yamashita, R.A., Zhang, D.C., and Bryant, S.H. (2013). CDD: conserved domains and protein three-dimensional structure. Nucleic Acids Research **41,** D348-D352.

Marchler-Bauer, A., Lu, S., Anderson, J.B., Chitsaz, F., Derbyshire, M.K., et al. (2011). CDD: a Conserved Domain Database for the functional annotation of proteins. Nucleic Acids Research **39,** D225-229.

Marnef, A., and Standart, N. (2010). Pat1 proteins: a life in translation, translation repression and mRNA decay. Biochemical Society Transactions **38,** 1602-1607.

Maruta, T., Noshi, M., Tanouchi, A., Tamoi, M., Yabuta, Y., Yoshimura, K., Ishikawa, T., and Shigeoka, S. (2012). H_2O_2-triggered retrograde signaling from chloroplasts to nucleus plays specific role in response to stress. Journal of Biological Chemistry **287,** 11717-11729.

Mccord, J.M., and Fridovic.I. (1969). Superoxide dismutase-an enzymic function for erythrocuprein. Federation proceedings **28,** 346-&.

Mehdy, M.C. (1994). Active oxygen species in plant defense against pathogens. Plant Physiology **105,** 467-472.

Mehler, A.H. (1951). Studies on reactions of illuminated chloroplasts. I. Mechanism of the reduction of oxygen and other Hill reagents. Archives of Biochemistry and Biophysics **33,** 65-77.

Melonek, J., Mulisch, M., Schmitz-Linneweber, C., Grabowski, E., Hensel, G., and Krupinska, K. (2010). Whirly1 in chloroplasts associates with intron containing RNAs and rarely co-localizes with nucleoids. Planta **232,** 471-481.

Meskauskiene, R., Nater, M., Goslings, D., Kessler, F., den Camp, R.O., and Apel, K. (2001). FLU: A negative regulator of chlorophyll biosynthesis in *Arabidopsis thaliana*. Proceedings of the National Academy of Sciences USA **98,** 12826-12831.

Meskauskiene, R., Wursch, M., Laloi, C., Vidi, P.A., Coll, N.S., Kessler, F., Baruah, A., Kim, C., and Apel, K. (2009). A mutation in the Arabidopsis mTERF-related plastid protein SOLDAT10 activates retrograde signaling and suppresses $^1O_{(2)}$-induced cell death. The Plant Journal **60,** 399-410.

Mittler, R., Vanderauwera, S., Gollery, M., and Van Breusegem, F. (2004). Reactive oxygen gene network of plants. Trends in Plant Science **9,** 490-498.

Mittler, R., Vanderauwera, S., Suzuki, N., Miller, G., Tognetti, V.B., Vandepoele, K., Gollery, M., Shulaev, V., and Van Breusegem, F. (2011). ROS signaling: the new wave? Trends in Plant Science **16,** 300-309.

Mochizuki, N., Brusslan, J.A., Larkin, R., Nagatani, A., and Chory, J. (2001). Arabidopsis genomes uncoupled 5 (GUN5) mutant reveals the involvement of Mg-chelatase H subunit in plastid-to-nucleus signal transduction. Proceedings of the National Academy of Sciences USA **98,** 2053-2058.

Moller, I.M., and Sweetlove, L.J. (2010). ROS signalling - specificity is required. Trends in Plant Science **15,** 370-374.

Monaghan, J., Xu, F., Gao, M.H., Zhao, Q.G., Palma, K., Long, C.Z., Chen, S., Zhang, Y.L., and Li, X. (2009). Two Prp19-Like U-Box Proteins in the MOS4-Associated Complex Play Redundant Roles in Plant Innate Immunity. Plos Pathog **5**.

Morgan, D. (2007). The Cell Cycle: Principles of Control. (London: New Science Press).

Mostafavi, S., Ray, D., Warde-Farley, D., Grouios, C., and Morris, Q. (2008). GeneMANIA: a real-time multiple association network integration algorithm for predicting gene function. Genome Biology **9 Suppl 1,** S4.

Mullineaux, P., and Karpinski, S. (2002). Signal transduction in response to excess light: getting out of the chloroplast. Current Opinion in Plant Biology **5,** 43-48.

Mullineaux, P.M., Karpinski, S., Jimenez, A., Cleary, S.P., Robinson, C., and Creissen, G.P. (1998). Identification of cDNAS encoding plastid-targeted glutathione peroxidase. The Plant Journal: for cell and molecular biology **13,** 375-379.

Munne-Bosch, S. (2005). The role of alpha-tocopherol in plant stress tolerance. Journal of Plant Physiology **162,** 743-748.

Munne-Bosch, S., JOURNAL OFubany-Mari, T., and Alegre, L. (2003). Enhanced photo- and antioxidative protection, and hydrogen peroxide accumulation in drought-stressed Cistus clusii and Cistus albidus plants. Tree Physiology **23,** 1-12.

Nanda, A.K., Andrio, E., Marino, D., Pauly, N., and Dunand, C. (2010). Reactive oxygen species during plant-microorganism early interactions. Journal of Integrative Plant Biology **52,** 195-204.

Niki, E. (1987). Interaction of ascorbate and alpha-tocopherol. Annals of the New York Academy of Sciences **498,** 186-199.

Nishida, S., Tsuzuki, C., Kato, A., Aisu, A., Yoshida, JOURNAL OF., and Mizuno, T. (2011). AtIRT1, the primary iron uptake transporter in the root, mediates excess nickel accumulation in *Arabidopsis thaliana*. Plant & Cell Physiology **52,** 1433-1442.

Noctor, G., and Foyer, C.H. (1998). Ascorbate and Glutathione: keeping active oxygen under control. Annual review of Plant Physiologyogy and Plant Molecular Biology **49,** 249-279.

Noordally, Z.B., Ishii, K., Atkins, K.A., Wetherill, S.JOURNAL OF., Kusakina, JOURNAL OF., Walton, E.JOURNAL OF., Kato, M., Azuma, M., Tanaka, K., Hanaoka, M., and Dodd,

A.N. (2013). Circadian control of chloroplast transcription by a nuclear-encoded timing signal. Science **339,** 1316-1319.

Ogawa, K., Sun, JOURNAL OF., Taketani, S., NakaJournal ofima, O., Nishitani, C., Sassa, S., Hayashi, N., Yamamoto, M., Shibahara, S., FuJournal ofita, H., and Igarashi, K. (2001). Heme mediates derepression of Maf recognition element through direct binding to transcription repressor Bach1. The EMBO Journal **20,** 2835-2843.

op den Camp, R.G., Przybyla, D., Ochsenbein, C., Laloi, C., Kim, C., Danon, A., Wagner, D., Hideg, E., Gobel, C., Feussner, I., Nater, M., and Apel, K. (2003). Rapid induction of distinct stress responses after the release of singlet oxygen in Arabidopsis. The plant cell **15,** 2320-2332.

Palma, K., Zhao, Q.G., Cheng, Y.T., Bi, D.L., Monaghan, JOURNAL OF., Cheng, W., Zhang, Y.L., and Li, X. (2007). Regulation of plant innate immunity by three proteins in a complex conserved across the plant and animal kingdoms. Genes & Development **21,** 1484-1493.

Park, S., Rancour, D.M., and Bednarek, S.Y. (2008). In planta analysis of the cell cycle-dependent localization of AtCDC48A and its critical roles in cell division, expansion, and differentiation. Plant Physiology **148,** 246-258.

Patel, R.V., Nahal, H.K., Breit, R., and Provart, N.JOURNAL OF. (2012). BAR expressolog identification: expression profile similarity ranking of homologous genes in plant species. The Plant Journal **71,** 1038-1050.

Pei, Z.M., Murata, Y., Benning, G., Thomine, S., Klusener, B., Allen, G.JOURNAL OF., Grill, E., and Schroeder, JOURNAL OF.I. (2000). Calcium channels activated by hydrogen peroxide mediate abscisic acid signalling in guard cells. Nature **406,** 731-734.

Pena-Ahumada, A., Kahmann, U., Dietz, K.JOURNAL OF., and Baier, M. (2006). Regulation of peroxiredoxin expression versus expression of Halliwell-Asada-Cycle enzymes during early seedling development of *Arabidopsis thaliana*. Photosynthesis Research **89,** 99-112.

Pesaresi, P., Schneider, A., Kleine, T., and Leister, D. (2007). Interorganellar communication. Current Opinion in Plant Biology **10,** 600-606.

Pesaresi, P., Pribil, M., Wunder, T., and Leister, D. (2011). Dynamics of reversible protein phosphorylation in thylakoids of flowering plants: The roles of STN7, STN8 and TAP38. BBA-Bioenergetics **1807,** 887-896.

Pfannschmidt, T. (2003). Chloroplast redox signals: how photosynthesis controls its own genes. Trends in Plant Science **8,** 33-41.

Pfannschmidt, T., Schutze, K., Brost, M., and Oelmuller, R. (2001). A novel mechanism of nuclear photosynthesis gene regulation by redox signals from the chloroplast during photosystem stoichiometry adJournal ofustment. Journal of Biological Chemistry **276,** 36125-36130.

Qi, Z., Hamza, I., and O'Brian, M.R. (1999). Heme is an effector molecule for iron-dependent degradation of the bacterial iron response regulator (Irr) protein. Proceedings of the National Academy of Sciences USA **96,** 13056-13061.

Quintero, F.JOURNAL OF., Garciadeblas, B., and Rodriguez-Navarro, A. (1996). The SAL1 gene of Arabidopsis, encoding an enzyme with 3'(2'),5'-bisphosphate nucleotidase and

inositol polyphosphate 1-phosphatase activities, increases salt tolerance in yeast. The plant cell **8,** 529-537.

Ramos, JOURNAL OF., Matamoros, M.A., Naya, L., JOURNAL OFames, E.K., Rouhier, N., Sato, S., Tabata, S., and Becana, M. (2009). The glutathione peroxidase gene family of Lotus Journal ofaponicus: characterization of genomic clones, expression analyses and immunolocalization in legumes. The New Phytologist **181,** 103-114.

Ramu, S.K., Peng, H.M., and Cook, D.R. (2002). Nod factor induction of reactive oxygen species production is correlated with expression of the early nodulin gene rip1 in Medicago truncatula. Molecular Plant-Microbe Interactions **15,** 522-528.

Rancour, D.M., Dickey, C.E., Park, S., and Bednarek, S.Y. (2002). Characterization of AtCDC48. Evidence for multiple membrane fusion mechanisms at the plane of cell division in plants. Plant Physiology **130,** 1241-1253.

Rancour, D.M., Park, S., Knight, S.D., and Bednarek, S.Y. (2004). Plant UBX domain-containing protein 1, PUX1, regulates the oligomeric structure and activity of Arabidopsis CDC48. Journal of Biological Chemistry **279,** 54264-54274.

Rice, P., Longden, I., and Bleasby, A. (2000). EMBOSS: The European molecular biology open software suite. Trends in Genetics **16,** 276-277.

Richly, E., and Leister, D. (2004). An improved prediction of chloroplast proteins reveals diversities and commonalities in the chloroplast proteomes of Arabidopsis and rice. Gene **329,** 11-16.

Rodermel, S. (2001). Pathways of plastid-to-nucleus signaling. Trends in Plant Science **6,** 471-478.

Rodriguez Milla, M.A., Maurer, A., Rodriguez Huete, A., and Gustafson, JOURNAL OF.P. (2003). Glutathione peroxidase genes in Arabidopsis are ubiquitous and regulated by abiotic stresses through diverse signaling pathways. The Plant Journal **36,** 602-615.

Rouhier, N., Gelhaye, E., Gualberto, JOURNAL OF.M., JOURNAL OFordy, M.N., De Fay, E., Hirasawa, M., Duplessis, S., Lemaire, S.D., Frey, P., Martin, F., Manieri, W., Knaff, D.B., and JOURNAL OFacquot, JOURNAL OF.P. (2004). Poplar peroxiredoxin Q. A thioredoxin-linked chloroplast antioxidant functional in pathogen defense. Plant Physiology **134,** 1027-1038.

Santos, R., Herouart, D., Sigaud, S., Touati, D., and Puppo, A. (2001). Oxidative burst in alfalfa-Sinorhizobium meliloti symbiotic interaction. Molecular plant-microbe interactions : MPMI **14,** 86-89.

Scandalios, JOURNAL OF.G. (2005). Oxidative stress: molecular perception and transduction of signals triggering antioxidant gene defenses. Brazilian Journal of medical and biological research **38,** 995-1014.

Schneeberger, K., Ossowski, S., Lanz, C., JOURNAL OFuul, T., Petersen, A.H., Nielsen, K.L., JOURNAL OForgensen, JOURNAL OF.E., Weigel, D., and Andersen, S.U. (2009). SHOREmap: simultaneous mapping and mutation identification by deep sequencing. Nature Methods **6,** 550-551.

Schroter, Y., Steiner, S., Matthai, K., and Pfannschmidt, T. (2010). Analysis of oligomeric protein complexes in the chloroplast sub-proteome of nucleic acid-binding proteins from

mustard reveals potential redox regulators of plastid gene expression. Proteomics **10,** 2191-2204.

Schutzendubel, A., and Polle, A. (2002). Plant responses to abiotic stresses: heavy metal-induced oxidative stress and protection by mycorrhization. Journal of Experimental Botany **53,** 1351-1365.

Schuurink, R.C., Shartzer, S.F., Fath, A., and JOURNAL OFones, R.L. (1998). Characterization of a calmodulin-binding transporter from the plasma membrane of barley aleurone. Proceedings of the National Academy of Sciences USA **95,** 1944-1949.

Shaikhali, JOURNAL OF., Heiber, I., Seidel, T., Stroher, E., Hiltscher, H., Birkmann, S., Dietz, K.JOURNAL OF., and Baier, M. (2008). The redox-sensitive transcription factor Rap2.4a controls nuclear expression of 2-Cys peroxiredoxin A and other chloroplast antioxidant enzymes. BMC Plant Biology **8**.

Shigeoka, S., Ishikawa, T., Tamoi, M., Miyagawa, Y., Takeda, T., Yabuta, Y., and Yoshimura, K. (2002). Regulation and function of ascorbate peroxidase isoenzymes. Journal of Experimental Botany **53,** 1305-1319.

Shimizu, M., Kato, H., Ogawa, T., Kurachi, A., Nakagawa, Y., and Kobayashi, H. (2010). Sigma factor phosphorylation in the photosynthetic control of photosystem stoichiometry. Proceedings of the National Academy of Sciences USA **107,** 10760-10764.

Smirnoff, N., and Wheeler, G.L. (2000). Ascorbic acid in plants: biosynthesis and function. Critical Reviews in Biochemistry and Molecular Biology **35,** 291-314.

Soitamo, A.JOURNAL OF., Piippo, M., Allahverdiyeva, Y., Battchikova, N., and Aro, E.M. (2008). Light has a specific role in modulating Arabidopsis gene expression at low temperature. BMC Plant Biology **8,** 13.

Soukenik, M., Diehl, A., Leidert, M., Sievert, V., Bussow, K., Leitner, D., Labudde, D., Ball, L.JOURNAL OF., Lechner, A., Nagler, D.K., and Oschkinat, H. (2004). The SEP domain of p47 acts as a reversible competitive inhibitor of cathepsin L. FEBS letters **576,** 358-362.

Stacy, R.A., Nordeng, T.W., Culianez-Macia, F.A., and Aalen, R.B. (1999). The dormancy-related peroxiredoxin anti-oxidant, PER1, is localized to the nucleus of barley embryo and aleurone cells. The Plant Journal **19,** 1-8.

Stael, S., Rocha, A.G., Wimberger, T., Anrather, D., Vothknecht, U.C., and Teige, M. (2012). Cross-talk between calcium signalling and protein phosphorylation at the thylakoid. Journal of Experimental Botany **63,** 1725-1733.

Steiner, S., Dietzel, L., Schroter, Y., Fey, V., Wagner, R., and Pfannschmidt, T. (2009). The Role of phosphorylation in redox regulation of photosynthesis genes psaA and psbA during photosynthetic acclimation of mustard. Molecular plant **2,** 416-429.

Storz, G., JOURNAL OFacobson, F.S., Tartaglia, L.A., Morgan, R.W., Silveira, L.A., and Ames, B.N. (1989). An alkyl hydroperoxide reductase induced by oxidative stress in *Salmonella-typhimurium* and *Escherichia-coli* genetic characterization and cloning of Ahp. Journal of Bacteriologyl **171,** 2049-2055.

Strand, A. (2004). Plastid-to-nucleus signalling. Current Opinion in Plant Biology **7,** 621-625.

Stratton, S.P., and Liebler, D.C. (1997). Determination of singlet oxygen-specific versus radical-mediated lipid peroxidation in photosensitized oxidation of lipid bilayers: Effect of beta-carotene and alpha-tocopherol. Biochemistry **36,** 12911-12920.

Straus, M.R., Rietz, S., van Themaat, E.V.L., Bartsch, M., and Parker, JOURNAL OF.E. (2010). Salicylic acid antagonism of EDS1-driven cell death is important for immune and oxidative stress responses in Arabidopsis. The Plant Journal **62,** 628-640.

Sun, X., Feng, P., Xu, X., Guo, H., Ma, JOURNAL OF., Chi, W., Lin, R., Lu, C., and Zhang, L. (2011). A chloroplast envelope-bound PHD transcription factor mediates chloroplast signals to the nucleus. Nature Communications **2,** 477.

Susek, R.E., Ausubel, F.M., and Chory, JOURNAL OF. (1993). Signal transduction mutants of Arabidopsis uncouple nuclear CAB and RBCS gene expression from chloroplast development. Cell **74,** 787-799.

Suzuki, N., and Mittler, R. (2012). Reactive oxygen species-dependent wound responses in animals and plants. Free Radical Biology & Medicine **53,** 2269-2276.

Suzuki, N., Koussevitzky, S., Mittler, R., and Miller, G. (2012). ROS and redox signalling in the response of plants to abiotic stress. Plant, Cell & Environment **35,** 259-270.

Swanson, S., and Gilroy, S. (2010). ROS in plant development. Physiologia Plantarum **138,** 384-392.

Swarbreck, D., Wilks, C., Lamesch, P., Berardini, T.Z., Garcia-Hernandez, M., Foerster, H., Li, D., Meyer, T., Muller, R., Ploetz, L., Radenbaugh, A., Singh, S., Swing, V., Tissier, C., Zhang, P., and Huala, E. (2008). The Arabidopsis Information Resource (TAIR): gene structure and function annotation. Nucleic Acids Research **36,** D1009-D1014.

Swarup, K., Alonso-Blanco, C., Lynn, JOURNAL OF.R., Michaels, S.D., Amasino, R.M., Koornneef, M., and Millar, A.JOURNAL OF. (1999). Natural allelic variation identifies new genes in the Arabidopsis circadian system. The Plant Journal **20,** 67-77.

Tikkanen, M., Gollan, P.JOURNAL OF., Suorsa, M., KangasJournal ofarvi, S., and Aro, E.M. (2012). STN7 operates in retrograde signaling through controlling redox balance in the electron transfer chain. Frontiers in Plant Science **3,** 277.

Torres, M.A., JOURNAL OFones, JOURNAL OF.D.G., and Dangl, JOURNAL OF.L. (2006). Reactive oxygen species signaling in response to pathogens. Plant Physiology **141,** 373-378.

Vanhee, C., Zapotoczny, G., Masquelier, D., Ghislain, M., and Batoko, H. (2011). The Arabidopsis multistress regulator TSPO is a heme binding membrane protein and a potential scavenger of porphyrins via an autophagy-dependent degradation mechanism. The plant cell **23,** 785-805.

Vert, G., Barberon, M., Zelazny, E., Seguela, M., Briat, JOURNAL OF.F., and Curie, C. (2009). Arabidopsis IRT2 cooperates with the high-affinity iron uptake system to maintain iron homeostasis in root epidermal cells. Planta **229,** 1171-1179.

Vert, G., Grotz, N., Dedaldechamp, F., Gaymard, F., Guerinot, M.L., Briat, JOURNAL OF.F., and Curie, C. (2002). IRT1, an Arabidopsis transporter essential for iron uptake from the soil and for plant growth. The plant cell **14,** 1223-1233.

Vinti, G., Hills, A., Campbell, S., Bowyer, JOURNAL OF.R., Mochizuki, N., Chory, JOURNAL OF., and Lopez-JOURNAL OFuez, E. (2000). Interactions between hy1 and gun mutants of Arabidopsis, and their implications for plastid/nuclear signalling. The Plant Journal **24,** 883-894.

Voinnet, O., Rivas, S., Mestre, P., and Baulcombe, D. (2003). An enhanced transient expression system in plants based on suppression of gene silencing by the p19 protein of tomato bushy stunt virus. The Plant Journal **33,** 949-956.

Voss, B., Meinecke, L., Kurz, T., Al-Babili, S., Beck, C.F., and Hess, W.R. (2011). Hemin and magnesium-protoporphyrin IX induce global changes in gene expression in Chlamydomonas reinhardtii. Plant Physiology **155,** 892-905.

Vranova, E., Inze, D., and Van Breusegem, F. (2002). Signal transduction during oxidative stress. Journal of Experimental Botany **53,** 1227-1236.

Wagner, D., Przybyla, D., Camp, R.O.D., Kim, C., Landgraf, F., Lee, K.P., Wursch, M., Laloi, C., Nater, M., Hideg, E., and Apel, K. (2004). The genetic basis of singlet oxygen-induced stress responses of *Arabidopsis thaliana*. Science **306,** 1183-1185.

Wang, X.Q., Watt, P.M., Louis, E.JOURNAL OF., Borts, R.H., and Hickson, I.D. (1996). Pat1: A topoisomerase II-associated protein required for faithful chromosome transmission in Saccharomyces cerevisiae. Nucleic Acids Research **24,** 4791-4797.

Warde-Farley, D., Donaldson, S.L., Comes, O., Zuberi, K., Badrawi, R., Chao, P., Franz, M., Grouios, C., Kazi, F., Lopes, C.T., Maitland, A., Mostafavi, S., MontoJournal ofo, JOURNAL OF., Shao, Q., Wright, G., Bader, G.D., and Morris, Q. (2010). The GeneMANIA prediction server: biological network integration for gene prioritization and predicting gene function. Nucleic Acids Research **38,** W214-220.

Waters, M.T., Wang, P., Korkaric, M., Capper, R.G., Saunders, N.JOURNAL OF., and Langdale, JOURNAL OF.A. (2009). GLK transcription factors coordinate expression of the photosynthetic apparatus in Arabidopsis. The plant cell **21,** 1109-1128.

Weigel D, G.JOURNAL OF. (2002). Arabidopsis: A Laboratory Manual. (Cold Spring Harbor Laboratory Press).

Wiermer, M., Feys, B.JOURNAL OF., and Parker, JOURNAL OF.E. (2005). Plant immunity: the EDS1 regulatory node. Current Opinion in Plant Biology **8,** 383-389.

Willems, A.R., Schwab, M., and Tyers, M. (2004). A hitchhiker's guide to the cullin ubiquitin ligases: SCF and its kin. BBA - Biochimica et Biophysica Acta **1695,** 133-170.

Wilson, K.E., Sieger, S.M., and Huner, N.P.A. (2003). The temperature-dependent accumulation of Mg-protoporphyrin IX and reactive oxygen species in Chlorella vulgaris. Physiologia Plantarum **119,** 126-136.

Winter, D., Vinegar, B., Nahal, H., Ammar, R., Wilson, G.V., and Provart, N.JOURNAL OF. (2007). An "Electronic Fluorescent Pictograph" browser for exploring and analyzing large-scale biological data sets. PloS ONE **2,** e718.

Woodson, JOURNAL OF.D., and Chory, JOURNAL OF. (2008). Coordination of gene expression between organellar and nuclear genomes. Nature Reviews Genetics **9,** 383-395.

Woodson, JOURNAL OF.D., Perez-Ruiz, JOURNAL OF.M., and Chory, JOURNAL OF. (2011). Heme synthesis by plastid ferrochelatase I regulates nuclear gene expression in plants. Current Biology : CB **21,** 897-903.

Xiao, Y., Savchenko, T., Baidoo, E.E., Chehab, W.E., Hayden, D.M., Tolstikov, V., Corwin, JOURNAL OF.A., Kliebenstein, D.JOURNAL OF., Keasling, JOURNAL OF.D., and Dehesh, K. (2012). Retrograde signaling by the plastidial metabolite MEcPP regulates expression of nuclear stress-response genes. Cell **149,** 1525-1535.

Yang, M.S., Chan, H.W., and Yu, L.C. (2006). Glutathione peroxidase and glutathione reductase activities are partially responsible for determining the susceptibility of cells to oxidative stress. Toxicology **226,** 126-130.

Yuan, X.M., Simpson, P., Mckeown, C., Kondo, H., Uchiyama, K., Wallis, R., Dreveny, I., Keetch, C., Zhang, X.D., Robinson, C., Freemont, P., and Matthews, S. (2004). Structure, dynamics and interactions of p47, a maJournal ofor adaptor of the AAA ATPase, p97. EMBO Journal **23,** 1463-1473.

Zhang, L., and Hach, A. (1999). Molecular mechanism of heme signaling in yeast: the transcriptional activator Hap1 serves as the key mediator. Cellular and Molecular Life Sciences **56,** 415-426.

Zimmermann, P., Hennig, L., and Gruissem, W. (2005). Gene-expression analysis and network discovery using Genevestigator. Trends in Plant Science **10,** 407-409.

Zimmermann, P., Hirsch-Hoffmann, M., Hennig, L., and Gruissem, W. (2004). GENEVESTIGATOR. Arabidopsis microarray database and analysis toolbox. Plant Physiology **136,** 2621-2632.

Appendix

A.1 Primers used for mapping PCR

Gene	Forward primer	Tm [°C]	Reverse primer	Tm [°C]
AtSO392	GTTGATCGCAGCTTGATAAGC	62	TTTGGAGTTAGACACGGATCTG	62
nga280	GGCTCCATAAAAAGTGCACC	62	CTGATCTCACGGACAATAGTGC	63
nga111	CTCCAGTTGGAAGCTAAAGGG	63	TGTTTTTTAGGACAAATGGCG	59
cer 461704	TGGGCAGAAGATCTGTACTC	61	TTGGACAGAGATCTTGCCTG	62
cer458709	AGCAGAGTCTTGTTGGTG	60	CGGTTACGTAGAGTAAGC	57
cer449005	CTTTCATGCGGAAGTGAGTG	62	TCCTCGTGCTTGGTTTGAC	63
cer451562	GCAAGAACCAATAAGCTCCC	62	AAGGGCATCATGAAAAGGGC	67
cer459016	CTATTAAGTGCACACGGCAG	61	ATTTGCACCCATTTCCTTAC	60
cer460565	TACTTGGATTCAGGACATTC	57	CTCCTCGGTTATTTCCACGC	66
cer451817	CCTAGCCTTCTTTTGACC	57	AAGCTTCTGACTCAACTCTC	59
cer452410	TTCTCAACACCACCTCTG	59	AAGACAAAATCTGAGGCG	57
cer464712	TTGAGGATGCAAGAGAGTC	59	GAGGTACGTGAATGAACAC	58
M1	CAAGAAAAACCGAATTCACG	57	AGAACTAGAATTTCCATGTC	54
cer455387	AAACCCTACTAGAGTGTGAC	52	TCTCTGTCACTCTTTTCCTC	56
cer455755	ACTGTTTTGTGGTAGTCCTG	57	GTATAACCCTTTTCATAGAC	55
cer455911	GCTTCAGACATAAACTACAG	51	GATACATTGAATTCGACATCC	58
cer455003	TAACCACAGCTATGAGGTCG	60	CTGAACCTTTCTAGTTACCC	55
cer459593	TATCATGACAGCCAGCCAC	63	GTGAGGGACACAATTCGTC	61
M2	AAATAGACCCCACGAAGTCG	62	GAGAGAAAGAGAGATGACG	57
cer470812	TCACCCATAAACCCAAACAC	62	TAGAAGTGTGGTTTTGGTCC	59
F5N16	AACCGTTACATTTCGACTAC	56	TGAACATTCAATCTAATACTATGAG	56
nga8	TGGCTTTCGTTTATAAACATCC	59	GAGGGCAAATCTTTATTTCGG	59
cer452834	AGGAGGAGGTGCAGGAAGA	59	AGCGTATACGACATGTATAAG	56
cer458607	GGAAACAACTTATTTTTCGAACC	58	GCAAGTCTCAACCTTTAATCACTT	58
cer458584	GTTTTGTCATTCGCCAAGATTC	60	TCTCAATGTTCGTGGGGTTT	60
cer449366	AAAGTTTACTCGAGTGGTCC	57	CTGTAAATTTTTGTAACGGC	56
nga249	GGATCCCTACTGTAAAATCCC	60	TACCGTCAATTTCATCGCC	60
nga139	GGTTTCGTTTCACTATCCAGG	61	AGAGCTACCAGATCCGATGG	64
MCO15	TAACCGAGCGAGGGCTACAG	67	ACGAGGTAAAAGGTCGGTCC	65

A.2 Primers used for genotyping

Primer	Sequence	Tm [°C]
SAIL-LB3	TAGCATCTGAATTTCATAACCAATCTCGATACAC	70
GABI-o8409	ATATTGACCATCATACTCATTGC	59
FLAG-RB4	TCACGGGTTGGGGTTTCTACAGGAC	73
FLAG-LB4	CGTGTGCCAGGTGCCCACGGAATAGT	78
SAIL-RB3	CATGGCATATGCTAGCATGC	64
SAIL-LB3	TTCATAACCAATCTCGATACAC	58
INRA-LB	GCCAGGTGCCCACGGAATAG	70
INRA-RB	CGGGTTGGGGTTTCTACAGGAC	69
AT3G21570-SALK_130153-F	GGCGGTTTCCGGTGAAAATG	65
AT3G21570-SALK_130153-R	GCGAAAAGCCAGGTTGTTG	63
AT3G21610-SALK_086303-F	GTCATCACCTCGTCCATAGG	62
AT3G21610-SALK_086303-R	CACAATAATTGATCCTTCCC	56
AT3G21620-Flag619b12-F	CCGAAAACATGGAACATCCT	61
AT3G21620-Flag619b12-R	CCTGAGCAGATTGGTTTCCT	63
AT3G21630-SALK_007193-F	GAAGCTTCCTTAGATTCCCC	60
AT3G21630-SALK_007193-R	AGAAATGGCGGTCTTCATAG	60
AT3G21630-GK-096F09.02-F	CTGGTGCCATGTAACCAAATG	62
AT3G21630-GK-096F09.02-R	GGCATGTATGTGGATCACTT	60
AT3G21650-SALK_059659-F	CCACGCGTGTTTCTCTCAAG	64
AT3G21650-SALK_059659-R	GTGTCCTCAGTCAATCTTAC	57
AT3G21660-GABI_400B11-F	CCTGTAATACACAAGATCC	54
AT3G21660-GABI_400B11-R	GGCTCTTCCGGTTACTCTCC	65
AT3G21660-SAIL_743_A08-F	CTAATGTGCTTAGAAAAGAG	53
AT3G21660-SAIL_743_A08-R	TCCAGCTTATATTAGCAGAC	56
AT3G21670-SALK_001553-F	CGCTTGTTCGACCGTGAAAG	65
AT3G21670-SALK_001553-R	GGCTGTAGCCGCGGTTATAG	66
AT4G01290-SALK_038452-F	LP GTATTGTTGGGGATGTTGGTG	59
AT4G01290-SALK_038452-R	RP GAAATACGAAGCCCTCAGACC	60

A.3 Primers used for qRT-PCR

Gene	Gene code	Forward primer	Reverse primer	Tm [°C]
actin-7	At5g09810	GTTGCCATTCAGGCCGTTCTTTC	CAGAATCGAGCACAATAC-CGGTTG	60
sAPX	At4g08390	AGAATGG-GATTAGATGACAAGGAC	TCCTTCTTTCGTGTACTTCGT	60
tAPX	At1g77490	GCTAGTGCCACAGCAATAGAG-GAG	TGATCAGCTGGTGAAGGAGGTC	60
RMB1	At1g32230	TTCCTCCTCAATTGGAG-TCAAACC	AACCAACACTGTTTGCAC-TTCCTG	68
RIMB3	At4g01290	CGTCACAAGGCTTTCCCTTTGC	CTCCTCTGTTGACTTGAGAAC-CTG	68
2CPA	At3g11630	CCCAACAGAGATTACTGCCT	ATAGTTCAGATCACCAAGCCC	60
2CPB	At5g06290	TCATACCCTCTTCCTCGGCAT	ACCGACCAGTGG-TAAATCATCAGC	60

A.4 Other primers

Primer	Sequence	Tm [°C]
Luc-RT1	ATTGACAAGGATGGATGGCTAC	58
Luc-RT3	AGACCTTTCGGTACTTCGTC	57
M13-F(-20)	GTAAAACGACGGCCAG	57
M13-R	CAGGAAACAGCTATGAC	50
2CPAProm-entry-F	CACCATCCAACTAATGGAC	57
2CPAProm-entry-R	TGCTACACACACTTTGTGAC	57
pHGWFS7-2016bp-F	CTCAGTGGCTCCTTCAACG	64
pHGWFS7-4089bp-R	GTGGTGCAGATGAACTTCAGG	64

List of publication

Baier M,. Pitsch N.T., Mellenthin M, and **Guo W.** (2010) Regulation of Genes Encoding Chloroplast Antioxidant Enzymes in Comparison to Regulation of the Extra-plastidic Antioxidant Defense System. Naser A. Anjum N. A., Umarm S., Chan MT. (Eds.) Ascorbate-Glutathione Pathway and Stress Tolerance in Plants (pp. 337 -386) New York, NY: Springer.

Meeting abstracts

Wei G, Baier M, (2009) Identification of transcriptional regulators of 2CPA using EMS-mutagenesis and reporter gene based QTL-mapping. Deutsche Botanikertagung 2009, Leipzig, Germany (poster presentation)

Wei G, Hiltscher H, Heiber I, Baier M (2010) A mutant screen for identification of regulators involved in chloroplast-to-nucleus redox signaling. 21th International Conference on Arabidopsis Research, Yokohama, Japan (poster presentation)

Wei G, Hiltscher H, Heiber I, Baier M (2010) A mutant screen for identification of regulators involved in chloroplast-to-nucleus redox signaling.19th Photosynthesis workshop, Frankfurt, Germany (poster presentation)

Wei Guo, Frenkel M, Hilscher H and Baier M (2010) Identification of regulators involved in chloroplast-to-nucleus redox signaling and their effects on growth and fitness signals. 4th SFB 429 International Symposium: ‘‘Sensing and plant primary metabolism.’’ Potsdam, Germany (poster presentation)

Wei G, Hiltscher H, Heiber I, Baier M (2011), Identification of regulators involved in chloroplast to nucleus redox signaling. Plant Biology 2011 Meeting, Minneapolis, United States (poster presentation)

Wei G, Hiltscher H, Heiber I, Baier M (2011), Identification of regulators rnvolved in chloroplast to nucleus redox signaling Molecular interactions workshop 2011, Berlin, Germany (poster presentation)

Wei G, Hiltscher H, Heiber I, Baier M (2011) Identification of transcriptional regulators of 2CPA using EMS-mutagenesis and reporter gene based QTL-mapping. Deutsche Botanikertagung 2011, Berlin, Germany (poster presentation)

Wei G, Hiltscher H, Heiber I, Baier M (2012) Identification and characterization of regulators of 2-Cys-Peroxiredoxin A in *Arabidopsis thaliana.* Havel-Spree-Colloquium, Potsdam, Germany (oral presentation)

Acknowledgement

Foremost, I would like to express my sincere gratitude to my supervisor Prof. Dr. Magarete Baier for the support of my Ph.D study and research, with her patience, motivation, enthusiasm, and immense knowledge. Especially, I would like to thank her for her tolerance to my disorderness in the laboratory. Her guidance helped me throughout my research and writing of this thesis. I could not have imagined having a better advisor and mentor for my Ph.D study. I am also thankful to the financial support of the DFG.

I would like to thank our collaboration partner Prof. Dr Ute Krämer for ICP-MS measurement and Dr. Beth Rowan for the NGS projects.

I extend my thanks to present and former members of the research group of Prof. Dr. Baier, who helped me during my stay in the laboratory. The group has been a source of friendship as well as good advice and collaboration. I am grateful to Dr. Jote Bulcha for his help during my research and thesis writing. He is not only my labmate but also my friend for life. My warm appreciation also goes to Dr. Marina Mellenthin, Ms. Sabine Matuszak and Ms. Ulrike Ellersiek for their friendly help in and out of laboratory.

I would like to express my thanks to Ms. Anting Zhu, who helped me to check my thesis.

I also would like to thank my thesis examination committee member and second supervisor, Prof. Dr. Wolfgang Schuster, who encouraged me during my Ph.D study and took time to review my thesis.

Very special thanks go to Mr. Yunpeng Bai. He suggested me of an alternative career path besides scientific research after my Ph.D study.

Finally, I would like to thank my family, my father Genkui Guo and my mother Meiying Pan and my sister Ting Guo, who support me spiritually throughout my life.

I hereby declare that I have prepared and written the presented doctoral thesis myself using only the presented methods and sources. All sources from literature are marked as such and are properly cited

Berlin, August 2013

Wei Guo